# Cysteine in signaling and plant pathogen response



**Doctoral thesis** 

for

the award of the doctoral degree
of the Faculty of Mathematics and Natural Sciences
of the University of Cologne

submitted by

**Jannis Moormann** 

Köln, 04.07.2025

accepted in 2025

#### **Abstract**

Beyond their role as building blocks of proteins, amino acids serve a variety of additional functions in plants. Since plants are sessile organisms, they need to identify and properly deal with a plethora of adverse environmental circumstances. Amino acids are known to be implicated in plant stress responses in different ways. While some aspects are already well understood, many remain elusive to date. Here, we reviewed the recent research progress on amino acids in plant-microbe interactions (chapter 2). There, we explored how specialized metabolites and amino acid transporters shape the plant microbiome and elaborated on how amino acids impact plant immunity. Furthermore, we aimed to elucidate the role of cysteine in signaling and plant pathogen response (chapter 3). To that end, we set up a liquid culture approach in which Arabidopsis thaliana seedlings were incubated with 1 mM cysteine for 24 hours. Subsequent shotgun proteome analysis revealed that elevated cysteine levels are interpreted as a biotic threat by the plant. Consistent with this, cysteine both primed adult Arabidopsis plants against infection with the hemibiotrophic leaf pathogen Pseudomonas syringae (Pst) and its levels increased in response to Pst infection. Comparing proteome responses of cysteine-treated and Pst-infected plants revealed potential mediators of the cysteine-induced defense response. Unlike other amino acids, cysteine can be synthesized in multiple subcellular compartments by different O-acetylserine(thiol)lyase (OASTL) isoforms. Here, we found that the lack of mitochondrial OASTL-C renders Arabidopsis plants more susceptible to infection with Pst. Remarkably, mitochondria allow for the complete oxidation of cysteine facilitated by a four-step enzymatic process. This is the only pathway to degrade cysteine without producing sulfide, which becomes toxic in high concentrations. However, the first enzyme catalyzing the transamination of cysteine is unknown. Here, we aimed to identify the missing aminotransferase to complete the mitochondrial cysteine degradation pathway (chapter 4). Thus, we established mass spectrometry-based thermal proteome profiling (TPP) with mitochondrial fractions to find novel proteins binding or interacting with cysteine. Consequently, selected candidate proteins were produced in Escherichia coli and purified using immobilized metal affinity- and size exclusion chromatography. Strikingly, alanine aminotransferase 1 and aspartate aminotransferase 1 showed activity using cysteine as an amino donor. Moreover, both enzymes were able to complete the mitochondrial cysteine degradation pathway in vitro. The findings in this dissertation expand our understanding of cysteine as an infochemical in the plant pathogen response, highlight the importance of plant mitochondria for biotic stress adaptation and suggest potent targets for future research in plant immunity. Additionally, we present a powerful tool to identify novel protein metabolite interactions and, thereby, further our knowledge about the mitochondrial cysteine metabolism.

### **Table of content**

Abstı	Abstractii					
List of Abbreviationsvii						
List of Figuresix						
1 lı	ntroduction	1				
1.1	Amino acids beyond proteins	1				
1.2	Cysteine in Plants	2				
1.3	Sulfur Assimilation and the Compartmentalized Cysteine Metabolism	2				
1.4	Cysteine as a Source of reduced Sulfur in the Plant Cell	5				
1.5	From Sulfate to Signal: Cysteine in ABA-dependent stomatal closure	6				
1.6	Aim of this study	9				
1.7	References	10				
2 N	News about amino acid metabolism in plant-microbe interactions	16				
2.1	Abstract	16				
2.2 nutrie	Plant amino acid metabolism provides signaling molecules, defense compounds ents to shape interactions with microbes					
2.3 shapi	Aromatic amino acids are converted to a set of specialized metabolites involved					
2.4	Amino acid transport controls nutrient exchange between plants and microbes	21				
2.5	Specific perturbations in amino acid homeostasis constitutively activate plant defen					
2.6 signa	Amino acid activated calcium channels (GLRs) mediate amino acid sensing a	and				
2.7	Lysine metabolism is essential for systemic immune signaling	26				
2.8	Concluding remarks	28				
2.9	Glossary	28				
2.10	References	30				
3 (	Cysteine signaling in plant pathogen response	39				
3.1	Abstract	39				
3 2	Introduction	39				

3.3	Resul	ts	.42
	3.3.1 biotic str	The seedling proteome response to increased cysteine concentrations indicaress signaling	
	3.3.2	Cysteine treatment induces pathogen resistance	44
	3.3.3 cysteine	Pathogen attack induces cysteine synthesis, and proteome responses treatment and pathogen interaction overlap	
	3.3.4	Compartment specific cysteine synthesis is required for pathogen resistance	.47
3.4	Discus	ssion	49
	3.4.1	Links of cysteine homeostasis to plant immune signaling	49
	3.4.2	Compartment specific functions of cysteine synthesis in immune signaling	51
	3.4.3	Potential mechanisms of cysteine immune signaling	52
3.5	Mater	ials and Methods	.54
	3.5.1	Plant Material and growth conditions	.54
	3.5.2	Cysteine treatment	54
	3.5.3	Quantification of total lipids	55
	3.5.4	Quantification of total carbohydrates	55
	3.5.5	Extraction and quantification of total protein	55
	3.5.6	Quantification of chlorophyll	.55
	3.5.7	Analysis of seedling respiration	55
	3.5.8	Reactive oxygen species staining	56
	3.5.9	Glutathione-S-transferase activity assay	56
	3.5.10	Analysis of photosynthetic performance	.56
	3.5.11	Pseudomonas syringae infection assays	.56
	3.5.12	Quantification of sulfur metabolites	.57
	3.5.13	Quantification of camalexin	.57
	3.5.14	Protein extraction, digestion and sample preparation for proteome analysis	via
	mass sp	ectrometry	.57
	3.5.15	Shotgun proteomics by ion mobility mass spectrometry (IMS-MS/MS)	.58
	3.5.16	Data Processing and Evaluation	.58
	3.5.17	Data availability	59

3.6	Supplementary Figures60		
3.7	Refer	rences	63
4 cys		al proteome profiling identifies mitochondrial aminotransferases involved tabolism via persulfides in plants	
4.1	Abstr	act	72
4.2	Introd	duction	73
4.3	Resu	lts	76
	4.3.1	Thermal proteome profiling of the Arabidopsis thaliana mitochondrial proteon	
	4.3.2 proteon	Cysteine-induced thermal stability shifts in the Arabidopsis thaliana mitochondine	
	4.3.3 aminotr	Identification and biochemical characterization of mitochondrial cystem	
	4.3.4	Reconstruction of the complete plant mitochondrial cysteine catabolic pathw	•
4.4	Discu	ussion	82
	4.4.1	Thermostability of plant mitochondrial proteins	82
	4.4.2	Thermal proteome profiling identifies mitochondrial cysteine aminotransferas	
	4.4.3	Metabolic integration of mitochondrial cysteine aminotransferases	85
4.5	Conc	lusion	86
4.6	Mate	rials & Methods	87
	4.6.1	Plant material and protein extraction	87
	4.6.2	Temperature gradient precipitation	87
	4.6.3 spectro	Protein digestion and sample preparation for proteome analysis via ma	
	4.6.4	Quantitative proteomics by shotgun mass spectrometry (LC-MS/MS)	88
	4.6.5	Thermal proteome profiling data analysis	88
	4.6.6	Cloning of Arabidopsis cysteine binding candidates	89
	4.6.7	Protein overexpression and purification	89
	4.6.8	Enzyme activity tests	91

	4.6.9	Pathways Reconstruction	91		
	4.6.10	Data availability	92		
4.7	Suppl	ementary Figures	93		
4.8	Refer	ences	99		
5	Closing	Remarks	105		
Eidesstattliche Erklärung Fehler! Textmarke nicht definiert.					
Declaration of Contribution108					
Acknowledgements Fehler! Textmarke nicht definier					

#### **List of Abbreviations**

1,2-DP: 1,2-dehydropipecolic acid

**3-MP**: 3-mercaptopyruvate

**AAAP**: Amino acid/auxin permease **AAO3**: Abscisic aldehyde oxidase 3

**ABA**: Abscisic acid

ABA3: Molybdenum cofactor sulfurylase

ABI4: ABA-insensitive 4

ABF2: ABA response binding factor 2

ACC: Aminocyclopropane-1- carboxylic acid

Ala: Alanine

Ala-AT: Alanine aminotransferase 1

**ALD1**: AGD2-LIKE DEFENSE RESPONSE PROTEIN1

AOX: Alternative oxidase

**APC**: Amino acid polyamine organocation

APK: APS kinase

**APS**: Adenosine 5-phosphosulfate

Asn: Asparagine

Asp-AT: Aspartate aminotransferase 1

ATP: Adenosine triphosphate

**ATPS**: ATP sulfurylase **BTH**: Benzothiadiazole

**CAS-C1**: Cyanoalanine synthase

**CAT1**: CATIONIC AMINO ACID TRANSPORTER 1

**CSC**: Cysteine synthase complex **CESTA**: Cellular thermal shift assay

Cys: Cysteine

**DAP**: 3,3'-diaminobenzidine

**DAMP**: Damage-associated molecular pattern

**DES1**: L-cysteine desulfhydrase

DHS: 3-deoxy-d-arabino-heptulosonate 7-phosphate synthase

**ETC**: Electron transport chain

ETHE1: Sulfur/persulfide dioxygenase

ETI: Effector-triggered immunity

FMO1: FLAVIN-DEPENDENT MONOOXYGENASE1

**GABA**: γ-aminobutyrate

**GABA-AT**: GABA aminotransferase

GLR: Glutamate receptor-like calcium channels

**Glu**: Glutamate **Gly**: Glycine

**γ-EC**: γ-glutamylcysteine **GDU1**: Glutamine dumper 1

**GSH**: Glutathione **GSH1**: γ-EC synthase

**GSH2**: Glutathione synthetase

**GSSH**: GSH persulfide

**GST**: Glutathione-S-transferase

His: Histidine

hpi: Hours past infection

**HPLC**: High performance liquid chromatography

JA: Jasmonic acid

**KAC**: α-ketocaproic acid

**LHT1**: LYSINE HISTIDINE TRANSPORTER1

Lys: Lysine

MAPKKK18: Mitogen-Activated Protein Kinase Kinase Kinase 18

**MAMP**: Microbe-associated molecular pattern **MPST**: 3-mercaptopyruvate sulfurtransferase **NCED3**: 9-cis-epoxycarotenoid dioxygenase 3

NFS: Cysteine desulfurase NHP: N-hydroxypipecolic acid NHPG: NHP-N-O-glucoside Ni-NTA: Nickel-nitrilotriacetic acid

**OAS**: O-acetylserine **OASTL**: OAS-(thiol)lyase

PAPS: 3-phosphoadenosine 5-phosphosulfate

**PCA**: Principle component analysis

**Phe**: Phenylalanine **Pip**: Pipecolic acid

PLP: Pyridoxal phosphate

**PMP**: Pyridoxamine-5'-phosphate **PPR**: Pentatricopeptide repeat

Pst: Pseudomonas syringae pv tomato DC3000

PTI: Pattern-triggered immunity

SA: Salicylic acid

**SAM**: S-adenosylmethionine

**SAR**: Systemic acquired resistance

**SARD4**: SAR-DEFICIENT4

Ser: Serine

**SERAT**: Serine acetyltransferase **SnRK2**: SNF1-RELATED KINASE 2 **STR1**: (3-MP) Sulfur transferase

**SULTR**: Sulfate transporter

**RBOHD**: Respiratory Burst Oxidase Homolog Protein D

**ROS**: Reactive oxygen species

TCA: Tricarboxylic acid

**TPP**: Thermal proteome profiling

**Tm**: Melting temperature

**Trp**: Tryptophan **Tyr**: Tyrosine

**UDP**: Uridine diphosphate

**UGT**: UDP-glucosyltransferases

**UMAMIT: USUALLY MULTIPLE ACIDS MOVE IN AND OUT TRANSPORTERS** 

### **List of Figures**

Figure 1.1: Cellular organization of sulfur metabolism 4
Figure 1.2: Representation of cysteine-mediated ABA signaling in guard cells 8
Figure 2.1: Plant amino acid metabolism provides active compounds for interacting with
microbes at different levels
Figure 2.2: Specialized metabolites derived from aromatic amino acids shape the root
microbiome20
Figure 2.3: Perturbations in amino acid transport and metabolism can trigger immune
signaling24
Figure 2.4: Lysine is converted to the mobile immune signal N-hydroxypipecolic acid to induce
systemic acquired resistance27
Figure 3.1: Seedling proteome response to cysteine treatment
Figure 3.2: Cysteine treatment induces resistance to the virulent pathogen Pseudomonas
syringae44
Figure 3.3: Cysteine accumulation and proteome response during pathogen interaction46
Figure 3.4: Compartmentalization of cysteine synthesis in pathogen resistance48
Figure 4.1: Mitochondrial cysteine metabolism75
Figure 4.2: Thermal proteome profiling (TPP) workflow76
Figure 4.3: Thermal proteome profiling of the <i>Arabidopsis thaliana</i> mitochondrial proteome78
Figure 4.4: Candidates for a mitochondrial cysteine aminotransferase identified by thermal
proteome profiling
Figure 4.5: Biochemical characterization of mitochondrial cysteine aminotransferase
candidates80
Figure 4.6: Reconstruction of the complete plant mitochondrial cysteine catabolic pathway in
vitro
Figure 5.1 Working model of cysteine in signaling and plant pathogen response107
J J J J J J J J J J J J J J J J J J J

#### 1 Introduction

#### 1.1 Amino acids beyond proteins

Plants are sessile organisms and subject to changing environmental conditions. To withstand adverse circumstances, they need to evaluate stressors accurately and mount proper defense responses. A number of strategies to survive such stresses involve the amino acid metabolism. However, many of the underlying mechanisms are still unknown. While amino acids are best known as the building blocks of proteins, the molecules also serve a multitude of additional functions in plant physiology. Their tight connection to the protein and carbohydrate metabolism, as well as nitrogen and sulfur assimilation makes them important hubs for metabolic adaptation (Liu et al. 2022; Takahashi et al. 2011). Hence, amino acids are part of vital processes such as plant growth and development, intracellular pH control and generation of metabolic energy or redox power (Amir et al. 2018; Watanabe et al. 2013; Galili et al. 2014). Furthermore, amino acids are involved in the response to environmental stress and their role as signaling molecules is increasingly being looked at. Notably, they are implicated in a number of different processes. Under carbon starvation, amino acids serve as alternative respiratory substrates (Hildebrandt et al. 2015). Osmotic stress elicited by drought or high salinity prompts the accumulation of proline, which functions as both an osmolyte and a molecular chaperone, protecting protein integrity (Szabados & Savouré 2010). During hypoxic conditions, the nonproteinogenic amino acid y-aminobutyrate (GABA) inhibits membrane depolarization to prevent programmed cell death and possibly contributes to energy and redox homeostasis via the so-called GABA-shunt pathway (van Veen et al. 2024). Cysteine elicits abscisic acidmediated stomatal closure in response to water deficit stress in guard cells (see chapter 1.5) and glutamate triggers long distance, calcium-based plant defense signaling in response to wounding (Toyota et al. 2018). What is more, amino acids are precursors for several specialized molecules that aid during pathogen infection. For example, the phloem-mobile immune signaling molecule N-hydroxypipecolic acid (NHP) is synthesized from lysine (Hartmann & Zeier 2019) and the backbones of glucosinolates, working as defense compounds, are made from multiple amino acids such as phenylalanine, tryptophan or valine (Blažević et al. 2020). These examples illustrate the diverse roles of amino acids in situations where adaptation is necessary to survive. This dissertation comprises three manuscripts that contribute to our understanding of amino acid metabolism in general and, more specifically, during biotic interactions. The recent progress of research concerning the amino acid metabolism during plant-microbe interactions was reviewed in chapter 2. The review article covers amino acid-derived specialized metabolites shaping the rhizosphere, the NHP metabolism, amino acid transporters during plant-microbe interactions and perturbations in amino acid homeostasis affecting plant immunity. The latter section includes reports on

Arabidopsis mutants compromised in different aspects of cysteine metabolism which was accompanied by evident changes in immunity. This suggests that cysteine plays a role during the plant's response to pathogens. However, the potential underlying mechanisms by which this is mediated remain largely unknown. Hence, more research is needed to unravel how cysteine is involved in plant immune signaling processes. In chapter 3, by monitoring the response of Arabidopsis to elevated cysteine levels we aimed to elucidate potential mechanisms involved in cysteine-mediated immune signaling. In chapter 4, by identifying novel enzymes that interact with cysteine, we aspired to further the knowledge about the cysteine metabolism in general.

#### 1.2 Cysteine in Plants

Among the 20 proteinogenic amino acids cysteine stands out for its distinct chemical features owed to the presence of the sulfur atom in the thiol group of its side chain, making this amino acid highly reactive. Next to its universal role as part of proteins it inhabits multiple other functions in the plant cell. It is the first organic acceptor of reduced sulfur during assimilation, which makes it the starting point for a range of vital compounds in plant metabolism (Takahashi et al. 2011). In addition, cysteine can be synthesized and degraded in multiple compartments, again, making it stand out among amino acids (Heeg et al. 2008; Alvarez et al. 2010; Höfler et al. 2016). In recent years, cysteine was found to be involved in both abiotic and biotic stress responses via different mechanisms (Álvarez et al. 2012; Ingrisano et al. 2023; Romero et al. 2014). The following paragraphs summarize the role of cysteine in plant metabolism, explore its relevance for stress adaptation and signaling and introduce the research conducted in chapter 3 and chapter 4.

#### 1.3 Sulfur Assimilation and the Compartmentalized Cysteine Metabolism

Sulfur is an essential mineral nutrient in plants and constitutes about 1.3 % of leaf and 3.6 % of seed elements in Arabidopsis ((w/w) dry weight, Campos et al. 2021). In the soil, sulfur is commonly found in the form of sulfate, which contains sulfur in its most oxidized form. Available sulfate is taken up by the roots and distributed within the plant via sulfate transporter proteins called SULTR. In the cell, sulfate can be translocated into the vacuole for storage or into the plastids where primary sulfate assimilation takes place. Before reduction, sulfate needs to be activated by adenylation catalyzed by ATP sulfurylase (ATPS) to form adenosine 5-phosphosulfate (APS). Consecutively, APS either undergoes further reduction following the sulfur assimilation pathway or it is phosphorylated by APS kinase resulting in 3-phosphoadenosine 5-phosphosulfate (PAPS). PAPS is used in sulfation reactions which

commonly modify metabolites and proteins in plant cells. The nitrogen- and sulfur-rich defense compounds of the Brassicaceae family, known as glucosinolates are well known sulfated molecules. In plastids, APS is reduced by APS reductase to form sulfite, which is again reduced to sulfide by sulfite reductase. In the next and final step of the sulfur assimilatory pathway, sulfide is incorporated into cysteine. The carbon skeleton originates from serine which is activated by serine acetyltransferase (SERAT) to form O-acetylserine (OAS). The acetyl moiety of OAS is exchanged by sulfide through the activity of OAS-(thiol)lyase (OASTL) resulting in cysteine. SERAT and OASTL are associated in a hetero-oligomeric cysteine synthase complex (CSC; (Takahashi et al. 2011)). Major isoforms of both enzymes exist in the cytosol (OASTL-A; SERAT1;1), plastids (OASTL-B; SERAT2;1) and mitochondria (OASTL-C, SERAT2;2) (Figure 1.1; (Heeg et al. 2008; Noji et al. 1998), allowing for the establishment of the CSC in multiple cellular compartments. Notably, SERAT and OASTL activities differ significantly between compartments. Despite the fact that sulfide is produced in chloroplasts, the main site of cysteine synthesis in the cell was found to be the cytosol. Interestingly, knock-out of the individual OASTL genes in Arabidopsis lead to viable single mutant plants with fairly stable cysteine and glutathione (GSH) contents. Even though, lack of OASTL-A resulted in slightly but significantly decreased cysteine levels, growth retardation was only visible in the mitochondrial OASTL-C mutant. What is more, OASTL-C, despite constituting only about 5 % of the total OASTL activity, was sufficient to compensate for the absence of OASTL-A and OASTL-B in the double knock-out mutant oastIAB. The study from Heeg et al. (2008) highlights the importance of stable and sufficient cysteine levels and shows the potential of different compartment-specific OASTL isoforms to contribute to that end. Here, we investigated how the plant reacts to disturbed cysteine levels as we set up a cysteine feeding approach and monitored the proteomic response. Additionally, we explored the role of compartment-specific cysteine synthesis in response to pathogen infection (Chapter 3).

In total, the OASTL gene family contains nine isoforms in Arabidopsis. Next to the isoforms introduced above, three more genes with critical functions in cysteine metabolism have been identified. (i) CAS-C1, formerly known as CysC1, encodes for a  $\beta$ -cyanoalanine synthase in mitochondria. It catalyzes the formation of  $\beta$ -cyanoalanine from cysteine and cyanide, allowing for the detoxification of the latter (Yamaguchi et al. 2000; Hatzfeld et al. 2000). (ii) Further, CS26 catalyzes the formation of S-sulfocysteine from OAS and thiosulfate to aid in redox regulation in chloroplasts (Bermúdez et al. 2010) and (iii) the L-cysteine desulfhydrase DES1 catalyzes the desulfhydration of cysteine to sulfide, ammonia and pyruvate in the cytosol (Alvarez et al. 2010). Another cysteine degradation pathway is located in mitochondria where it is postulated that a yet unknown amino transferase catalyzes the transamination of cysteine to form 3-mercaptopyruvate (3-MP). Next, the sulfhydryl group of 3-MP is transferred to GSH by the sulfur transferase STR1 resulting in pyruvate and GSH persulfide (GSSH). In turn,

GSSH is oxidized by the persulfide dioxygenase ETHE1 forming GSH and sulfite. Finally, thiosulfate is formed by the addition of another persulfide group from GSSH to sulfite by STR1 (Figure 1.1, (Höfler et al. 2016)). This pathway facilitates the complete oxidation of cysteine without sulfide as a byproduct. In contrast, DES1-catalyzed cysteine degradation produces

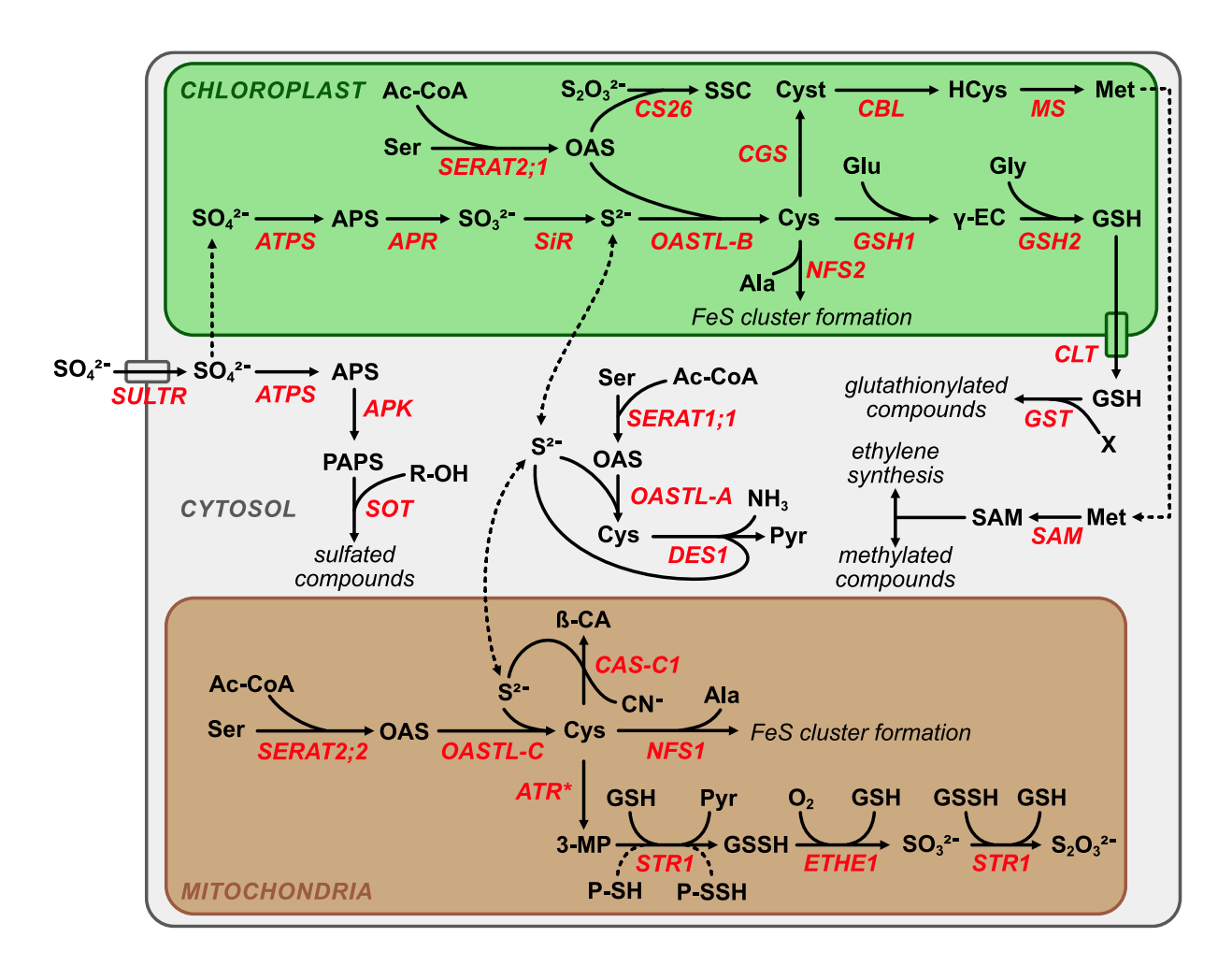


Figure 1.1: Cellular organization of sulfur metabolism

Enzymes and transporters are indicated in red. Dashed lines indicate putative pathways for metabolite transport or putative enzyme function. Abbreviations of metabolites: Ac-CoA, acetyl coenzyme A; APS, adenosine 5'-phosphosulfate; Cys, cysteine; Cyst, cystathionine; Glu, glutamate;  $\gamma$ -EC,  $\gamma$ -glutamylcysteine; GSH, glutathione; GSSH, glutathione persulfide; HCys, homocysteine; Met, methionine; OAS, O-acetylserine; PAPS, 3'-phosphoadenosine 5'-phosphosulfate; Pyr, pyruvate; R-OH, hydroxylated precursor; SAM, S-adenosylmethionine; Ser, serine; 3-MP, 3-mercaptopyruvate;  $\beta$ -CA;  $\beta$ -cyanoalanine Abbreviations of enzymes and transporters: APK, APS kinase; APR, APS reductase; ATR; amino transferase (\*yet unknown); ATPS, ATP sulfurylase; CAS-C1;  $\beta$ -cyanoalanine synthase; CBL, cystathionine  $\beta$ -lyase; CGS, cystathionine  $\gamma$ -synthase; CS26, s-sulfocysteine synthase; ETHE1, persulfide dioxygenase; GSH1,  $\gamma$ -glutamylcysteine synthetase; GSH2, glutathione synthetase; GST, glutathione-S-transferase; MS, methionine synthase; OASTL, OAS(thiol)lyase; SAM, S-adenosylmethionine synthetase; SERAT, serine acetyltransferase; SiR, sulfite reductase; SOT, sulfotransferase; STR1, sulfur transferase; SULTR, sulfate transporter. Figure adapted from Takahashi et al. (2011) and Höfler et al. (2016).

sulfide in the process, which must be controlled through its eventual reincorporation into cysteine. High concentrations of sulfide can be toxic due to its ability to inhibit the cytochrome

c oxidase and, consequently, the mitochondrial electron transport chain (ETC) (Cooper & Brown 2008). In connection with that, ETHE1 was found to be essential for early embryo development in Arabidopsis (Holdorf et al. 2012). Moreover, the mitochondrial pathway produces persulfides from cysteine and is speculated to be involved in the persulfidation of proteins. This might be facilitated by STR1, as protein persulfidation activity was recently confirmed for its yeast homolog MPST (Pedre et al. 2023). Persulfidations are posttranslational protein modifications in which a cysteine thiol (-SH) is covalently bound to a sulfane sulfur to form a persulfide (-SSH) (Moseler et al. 2024). This would enable for another layer of regulation and poses a potential mode of cysteine-mediated signaling via mitochondria. The mitochondrial cysteine degradation pathway, therefore, plays a vital role in cysteine homeostasis, aids in proper sulfide detoxification and might mediate protein persulfidation. However, the protein to facilitate the first transamination step to produce 3-MP is yet to be identified. Here, mass spectrometry-based thermal proteome profiling (TPP) was used to find unknown proteins that interact with cysteine. In doing so, novel mitochondrial proteins were identified that showed transaminase activity using cysteine as amino donor in vitro (chapter 4).

#### 1.4 Cysteine as a Source of reduced Sulfur in the Plant Cell

Cysteine metabolism is intricately linked to sulfur assimilation, making it the key to distributing reduced sulfur to various compounds vital for plant metabolism and stress responses. In order to defend against pathogen invasion, cruciferous plants, like Arabidopsis, characteristically synthesize sulfur-containing indole alkaloids like camalexin. These molecules rely on the incorporation of sulfur from cysteine to be synthesized and available upon pathogen challenge (Pedras et al. 2000). Also, cysteine is used to provide sulfur for the formation of iron sulfur (FeS) clusters. FeS cluster are essential cofactors for multiple proteins involved in electron transfer reactions in the photosynthetic and respiratory ETCs or of enzymes involved in metabolic processes. NFS1 in mitochondria and NFS2 in chloroplasts facilitate the desulfuration of cysteine and, thus, the first step of the FeS cluster assembly. (Figure 1.1; (Turowski et al. 2012; Léon et al. 2002; Pilon-Smits et al. 2002). Another branching point from cysteine in the chloroplasts is a three-step enzymatic reaction synthesizing the second sulfurcontaining amino acid methionine. Methionine is converted to S-adenosylmethionine (SAM) in the cytosol by S-adenosylmethionine synthetase. SAM is used for transmethylation, leading to nucleic acid, protein and lipid modifications (Ravanel et al. 2004; Ravanel et al. 1998). To add to that, the gaseous phytohormone ethylene is produced from SAM (Bleecker & Kende 2000). Further, the tripeptide GSH is synthesized from cysteine in a two-step enzymatic process in chloroplasts. First, γ-glutamylcysteine (γ-EC) is formed from glutamate and cysteine, catalyzed

by y-EC synthase (GSH1; (May & Leaver 1994). Then, glutathione synthetase (GSH2) adds glycine to y-EC to produce GSH (Ullmann et al. 1996), which is exported by so-called CLTs in the plastid membrane (Maughan et al. 2010). GSH plays a pivotal role in several physiological processes such as redox homeostasis, reactive oxygen species (ROS) scavenging, development, defense responses and detoxification of xenobiotics (Foyer & Noctor 2011; Considine & Foyer 2014; Noctor et al. 2024). The latter is facilitated by the action of glutathione-S-transferases (GSTs), which catalyze the conjugation of GSH to electrophilic centers of a wide range of substrates. This conjugation renders substrates more water-soluble and facilitates their transport or sequestration. GSTs have been shown to be highly inducible by different stimuli and play a role during hormone homeostasis and biotic interactions (Cummins et al. 2011; Moons 2005; Gullner et al. 2018). The central position of cysteine for the distribution of reduced sulfur to a range of compounds makes it a promising candidate for a metabolic signaling molecule. As multiple sulfur-containing molecules facilitate defense responses (i.e. camalexin, GSH or, in turn, GSTs), the proposed signaling via cysteine could also be involved in response to pathogen challenge. In chapter 3, we show that increased cysteine levels in Arabidopsis are interpreted as biotic stress signal. However, there is little evidence regarding sensors or receptors for the amino acid. In chapter 4, we established TPP to find cysteine binding proteins which bears the potential to identify novel cysteine sensing proteins.

#### 1.5 From Sulfate to Signal: Cysteine in ABA-dependent stomatal closure

One well-studied example of the implication of cysteine in stress signaling is drought stress. There, it helps to mediate the process of closing the plants stomata. Stomata are small pores that are surrounded by a pair of guard cells in the leaf epidermis. When open, they allow CO2 and  $O_2$  to enter and exit the leaves and water to diffuse out of the leaves by transpiration. Conditions such as drought stress, darkness or invasion of pathogens trigger stomata to close (Shimazaki et al. 2007; Melotto et al. 2008; Kim et al. 2010). In recent years, cysteine was found to play a central role in the process of stomatal closure via multiple mechanisms. Upon drought, sulfate is transported from roots into leaves in maize plants (Ernst et al. 2010). Following this, it was shown that sulfate accumulation prompts stomatal closure in Arabidopsis. Strikingly, assimilation of sulfate into cysteine was necessary for the process. Additionally, it was found that cysteine activates the expression of 9-cis-epoxycarotenoid dioxygenase 3 (NCED3; (Batool et al. 2018). NCED3 catalyzes the rate-limiting step in the synthesis pathway of abscisic acid (ABA; Figure 1.2; (Nambara & Marion-Poll 2005). Furthermore, cysteine is a substrate for the molybdenum cofactor sulfurylase ABA3 and required for activation of abscisic aldehyde oxidase 3 (AAO3; (Bittner et al. 2001)), which catalyzes the last step of ABA production. ABA is a phytohormone key to induce stomatal closure by allowing for the

autophosphorylation of protein kinases SNF1-RELATED KINASE 2s (SnRK2s). SnRK2s, in turn, phosphorylate and activate downstream protein targets (Weiner et al. 2010; Heinemann & Hildebrandt 2021). In addition, ABA transcriptionally upregulates DES1, resulting in the accumulation of H<sub>2</sub>S (Scuffi et al. 2014). Consecutively, DES1 is further activated in the presence of ABA by H<sub>2</sub>S-triggered protein persulfidation (Chen et al. 2020; Shen et al. 2020). Interestingly, three additional proteins pivotal for ABA-dependent guard cell signaling were recently found to be activated by persulfidation (Figure 1.2): (i) The transcription factor ABI4, when persulfidated, induces the expression of Mitogen-Activated Protein Kinase Kinase Kinase 18 (MAPKKK18). MAPKKK18 propagates MAPK signaling cascades that lead to stomatal closure. Additionally, ABI4 can also transactivate DES1 to coordinate ABA and MAPK signals (Zhou et al. 2021). (ii) Persulfidated SnRK2.6 showed enhanced phosphorylation activity and stronger interaction with ABA response binding factor 2 (ABF2), which is a transcription factor acting downstream of ABA signaling (Chen et al. 2020). (iii) Persulfidation of the NADPH oxidase Respiratory Burst Oxidase Homolog Protein D (RBOHD) improves its ability to produces ROS. In turn, ROS not only promotes stomatal closure, but also contributes to a negative feedback mechanism through persulfide-oxidation (Shen et al. 2020). The role of cysteine in ABA-mediated guard cell signaling showcases the variety of mechanisms in which cysteine can affect the plant metabolism. Hence, similar dynamics, including signaling functions, might be present in other tissues or in response to stimuli other than drought stress. Here, we found that cysteine induces a biotic stress response at the level of the leaf as a whole (chapter 3). This contrasts its function in guard cells, since biotic and abiotic stress responses usually suppress each other and lead to different outcomes (Torres-Zabala et al. 2007; Torres Zabala et al. 2009). Therefore, a deviating mode of action might be underlying cysteineinduced biotic stress signaling. Nevertheless, protein persulfidation might still be a potential mechanism. Interestingly, we found mitochondrial cysteine synthesis to be of particular importance for a proper defense response. Consequently, it is tempting to speculate that protein persulfidation, possibly facilitated by mitochondrial STR1, plays a role during plant pathogen interactions. In chapter 4, we used TPP on mitochondrial protein fractions to identify novel cysteine binding proteins and illuminate unknown steps in the mitochondrial cysteine metabolism.

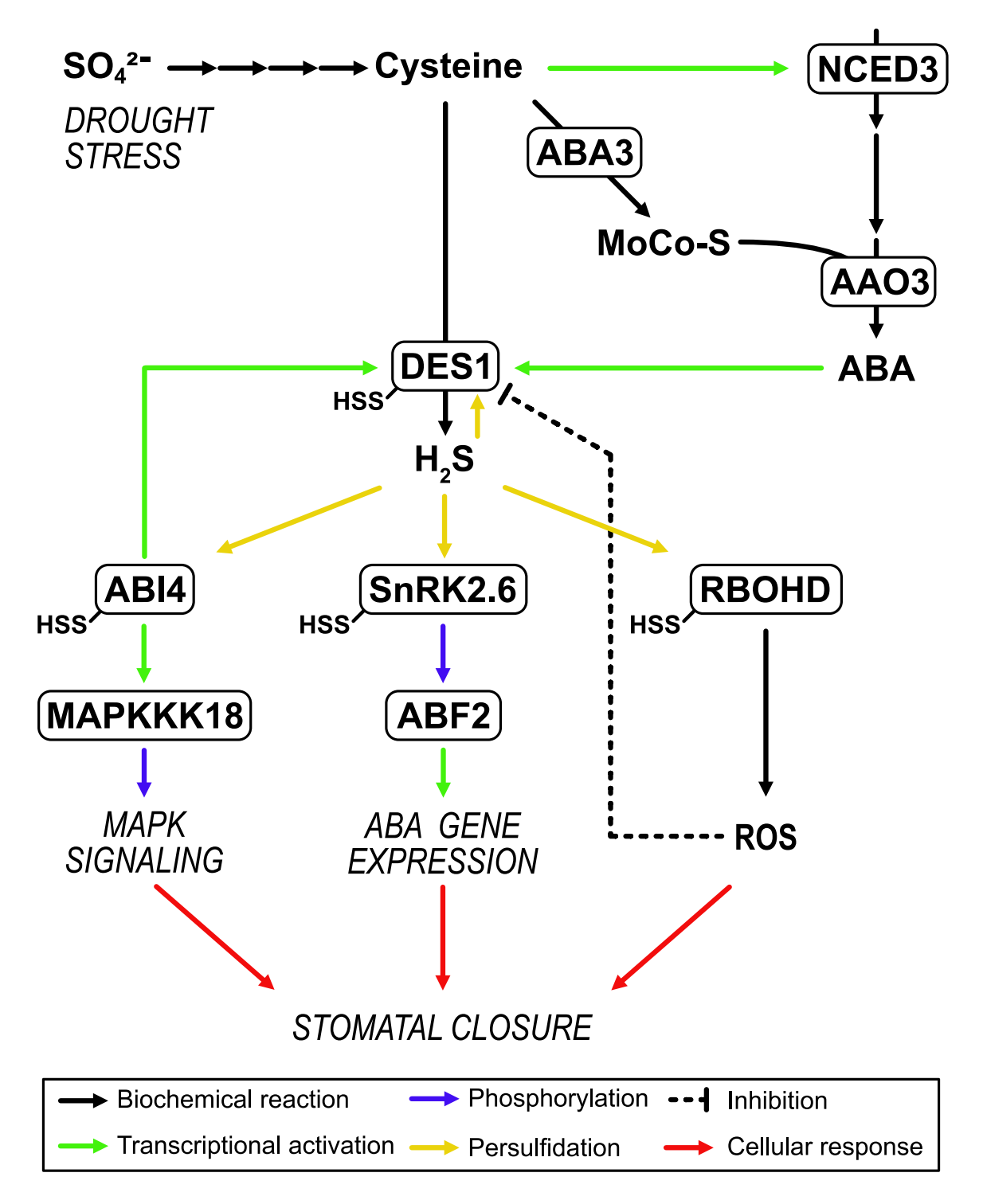


Figure 1.2: Representation of cysteine-mediated ABA signaling in guard cells

AAO3, abscisic aldehyde oxidase3; ABA, abscisic acid; ABA3, ABA deficient3; ABI4, ABA insensitive4; ABF2, ABA response binding factor 2; DES1, L-cysteine desulfhydrase1; MAPKKK18, mitogen-activated protein kinase kinase kinase18; NCED3, nine-cis-epoxycarotenoid dioxygenase3; RBOHD, respiratory burst oxidase homologue D; ROS, reactive oxygen species. Figure adapted from Ingrisano et al. (2023).

#### 1.6 Aim of this study

The aim of this dissertation was to elucidate the role of cysteine in plant stress signaling and how it acts as a so called infochemical. Using Arabidopsis seedling cultures, we monitored the proteomic response to artificially elevated cysteine levels and aimed to identify affected pathways. As defense responses were activated upon cysteine feeding, we further explored the contribution of compartment-specific cysteine synthesis during pathogen attack. Mitochondrial cysteine metabolism, in particular, seemed to play an important role during infection, which prompted us to take a closer look at this compartment. To that end, we aimed to establish mass spectrometry-based thermal proteome profiling (TPP) to identify novel mitochondrial proteins that interact with cysteine. Specifically, we looked for amino transferase candidate proteins and tested their ability to transaminate cysteine *in vitro*. In doing so, we aimed to identify a yet unknown enzyme that catalyzes the first step of the mitochondrial cysteine degradation pathway. In the end, this might also further our understanding of a potential cysteine-dependent protein persulfidation pathway. Moreover, we aspired to demonstrate the potential of TPP as a powerful tool for identifying protein metabolite interactions of genuine functional relevance.

#### 1.7 References

Alvarez, Consolacion; Calo, Leticia; Romero, Luis C.; Garcia, Irene; Gotor, Cecilia (2010): An O-Acetylserine(thiol)lyase Homolog with I-Cysteine Desulfhydrase Activity Regulates Cysteine Homeostasis in Arabidopsis. In: *Plant Physiol* 152 (2), S. 656–669. DOI: 10.1104/pp.109.147975.

Álvarez, Consolación; Ángeles Bermúdez, M.; Romero, Luis C.; Gotor, Cecilia; García, Irene (2012): Cysteine homeostasis plays an essential role in plant immunity. In: *New Phytol.* 193 (1), S. 165–177. DOI: 10.1111/j.1469-8137.2011.03889.x.

Amir, Rachel; Galili, Gad; Cohen, Hagai (2018): The metabolic roles of free amino acids during seed development. In: *Plant science : an international journal of experimental plant biology* 275, S. 11–18. DOI: 10.1016/j.plantsci.2018.06.011.

Batool, Sundas et al. (2018): Sulfate is Incorporated into Cysteine to Trigger ABA Production and Stomatal Closure. In: *Plant Cell* 30 (12), S. 2973–2987. DOI: 10.1105/tpc.18.00612.

Bermúdez, Maria Angeles; Páez-Ochoa, Maria Angeles; Gotor, Cecilia; Romero, Luis C. (2010): Arabidopsis S-sulfocysteine synthase activity is essential for chloroplast function and long-day light-dependent redox control. In: *Plant Cell* 22 (2), S. 403–416. DOI: 10.1105/tpc.109.071985.

Bittner, Florian; Oreb, Mislav; Mendel, Ralf R. (2001): ABA3 Is a Molybdenum Cofactor Sulfurase Required for Activation of Aldehyde Oxidase and Xanthine Dehydrogenase in Arabidopsis thaliana\*. In: *Journal of Biological Chemistry* 276 (44), S. 40381–40384. DOI: 10.1074/jbc.C100472200.

Blažević, Ivica et al. (2020): Glucosinolate structural diversity, identification, chemical synthesis and metabolism in plants. In: *Phytochemistry* 169, S. 112100. DOI: 10.1016/j.phytochem.2019.112100.

Bleecker, A. B.; Kende, H. (2000): Ethylene: a gaseous signal molecule in plants. In: *Annual review of cell and developmental biology* 16, S. 1–18. DOI: 10.1146/annurev.cellbio.16.1.1.

Campos, Ana Carolina A. L. et al. (2021): 1,135 ionomes reveal the global pattern of leaf and seed mineral nutrient and trace element diversity in Arabidopsis thaliana. In: *Plant J* 106 (2), S. 536–554. DOI: 10.1111/tpj.15177.

Chen, Sisi et al. (2020): Hydrogen Sulfide Positively Regulates Abscisic Acid Signaling through Persulfidation of SnRK2.6 in Guard Cells. In: *Molecular Plant* 13 (5), S. 732–744. DOI: 10.1016/j.molp.2020.01.004.

Considine, Michael J.; Foyer, Christine H. (2014): Redox regulation of plant development. In: *Antioxidants & redox signaling* 21 (9), S. 1305–1326. DOI: 10.1089/ars.2013.5665.

Cooper, Chris E.; Brown, Guy C. (2008): The inhibition of mitochondrial cytochrome oxidase by the gases carbon monoxide, nitric oxide, hydrogen cyanide and hydrogen sulfide: chemical mechanism and physiological significance. In: *Journal of Bioenergetics and Biomembranes* 40 (5), S. 533–539. DOI: 10.1007/s10863-008-9166-6.

Cummins, Ian; Dixon, David P.; Freitag-Pohl, Stefanie; Skipsey, Mark; Edwards, Robert (2011): Multiple roles for plant glutathione transferases in xenobiotic detoxification. In: *Drug Metabolism Reviews* 43 (2), S. 266–280. DOI: 10.3109/03602532.2011.552910.

Ernst, Laura et al. (2010): Sulphate as a xylem-borne chemical signal precedes the expression of ABA biosynthetic genes in maize roots. In: *J Exp Bot* 61 (12), S. 3395–3405. DOI: 10.1093/jxb/erq160.

Foyer, Christine Helen; Noctor, Graham (2011): Ascorbate and Glutathione: The Heart of the Redox Hub. In: *Plant Physiol* 155 (1), S. 2–18. DOI: 10.1104/pp.110.167569.

Galili, Gad; Avin-Wittenberg, Tamar; Angelovici, Ruthie; Fernie, Alisdair R. (2014): The role of photosynthesis and amino acid metabolism in the energy status during seed development. In: *Frontiers in Plant Science* 5, S. 447. DOI: 10.3389/fpls.2014.00447.

Gullner, Gábor; Komives, Tamas; Király, Lóránt; Schröder, Peter (2018): Glutathione S-Transferase Enzymes in Plant-Pathogen Interactions. In: *Frontiers in Plant Science* 9, S. 1836. DOI: 10.3389/fpls.2018.01836.

Hartmann, Michael; Zeier, Jürgen (2019): N-hydroxypipecolic acid and salicylic acid: A metabolic duo for systemic acquired resistance. In: *Curr. Opin. Plant Biol.* 50, S. 44–57. DOI: 10.1016/j.pbi.2019.02.006.

Hatzfeld, Yves; Maruyama, Akiko; Schmidt, Ahlert; Noji, Masaaki; Ishizawa, Kimiharu; Saito, Kazuki (2000): β-Cyanoalanine Synthase Is a Mitochondrial Cysteine Synthase-Like Protein in Spinach and Arabidopsis1. In: *Plant Physiol* 123 (3), S. 1163–1172. DOI: 10.1104/pp.123.3.1163.

Heeg, Corinna et al. (2008): Analysis of the Arabidopsis O-Acetylserine(thiol)lyase Gene Family Demonstrates Compartment-Specific Differences in the Regulation of Cysteine Synthesis. In: *Plant Cell* 20 (1), S. 168–185. DOI: 10.1105/tpc.107.056747.

Heinemann, Björn; Hildebrandt, Tatjana M. (2021): The role of amino acid metabolism in signaling and metabolic adaptation to stress-induced energy deficiency in plants. In: *J. Exp. Bot.* 72 (13), S. 4634–4645. DOI: 10.1093/jxb/erab182.

Hildebrandt, Tatjana M.; Nunes Nesi, Adriano; Araújo, Wagner L.; Braun, Hans-Peter (2015): Amino Acid Catabolism in Plants. In: *Molecular Plant* 8 (11), S. 1563–1579. DOI: 10.1016/j.molp.2015.09.005.

Höfler, Saskia et al. (2016): Dealing with the sulfur part of cysteine: four enzymatic steps degrade I-cysteine to pyruvate and thiosulfate in Arabidopsis mitochondria. In: *Physiologia Plantarum* 157 (3), S. 352–366. DOI: 10.1111/ppl.12454.

Holdorf, Meghan M. et al. (2012): Arabidopsis ETHE1 Encodes a Sulfur Dioxygenase That Is Essential for Embryo and Endosperm Development. In: *Plant Physiol.* 160 (1), S. 226–236. DOI: 10.1104/pp.112.201855.

Ingrisano, Rachele; Tosato, Edoardo; Trost, Paolo; Gurrieri, Libero; Sparla, Francesca (2023): Proline, Cysteine and Branched-Chain Amino Acids in Abiotic Stress Response of Land Plants and Microalgae. In: *Plants* 12 (19). DOI: 10.3390/plants12193410.

Kim, Tae-Houn; Böhmer, Maik; Hu, Honghong; Nishimura, Noriyuki; Schroeder, Julian I. (2010): Guard cell signal transduction network: advances in understanding abscisic acid, CO2, and Ca2+ signaling. In: *Annual review of plant biology* 61, S. 561–591. DOI: 10.1146/annurev-arplant-042809-112226.

Léon, Sébastien; Touraine, Brigitte; Briat, Jean-François; Lobréaux, Stéphane (2002): The AtNFS2 gene from Arabidopsis thaliana encodes a NifS-like plastidial cysteine desulphurase. In: *Biochem J* 366 (Pt 2), S. 557–564. DOI: 10.1042/BJ20020322.

Liu, Xiujie; Hu, Bin; Chu, Chengcai (2022): Nitrogen assimilation in plants: current status and future prospects. In: *Journal of genetics and genomics* = *Yi chuan xue bao* 49 (5), S. 394–404. DOI: 10.1016/j.jgg.2021.12.006.

Maughan, Spencer C. et al. (2010): Plant homologs of the Plasmodium falciparum chloroquine-resistance transporter, PfCRT, are required for glutathione homeostasis and stress responses. In: *Proceedings of the National Academy of Sciences of the United States of America* 107 (5), S. 2331–2336. DOI: 10.1073/pnas.0913689107.

May, M. J.; Leaver, C. J. (1994): Arabidopsis thaliana gamma-glutamylcysteine synthetase is structurally unrelated to mammalian, yeast, and Escherichia coli homologs. In: *Proceedings of the National Academy of Sciences of the United States of America* 91 (21), S. 10059–10063. DOI: 10.1073/pnas.91.21.10059.

Melotto, Maeli; Underwood, William; He, Sheng Yang (2008): Role of stomata in plant innate immunity and foliar bacterial diseases. In: *Annual Review of Phytopathology* 46, S. 101–122. DOI: 10.1146/annurev.phyto.121107.104959.

Moons, Ann (2005): Regulatory and functional interactions of plant growth regulators and plant glutathione S-transferases (GSTs). In: *Vitamins and hormones* 72, S. 155–202. DOI: 10.1016/S0083-6729(05)72005-7.

Moseler, Anna; Wagner, Stephan; Meyer, Andreas J. (2024): Protein persulfidation in plants: mechanisms and functions beyond a simple stress response. In: *Biological Chemistry* 405 (9-10), S. 547–566. DOI: 10.1515/hsz-2024-0038.

Nambara, Eiji; Marion-Poll, Annie (2005): Abscisic acid biosynthesis and catabolism. In: *Annual review of plant biology* 56, S. 165–185. DOI: 10.1146/annurev.arplant.56.032604.144046.

Noctor, Graham; Cohen, Mathias; Trémulot, Lug; Châtel-Innocenti, Gilles; van Breusegem, Frank; Mhamdi, Amna (2024): Glutathione: a key modulator of plant defence and metabolism through multiple mechanisms. In: *J Exp Bot* 75 (15), S. 4549–4572. DOI: 10.1093/jxb/erae194.

Noji, M.; Inoue, K.; Kimura, N.; Gouda, A.; Saito, K. (1998): Isoform-dependent differences in feedback regulation and subcellular localization of serine acetyltransferase involved in cysteine biosynthesis from Arabidopsis thaliana. In: *Journal of Biological Chemistry* 273 (49), S. 32739–32745. DOI: 10.1074/jbc.273.49.32739.

Pedras, M. S.; Okanga, F. I.; Zaharia, I. L.; Khan, A. Q. (2000): Phytoalexins from crucifers: synthesis, biosynthesis, and biotransformation. In: *Phytochemistry* 53 (2), S. 161–176. DOI: 10.1016/S0031-9422(99)00494-X.

Pedre, Brandán et al. (2023): 3-Mercaptopyruvate sulfur transferase is a protein persulfidase. In: *Nature chemical biology* 19 (4), S. 507–517. DOI: 10.1038/s41589-022-01244-8.

Pilon-Smits, Elizabeth A. H. et al. (2002): Characterization of a NifS-like chloroplast protein from Arabidopsis. Implications for its role in sulfur and selenium metabolism. In: *Plant Physiol* 130 (3), S. 1309–1318. DOI: 10.1104/pp.102.010280.

Ravanel, S.; Gakière, B.; Job, D.; Douce, R. (1998): The specific features of methionine biosynthesis and metabolism in plants. In: *Proceedings of the National Academy of Sciences of the United States of America* 95 (13), S. 7805–7812. DOI: 10.1073/pnas.95.13.7805.

Ravanel, Stéphane et al. (2004): Methionine metabolism in plants: chloroplasts are autonomous for de novo methionine synthesis and can import S-adenosylmethionine from the cytosol. In: *Journal of Biological Chemistry* 279 (21), S. 22548–22557. DOI: 10.1074/jbc.M313250200.

Romero, Luis C.; Aroca, M. Ángeles; Laureano-Marín, Ana M.; Moreno, Inmaculada; García, Irene; Gotor, Cecilia (2014): Cysteine and Cysteine-Related Signaling Pathways in Arabidopsis thaliana. In: *Molecular Plant* 7 (2), S. 264–276. DOI: 10.1093/mp/sst168.

Scuffi, Denise; Álvarez, Consolación; Laspina, Natalia; Gotor, Cecilia; Lamattina, Lorenzo; García-Mata, Carlos (2014): Hydrogen Sulfide Generated by I-Cysteine Desulfhydrase Acts Upstream of Nitric Oxide to Modulate Abscisic Acid-Dependent Stomatal Closure. In: *Plant Physiol* 166 (4), S. 2065–2076. DOI: 10.1104/pp.114.245373.

Shen, Jie et al. (2020): Persulfidation-based Modification of Cysteine Desulfhydrase and the NADPH Oxidase RBOHD Controls Guard Cell Abscisic Acid Signaling. In: *Plant Cell* 32 (4), S. 1000–1017. DOI: 10.1105/tpc.19.00826.

Shimazaki, Ken-ichiro; Doi, Michio; Assmann, Sarah M.; Kinoshita, Toshinori (2007): Light regulation of stomatal movement. In: *Annual review of plant biology* 58, S. 219–247. DOI: 10.1146/annurev.arplant.57.032905.105434.

Szabados, László; Savouré, Arnould (2010): Proline: a multifunctional amino acid. In: *Trends in Plant Science* 15 (2), S. 89–97. DOI: 10.1016/j.tplants.2009.11.009.

Takahashi, Hideki; Kopriva, Stanislav; Giordano, Mario; Saito, Kazuki; Hell, Rüdiger (2011): Sulfur Assimilation in Photosynthetic Organisms: Molecular Functions and Regulations of Transporters and Assimilatory Enzymes. In: *Annual review of plant biology* 62 (Volume 62, 2011), S. 157–184. DOI: 10.1146/annurev-arplant-042110-103921.

Torres Zabala, Marta de; Bennett, Mark H.; Truman, William H.; Grant, Murray R. (2009): Antagonism between salicylic and abscisic acid reflects early host–pathogen conflict and moulds plant defence responses. In: *Plant J* 59 (3), S. 375–386. DOI: 10.1111/j.1365-313X.2009.03875.x.

Torres-Zabala, Marta de et al. (2007): *Pseudomonas syringae* pv. *tomato* hijacks the *Arabidopsis* abscisic acid signalling pathway to cause disease. In: *The EMBO Journal* 26 (5), 1434-1443. DOI: 10.1038/sj.emboj.7601575.

Toyota, Masatsugu et al. (2018): Glutamate triggers long-distance, calcium-based plant defense signaling. In: *Science* 361 (6407), S. 1112–1115. DOI: 10.1126/science.aat7744.

Turowski, Valeria R.; Busi, Maria V.; Gomez-Casati, Diego F. (2012): Structural and functional studies of the mitochondrial cysteine desulfurase from Arabidopsis thaliana. In: *Molecular Plant* 5 (5), S. 1001–1010. DOI: 10.1093/mp/sss037.

Ullmann, P.; Gondet, L.; Potier, S.; Bach, T. J. (1996): Cloning of Arabidopsis thaliana glutathione synthetase (GSH2) by functional complementation of a yeast gsh2 mutant. In: *European Journal of Biochemistry* 236 (2), S. 662–669. DOI: 10.1111/j.1432-1033.1996.00662.x.

van Veen, Hans; Triozzi, Paolo Maria; Loreti, Elena (2024): Metabolic strategies in hypoxic plants. In: *Plant Physiol* 197 (1). DOI: 10.1093/plphys/kiae564.

Watanabe, Mutsumi et al. (2013): Comprehensive dissection of spatiotemporal metabolic shifts in primary, secondary, and lipid metabolism during developmental senescence in Arabidopsis. In: *Plant Physiol* 162 (3), S. 1290–1310. DOI: 10.1104/pp.113.217380.

Weiner, Joshua J.; Peterson, Francis C.; Volkman, Brian F.; Cutler, Sean R. (2010): Structural and functional insights into core ABA signaling. In: *Current Opinion in Plant Biology* 13 (5), S. 495–502. DOI: 10.1016/j.pbi.2010.09.007.

Yamaguchi, Y.; Nakamura, T.; Kusano, T.; Sano, H. (2000): Three Arabidopsis genes encoding proteins with differential activities for cysteine synthase and beta-cyanoalanine synthase. In: *Plant Cell Physiol* 41 (4), S. 465–476. DOI: 10.1093/pcp/41.4.465.

Zhou, Mingjian et al. (2021): Hydrogen sulfide-linked persulfidation of ABI4 controls ABA responses through the transactivation of MAPKKK18 in Arabidopsis. In: *Molecular Plant* 14 (6), S. 921–936. DOI: 10.1016/j.molp.2021.03.007.

#### 2 News about amino acid metabolism in plant-microbe interactions

**Moormann, Jannis**; Heinemann, Björn; Hildebrandt, Tatjana M. (2022): News about amino acid metabolism in plant microbe interactions. *Trends in Biochemical Sciences* 47 (10). S. 839 – 850. DOI: 10.1016/j.tibs.2022.07.001

#### 2.1 Abstract

Plants constantly get into contact with a diverse mix of pathogenic and beneficial microbes. The ability to distinguish between them and respond appropriately is essential for plant health. Here we review recent progress in understanding the role of amino acid sensing, signaling, transport, and metabolism during plant-microbe interactions. Biochemical pathways converting individual amino acids into active compounds were recently elucidated and comprehensive large-scale approaches brought amino acid sensors and transporters into focus. These findings show that plant central amino acid metabolism is closely interwoven with stress signaling and defense responses at various levels. The individual biochemical mechanisms and the interconnections between the different processes are just beginning to emerge and might serve as a foundation for new plant protection strategies.

# 2.2 Plant amino acid metabolism provides signaling molecules, defense compounds and nutrients to shape interactions with microbes

In a natural environment outside controlled lab conditions plants interact with complex microbial communities. Microbes usually benefit from the rich supply of organic compounds including amino acids in the vicinity of a plant. Some might manipulate plant metabolism to access nutrients, either in return for some kind of service during mutualistic interactions of without benefit for the plant in commensals, whereas pathogens even cause damage to the plant (Figure 2.1). In any case, microbes need to evade or suppress immune reactions and the plant needs to discriminate between potentially harmful and beneficial interactions to react accordingly. The plant's set of measures may include withdrawing nutrients to starve pathogens (for example, see (Mur et al. 2017)) or supplying a specific set of compounds to establish beneficial interactions (for example, see (Lanfranco et al. 2018)). In the case of a pathogen attack, plants also have to activate appropriate defense responses and to alert noneffected parts of the plant about impending danger to restrict pathogen growth (Zhou & Zhang 2020). Here we discuss how plant amino acid metabolism is involved in shaping these different interactions between plants and microbes. Recent studies shed light on interspecies communication during first contact and demonstrated how plants use amino acids to produce specialized metabolites as a means to selectively promote proliferation of beneficial microbes.

Amino acid transport is required for nutrient exchange and in combination with specific receptors might be involved in amino acid sensing and signaling mechanisms during interaction with microbes. Amino acid metabolism is also be crucial for immune signaling within plants during establishment of a systemic immune reaction.

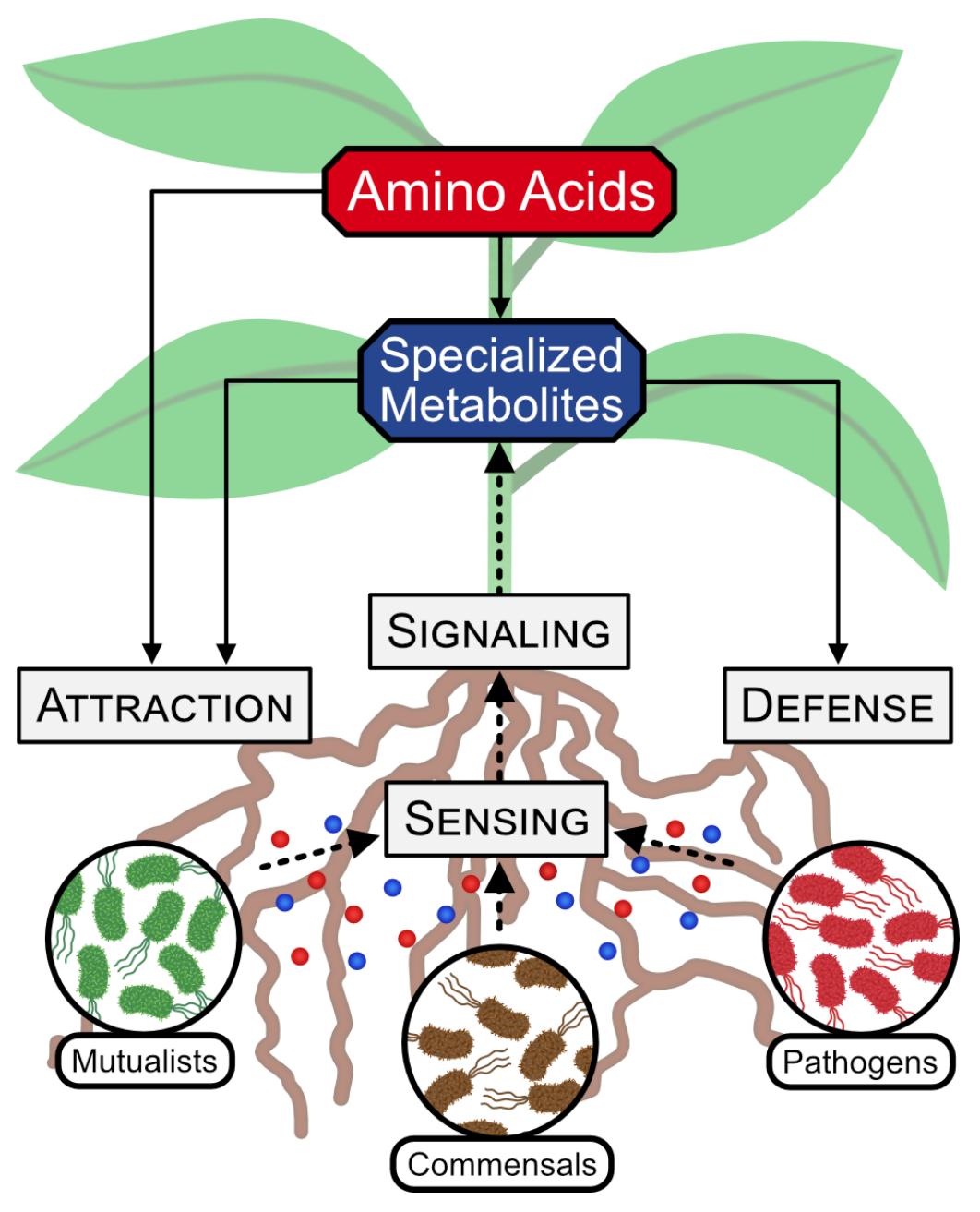


Figure 2.1: Plant amino acid metabolism provides active compounds for interacting with microbes at different levels

Plants interact with a multitude of microbes, which can be categorized according to their effect on plant health into mutualists (beneficial) commensals (neutral) and pathogens (detrimental). Plants convert amino acids into specialized metabolites that either act as signaling molecules within the plant or are exuded to shape the composition of the microbiome in favor of the plant. The microbes in turn require plant amino acids as a source of nutrients. Experimental results indicate that plants can sense specific patterns in changes in amino acid metabolism and interpret them as a fingerprint of a lurking pathogen. The mechanisms of amino acid sensing and signaling are however largely unknown.

### 2.3 Aromatic amino acids are converted to a set of specialized metabolites involved in shaping the plant microbiome

The aromatic amino acids Tyr, Phe, and Trp are synthesized in the plastids and also in the cytosol by the shikimate pathway (Lynch & Dudareva 2020). In addition to being incorporated into proteins they serve as precursors for a diverse set of specialized metabolites (Figure 2.2) (Yokoyama et al. 2021). A considerable share of carbon flow (≥ 30%) is directed through the shikimate pathway to produce pigments, defense compounds and the cell wall component lignin (Maeda & Dudareva 2012). Plant specialized metabolites can act as nutrient source, signaling molecules or toxins for individual microbial strains thereby shaping the overall composition of the **microbiome** (see Glossary) (Jacoby et al. 2020; Pascale et al. 2020). Recently there has been some significant progress in understanding both, the regulation of aromatic amino acid metabolism and the role of individual aromatic phytochemicals in coordinating plant microbe interactions.

The synthesis rates for the individual aromatic amino acids are regulated by product inhibition of the respective committed step, which is a common scheme in amino acid synthesis in plants (Lynch & Dudareva 2020; Maeda & Dudareva 2012). However, in addition the entry reaction of the shikimate pathway catalyzed by 3-deoxy-d-arabino-heptulosonate 7-phosphate synthase (DHS) is controlled via a complex pattern of allosteric feedback inhibition in a tissue-specific manner (Yokoyama et al. 2021). Notably, all the three DHS isoforms present in Arabidopsis are strongly inhibited by caffeate, an intermediate in phenylpropanoid biosynthesis from Phe, indicating that the flux through the shikimate pathway in general is adjusted to meet the demands of specialized metabolite production. A genome-wide **ribosome profiling** approach revealed that during **effector-triggered immunity (ETI)** Arabidopsis plants specifically induce the biosynthesis pathways for aromatic amino acids and derived specialized metabolites on the level of translation in coordination with increased transcription rates as an additional layer of upregulation (Yoo et al. 2020). Thus, the metabolism of aromatic amino acids is an important factor in the interaction between plants and microbes and serves as a toolbox for the production of a variety of tailored active compounds.

While the protective function of phytoalexins derived from aromatic amino acids during pathogen attack is well established, their role in recruiting beneficial microbes is just beginning to become clear (Jacoby et al. 2020; Jacoby et al. 2021). Coumarins are polar phenolic compounds produced from Phe via the general phenylpropanoid pathway and they are ubiquitious in plants (Stringlis et al. 2019). The synthesis pathway for two coumarins involved in plant-microbe interactions, fratexin and the redox-active sideretin has been clarified only recently (Rajniak et al. 2018; Siwinska et al. 2018). In addition, a suite of new publications has contributed to connecting two of the well established physiological functions of coumarins,

namely improving bioavailability of iron in alkaline soils and defense against pathogens (Figure 2.2B) (Stringlis et al. 2019; Tsai & Schmidt 2017). Using different coumarin-deficient Arabidopsis mutant lines in combination with either selected pathogenic and mutualistic microbes or a synthetic microbial community they revealed the role of coumarins in shaping the root microbiome to improve plant iron nutrition. Specific coumarins are secreted by the roots of Arabidopsis plants, which change the composition of the root microbiome by selectively inhibiting the growth of pathogenic microbes but not beneficial strains (Stringlis et al. 2018; Voges et al. 2019; Harbort et al. 2020). This effect is induced in iron-deficient soils and seems to involve redox-mediated toxicity (Voges et al. 2019).

Camalexin is an antifungal sulfur-containing indolic compound synthesized from Trp. It is specific for *Brassicacea* and the most prominent phytoalexin in Arabidopsis (Glawischnig 2007). Trp metabolism also produces a series of additional specialized metabolites including indolic glucosinolates and the auxin indole-3-acetic acid via common intermediates (Pastorczyk et al. 2020). Efficient camalexin synthesis without release of active intermediates is achieved by formation of a camalexin biosynthetic **metabolon**, a cytosolic protein complex attached to the endoplasmatic reticulum (Mucha et al. 2019). The pleiotropic drug resistance transporters PEN3 and PDR12 function redundantly to mediate camalexin secretion (He et al. 2019). Camalexin synthesis in the roots is required for recruiting mutualistic microbes to the **rhizosphere** and, interestingly, it is also prerequisite for actually receiving growth benefits by potentially growth-promoting bacterial strains (Figure 2.2B) (Koprivova et al. 2019). The mechanism of this interaction is yet to be discovered.

Poaceae such as maize, wheat and rye can synthesize large quantities of benzoxazinoids from the Trp precursor indol to regulate belowground as well as aboveground biotic interactions. A number of recent studies highlighted the pivotal role of these heteroaromatic metabolites in shaping the rhizosphere microbiota (Hu et al. 2018; Cotton et al. 2019; Kudjordjie et al. 2019). Benzoxazinoids serve as toxins towards pathogens and in addition as chemoattractants for beneficial microbes affecting both, bacterial and fungal root-associated communities. Soil conditioning even persisted into the next growing season and determined biotic interactions and plant performance in the next generation (Hu et al. 2018).

Plants potentially produce hundreds of thousands of different metabolites, and most of them have not been characterized yet (Jacobowitz & Weng 2020). Even with a focus on compounds derived from amino acids plant specialized metabolism is highly complex and has the potential to provide a high level of specificity during plant microbe interactions. Due to the high diversity of metabolites across plant species research on different model and non-model organisms holds the promise of new discoveries.

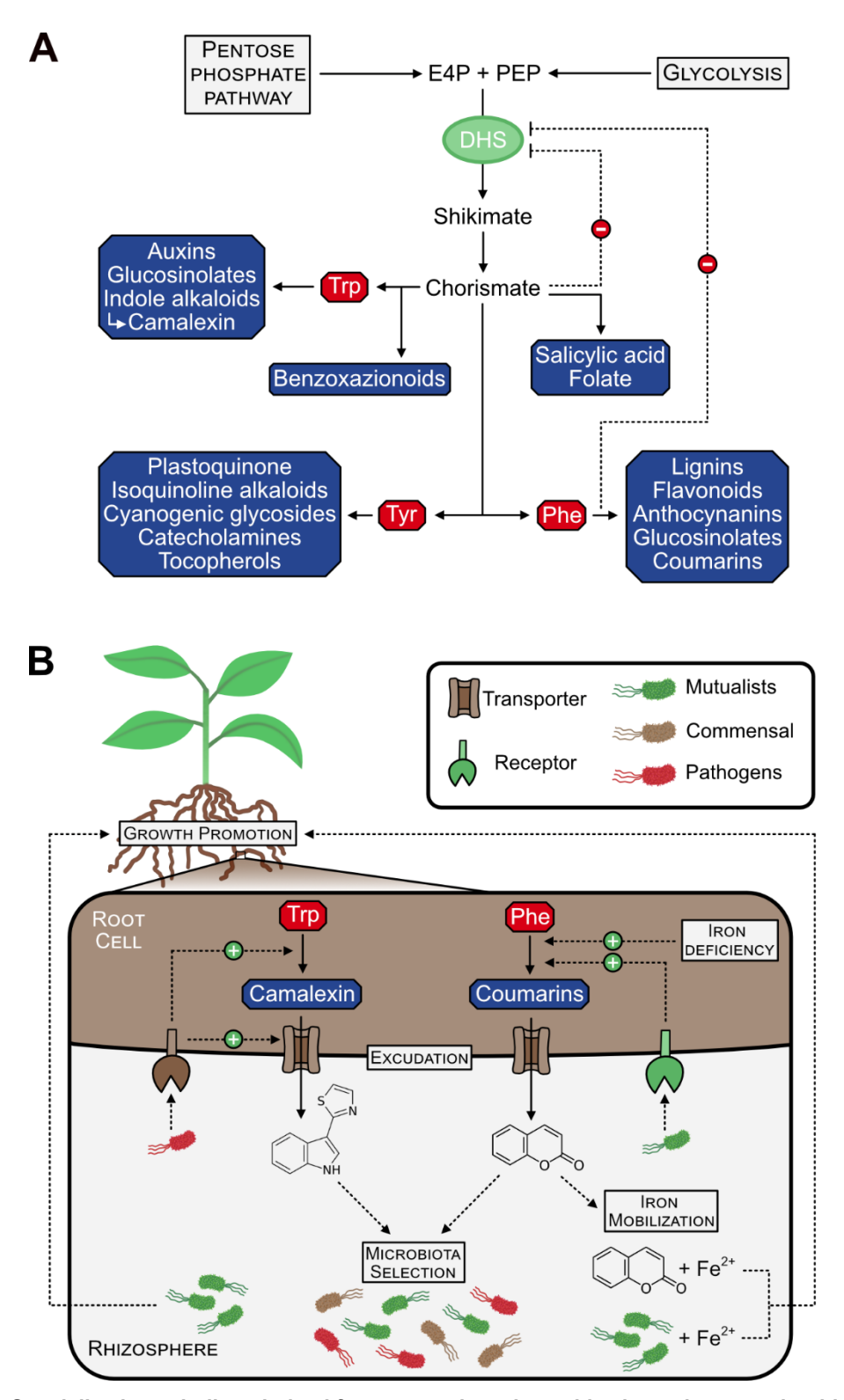


Figure 2.2: Specialized metabolites derived from aromatic amino acids shape the root microbiome

**A**. The shikimate pathway produces aromatic amino acids and a diverse set of specialized metabolites. The initial step catalyzed by 3-deoxy-d-arabino-heptulosonate 7-phosphate synthase (DHS) is regulated via feedback inhibition by several intermediates in a complex manner (dashed lines) (Yokoyama et al. 2021). **B**. Camalexin and coumarin shape the root microbiome in Arabidopsis by selectively inhibiting growth of pathogenic microbes. Camalexin synthesis from Trp and its secretion via the pleiotropic drug transporters PEN3 and PDR12 are induced in a coordinated fashion by MAP kinases and the downstream WRKY33 transcription factor upon pathogen recognition (He et al. 2019). During iron starvation probiotic rhizobacteria induce conversion of Phe to coumarins and their exudation into the rhizosphere via the transcription factor MYB72 (Stringlis et al. 2018). Coumarins as well as coumarin-tolerant microbes increase the bioavailability of iron in iron-limited alkaline soils (Stringlis et al. 2018; Voges et al. 2019; Harbort et al. 2020). DHS, 3-deoxy-d-arabino-heptulosonate 7-phosphate synthase; E4P, Erythrose-4-phosphate; PEP, phosphoenolpyruvate.

### 2.4 Amino acid transport controls nutrient exchange between plants and microbes

When a plant pathogen starts proliferating in the apoplast it is usually nutrient starved and depends on rapid assimilation of nutrients from the host. The plant in turn may reallocate resources for defense or withdraw nutrients from the site of infection. Thus, adaptations in plant nitrogen metabolism upon pathogen attack represent the combined effects of the plant's defense strategy and manipulation by the pathogen to increase nutrient availability. Plants exude 15% of assimilated nitrogen, and amino acids are a major nitrogen currency (Venturi & Keel 2016). Microbial **chemoreceptors** recognize a broad variety of amino acids and direct the microbes to the nutrient-rich niches surrounding plant roots (Yang et al. 2015). The ability to use amino acids supplied by the host plant for nutrition might be crucial for establishing symbiotic interactions. Three independent screening approaches identified **auxotrophy** for specific amino acids as a factor impairing the interaction of growth-promoting Pseudomonas strains with their host Arabidopsis (Cheng et al. 2017; Cole et al. 2017; Liu et al. 2010).

Amino acid exudation by the plant requires transport across several membranes (i) between apoplast and cytoplasm for exudation or uptake (ii) across membranes of intracellular compartments involved in amino acid synthesis, metabolism and storage (chloroplasts, mitochondria, vacuole), (iii) between different cells and plant organs to meet the increased local demand caused by microbial interactions (Figure 2.3). The Arabidopsis genome contains about 100 putative amino acid transporters belonging to three major families (Tegeder & Hammes 2018; Dhatterwal et al. 2021). Only about 20 % of them have been functionally characterized so far (Sonawala et al. 2018).

While transporters of the AAAP (amino acid/auxin permease) and APC (amino acid polyamine organocation) families and their role in amino acid uptake and secretion by the roots have been known for some time (Pratelli & Pilot 2014; Dinkeloo et al. 2018), the UMAMIT (USUALLY MULTIPLE ACIDS MOVE IN AND OUT TRANSPORTERS) family is currently the new center of interest. UMAMITs were originally identified as nodulins required for symbiotic interactions of **rhizobia** with legumes (Gamas 1996; Zhao et al. 2021). Zhao et al. (2021) characterized all 47 UMAMIT genes and proteins found in Arabidopsis in detail including tissue and subcellular localization as well as amino acid transport properties. Their results identify a set of particularly stress responsive UMAMITs as likely candidates for involvement in plant microbe interactions. UMAMIT14 and UMAMIT18 mediate the radial transport of amino acids in roots and their secretion to the soil (Besnard et al. 2016). The transcription factor bZIP11 is required for the induction of these two and an additional three UMAMITs (Cheng et al. 2017; Liu et al. 2010; Sonawala et al. 2018) alongside several nitrate and ammonium transporters and might be targeted by pathogens to secure access to nutrients from their hosts (Prior et al. 2021).

In addition, the stress-responsive W-BOX motif has recently been identified in the promotor regions of 40 amino acid transporter genes indicating that regulation by WRKY transcription factors could also play a role (Dhatterwal et al. 2021). Based on the same promotor profiling approach induction by the phytohormone salicylic acid can be postulated for 34 amino acid transporters. In the systemic (non-infected) leaves of Arabidopsis plants locally infected with Pseudomonas syringae the enzymatic pathways catalyzing amino acid synthesis are downregulated on a transcriptional level (Schwachtje et al. 2018). The lowered free contents in most amino acids might help to protect the non-infected leaves by reducing their nutritional value and thus making them less attractive for colonization by pathogens. The role of amino acid exudation in shaping the biochemical ecology of the rhizosphere is frequently discussed in recent reviews (Sasse et al. 2018; Kim et al. 2021; Dinkeloo et al. 2018; Sonawala et al. 2018) but not many mechanistic details are known yet. Plant amino acid transporters might be targeted by microbes to enhance nutrient availability and on the other hand could also be controlled by the plant immune system in order to selectively feed or starve beneficial or pathogenic microbes, respectively. Thus, an important aspect of future research efforts will be to unravel the connections between plant amino acid transporters and resistance or susceptibility to pathogens and pests.

## 2.5 Specific perturbations in amino acid homeostasis constitutively activate plant defenses

Several lines of evidence indicate that plants monitor their amino acid status and interpret specific alterations in metabolic activity, local amino acid concentrations or transport activities across membranes as a signature of an attacking pathogen (Figure 2.3A, (Sonawala et al. 2018)). Overexpression of the amino acid exporters UMAMIT14 and Glutamine dumper 1 (GDU1), or the importer CATIONIC AMINO ACID TRANSPORTER 1 (CAT1) leads to constitutive induction of immune signaling in Arabidopsis (Besnard et al. 2021; Liu et al. 2010; Yang et al. 2015). In contrast, knockout of LYSINE HISTIDINE TRANSPORTER1 (LHT1) or UMAMIT5 (WAT1) increases plant resistance towards a broad spectrum of pathogens (Liu et al. 2010; Denancé et al. 2013). However, since both of these amino acid transporters also accept additional substrates such as auxin or the ethylene precursor aminocyclopropane-1-carboxylic acid (ACC), a disturbance in hormone signaling might be the primary cause for activating defense responses in the knockout lines (Denancé et al. 2013; Shin et al. 2015).

An **autoimmune phenotype** has also been reported for mutant lines with different modifications in amino acid metabolic enzymes. An **RNAseq** approach recently identified the mitochondrial branched-chain aminotransferase BCAT1 as a potential regulator of rust infection in wheat (Corredor-Moreno et al. 2021). Knockout bcat1 mutants had moderately

increased levels of several amino acids and activated a systemic immune response. Transgenic Arabidopsis plants overexpressing pepper asparagine synthetase 1 exhibit enhanced resistance to *Pseudomonas syringae* pv. tomato DC3000 and *Hyaloperonospora arabidopsidis* (Hwang et al. 2011).

Cysteine can be synthesized and also metabolized in several different compartments of a plant cell and this compartmentalization seems to be important for signaling functions during abiotic stress (Hildebrandt et al. 2015; Heinemann & Hildebrandt 2021). Recent results indicate that specific pathways in cysteine metabolism might also be relevant for biotic interactions. Overexpression of the mitochondrial cysteine desulfurase NFS1, which degrades cysteine to provide sulfur during FeS cluster synthesis, results in constitutive upregulation of defenserelated genes and increased resistance against *Pseudomonas syringae* (Fonseca et al. 2020). In contrast, knockout of the cytosolic cysteine desulfhydrase DES1 leads to an autoimmune phenotype whereas knockout lines for OAS1 involved in cysteine synthesis in the cytosol are more susceptible to *Pseudomonas syringae* (Álvarez et al. 2012). Taken together these results indicate that increased cysteine degradation in the mitochondria and decreased cysteine degradation in the cytosol both induce a biotic stress response. Homoserine accumulation in the chloroplast due to homoserine kinase deficiency triggers a presently unknown mechanism of downy mildew resistance in Arabidopsis (van Damme et al. 2009), whereas threonine accumulation renders the plants unsuitable as an infection substrate for the adapted biotrophic pathogen Hyaloperonospora arabidopsidis without activating defense responses (Stuttmann et al. 2011). Intriguingly, several other defects in amino acid metabolic pathways or transporters also lead to altered amino acid steady state levels without an apparent effect on immune signaling (Dinkeloo et al. 2018). Even in those lines developing an autoimmune phenotype, there is no clear common trend for any specific amino acids being consistently altered. Thus, local changes in intracellular compartments or specific intermediates of amino acid metabolic pathways might be required to trigger a stress response.

Also, a sudden increase in exogenous amino acids could be interpreted by the plant as a common signature of pathogen induced cell damage or increased export stimulated by hungry microbes and thus be a useful alarm signal. Exogenous treatment with different amino acids has been shown to elicit immune reactions in Arabidopsis and rice (Goto et al. 2019; Kadotani et al. 2016). A diverse set of damage-associated molecular patterns (DAMPs) including extracelluar ATP has already been identified in Arabidopsis (Thoms et al. 2021). DAMPs are molecules that are normally localized inside the plant cell and elicit an immune response by binding to extracellular receptors. In combination with microbe-associated molecular patterns (MAMPs) they can elicit a robust and highly specific local immune response (Zhou et al. 2020). Some amino acids might be added to the list in the near future (see also next paragraph). Exploring the mechanistic details of amino acid sensing in plants and its role during

plant-microbe interactions will be a challenging task but also offers great potential for identifying central hubs in the integration of plant primary metabolism with biotic stress signaling.

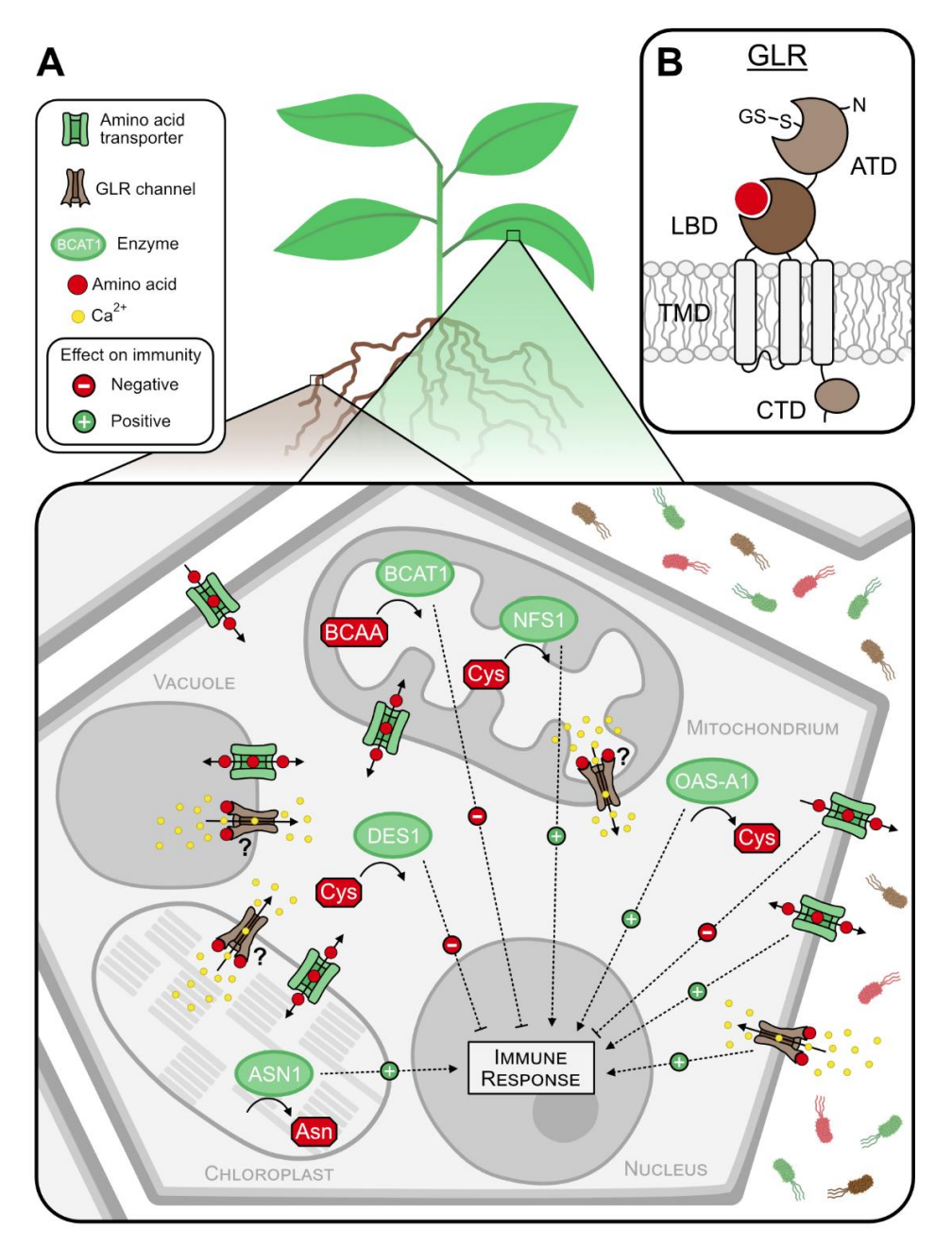


Figure 2.3: Perturbations in amino acid transport and metabolism can trigger immune signaling

**A**. Specific features in the structure of plant glutamate like receptors provide a basis for a high ligand diversity and additional regulation via glutathionlyation of a cysteine residue in the cleft of the aminoterminal domain. **B**. Amino acid metabolism within the plant and exudation into the apoplast requires transport across several membranes. A positive or negative role in plant immunity has been postulated for several amino acid transporters and also for individual enzymes involved in amino acid metabolism based on the suppression or induction of a pathogen response in mutant plants. GLRs might be involved in detecting local fluctuations in specific amino acids and triggering an immune response. The mechanism of amino acid sensing and signaling during plant-microbe interactions is largely unclear. ASN1, asparagine synthetase 1; ATD, aminoterminal domain; BCAA, branched-chain amino acids; BCAT1, branched-chain aminotransferase 1; CTD, carboxyterminal domain; DES1, cysteine desulfhyrease 1; GLR, glutamate receptor-like channel; GS-S-, glutathionylated cysteine residue; LBD, ligand-binding domain; NFS1, nitrogen fixation S-like 1; OAS-A1, O-acetylserine(thiol)lyase A1; TMD, transmembrane domain.

### 2.6 Amino acid activated calcium channels (GLRs) mediate amino acid sensing and signaling in plants

Based on a detailed transcriptome study a set of 39 core immunity response genes was recently defined, which are common to the initial signaling outputs during **pattern-triggered immunity (PTI)** establishment in response to a broad range of patterns in Arabidopsis (Bjornson et al. 2021). Strikingly, this set includes two genes for glutamate receptor-like calcium channels (GLRs). GLR proteins, which structurally resemble the neuronal glutamate receptors from metazoans, are involved in long-distance plant defense signaling in response to insect feeding (Figure 2.3B) (Toyota et al. 2018; Qiaolin et al. 2020). In contrast to their animal counterpart plant GLRs are activated by a broad range of amino acids including Glu, Gly, Ala, Asn, Ser, Cys, Met and the tripeptide glutathione (Alfieri et al. 2020) indicating a more general role in the perception of extracellular amino acids. The structural basis for this ligand diversity has been identified using **X-ray crystallography** and **single-particle cryo-EM**, which also revealed some additional plant specific features in GLR architecture and regulation (Figure 2.3B) (Alfieri et al. 2020; Green et al. 2021).

The Arabidopsis genome contains 20 GLR homologs belonging to three clades (Lam et al. 1998). Most of them are predicted to be localized in the plasma membrane or the vacuole (Wudick et al. 2018), but AtGLR3.4 was also detected in chloroplasts and a splice variant of AtGLR3.5 in the inner mitochondrial membrane (Teardo et al. 2011; Teardo et al. 2015). Specific isoforms have been implicated in several physiological processes in addition to longdistance wound signaling such as germination (Cheng et al. 2018), root growth (Singh et al. 2016), pollen tube growth (Michard Erwan et al. 2011) and hypocotyl elongation (Dubos et al. 2003). A general function of GLRs in mediating the calcium influx triggered by selected microbial epitopes has been postulated based on a pharmacological inhibitor study (Kwaaitaal et al. 2011). There is some experimental evidence indicating a role of GLR3.3 and GLR3.6 (the calcium channels required for systemic wound signaling) in plant microbe interactions (Li et al. 2013; Manzoor et al. 2013; Goto et al. 2019). However, both GLRs in the core set of immunity response genes belong to clade 2, which has not been studied in detail so far (Bjornson et al. 2021). The authors demonstrated a functional relevance of clade 2 GLRs in plant immunity by means of a glr2.7 2.8 2.9 triple mutant. Mutant plants were highly susceptible to the bacterial pathogen Pseudomonas syringae and showed a significantly impaired increase in cytosolic Ca<sup>2+</sup> concentration after elicitor treatment but not in response to salt or cold.

Since calcium signaling is involved in many different processes in the plant (Resentini et al. 2021; Tian et al. 2020) identification of the downstream components of the GLR signaling cascade will be crucial for understanding its role in plant microbe interactions. The 20 GLR isoforms with their potentially broad ligand spectrum may allow the plant to distinguish between

different kinds of threats. Amino acid sensing by GLRs might be the mechanism behind observations that specific modifications in amino acid homeostasis induce autoimmune reactions (discussed in the previous paragraph). If localization in membranes of subcellular compartments is confirmed maybe with splice variants of additional GLR isoforms it is tempting to speculate even about a role in intracellular amino acid sensing and signaling during plant-microbe interactions.

#### 2.7 Lysine metabolism is essential for systemic immune signaling

In the last decade, the basic amino acid Lys has attracted research interest as a precursor of a key signaling molecule in plant pathogen response. Pathogen attack elicits local immune responses but it also initiates signaling to the non-infected parts of the plant to establish systemic acquired resistance (SAR) (Zeier 2021). Extensive changes in gene transcription triggered during SAR put the plant immune system in a state of alert to prevent the pathogen from spreading over the entire foliage (Bernsdorff et al. 2016). The search for the mobile immune signal required for SAR induction recently culminated in the identification of Nhydroxypipecolic acid (NHP) and the final step of its synthesis pathway from Lys (Chen et al. 2018; Hartmann et al. 2018). All three enzymes required for converting Lys to NHP are strongly induced by biotic stress and have been shown to be essential for SAR induction by means of Arabidopsis mutant lines (Hartmann & Zeier 2018). In a first reaction, the aminotransferase ALD1 (AGD2-LIKE DEFENSE RESPONSE PROTEIN1) deaminates the α-amino group of L-Lys to generate α-ketocaproic acid (KAC), which is unstable and spontaneously reacts to 1,2dehydropipecolic acid (1,2-DP) and its tautomer 2,3-DP in planta (Figure 2.4; (Návarová et al. 2012; Hartmann et al. 2017; Ding et al. 2016). DP is then reduced to pipecolic acid (Pip) by the NAD(P)H-dependent ketimine reductase SAR-DEFICIENT4 (SARD4) (Hartmann et al. 2017; Ding et al. 2016). Pip accumulates in the leaves of infected plants and external application induces systemic immune reactions (Návarová et al. 2012). However, Nhydroxylation of Pip to NHP by FLAVIN-DEPENDENT MONOOXYGENASE1 (FMO1) is prerequisite for this function indicating that NHP is the active plant hormone mediating longdistance immune signaling during pathogen defense (Cheng et al. 2018; Hartmann et al. 2018).

Defense responses require many resources, so their constitutive induction would impair growth and reproduction (Huot et al. 2014). Therefore, the content of active immune signaling molecules must be tightly regulated by fine-tuning their synthesis rates as well as their inactivation (Zeier 2021). Recently, four independent studies simultaneously showed that UGT76B1 glucosylates NHP to produce the inactive NHP–N–O-glucoside (NHPG) (Bauer et al. 2021; Cai et al. 2021; Mohnike et al. 2021; Holmes et al. 2021). Notably, UGT76B1 also accepts the defense hormone salicylic acid (SA) as a substrate (Bauer et al. 2021; Cai et al.

2021). The metabolic pathways of SA and NHP share multiple common regulatory elements, and both molecules work in concert during SAR induction (Hartmann & Zeier 2019; Zeier 2021).

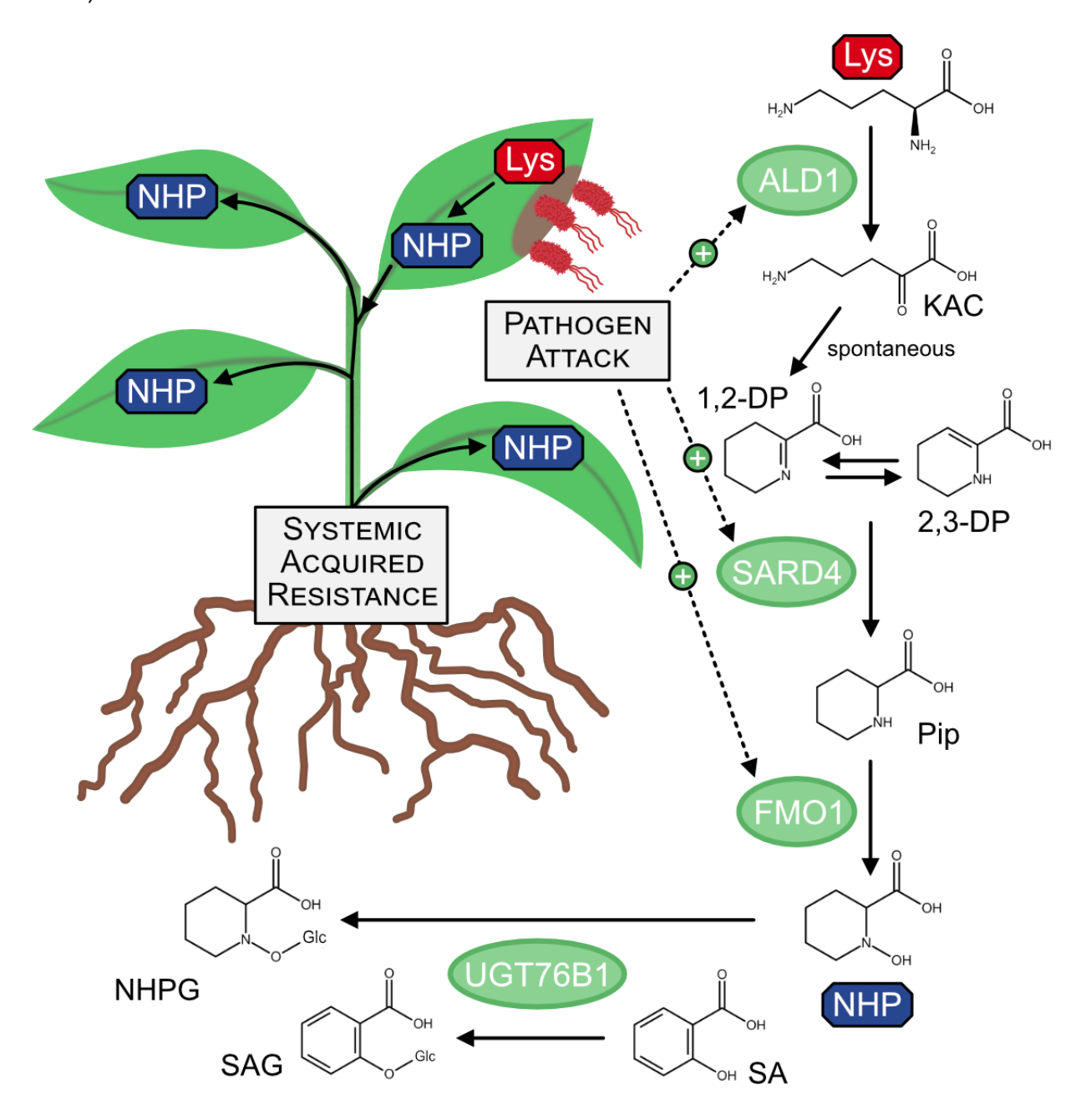


Figure 2.4: Lysine is converted to the mobile immune signal N-hydroxypipecolic acid to induce systemic acquired resistance

Local pathogen attack induces the synthesis pathway of N-hydroxypipecolic acid (NHP) from Lys catalyzed by three enzymes. NHP is transported to the non-infected systemic parts of the plant and triggers a systemic acquired resistance response that confers long-lasting protection against a broad spectrum of pathogens. The level of NHP is modulated via formation of the inactive  $\beta$ -glucoside catalyzed by the glycosyltransferase UGT76B1, which also accepts salicylic acid (SA) as a substrate. ALD1, AGD2-like defense response protein 1; DP, Dehydropipecolic acid; FMO1, Flavin-dependent monooxygenase 1; KAC,  $\alpha$ -ketocaproic; NHP, N-hydroxy pipecolic acid; NHPG, NHP-N-O-glucoside; Pip, Pipecolic acid; SA, Salicylic acid; SAG, SA- $\beta$ -glucoside; SARD4, SAR-deficient 4; UGT76B1, UDP-dependent glycosyltransferase 76B1.

The SAR signaling pathway was first elucidated in Arabidopsis but it is also prevalent in other species such as tobacco, cucumber, tomato and the monocot Brachypodium dystachyon (Holmes et al. 2019; Schnake et al. 2020). Transient expression of UGT76B1 in tomato confirmed glycosylation of NHP and the resulting mitigation of defense signaling (Holmes et al. 2021). Thus, conversion of the amino acid Lys into the defense hormone NHP seems to be a central component of plant immune response conserved among angiosperms. Changes in Lys metabolism will most likely have immediate consequences for immune signaling, which could be the reason for plants to strictly control the level of free Lys (Batista-Silva et al. 2019; Stepansky et al. 2006).

## 2.8 Concluding remarks

Amino acids are central components of protein, energy and nitrogen metabolism within the plant's primary metabolism. In addition, they are precursors for a variety of active compounds with specific functions in plant-microbe interactions that are far from being fully understood. Most likely, individual amino acids are also involved in signaling events during biotic interactions. In a complex environment plants need to integrate environmental information with intrinsic cues about their nutritional status and trigger appropriate metabolic and cellular responses during initial contact with microbes. A major aim of future research efforts will be to identify the biochemical mechanism of amino acid sensing in plants including the downstream signaling cascades but also to unravel the metabolic interactions between plants and microbes. There will most likely be substantial overlap with metabolic adaptations in plants during the interaction with multicellular organisms such as nematodes or mycorrhizal fungi (Lanfranco et al. 2018; Siddique et al. 2022). Also, the different organisms interacting with an individual plant compete for the allocation of resources and trigger specific response patterns with reciprocal effects (Bell et al. 2021). Thus, integrating advances in these research areas will contribute to a holistic understanding of plant biotic interactions.

#### 2.9 Glossary

**Autoimmune phenotype**: Natively elevated immunity in plants not exposed to pathogens commonly accompanied by growth defects.

**Auxotrophy**: Dependence of organisms to take up certain essential substances from the environment, which they are unable to synthesize on their own.

**Chemoreceptors**: Sensory proteins responsive to chemical stimuli. **Damage-associated molecular patterns (DAMPs)**: Endogenous molecules that serve as molecular marker for physical damage on extracellular receptors. **Effector-triggered immunity (ETI)**: Plant immunity elicited by pathogen virulence factors secreted into the plant cell usually to alter transcription of the host.

**Metabolon**: A temporary structural-functional complex formed between sequential enzymes of a metabolic pathway

**Microbe-associated molecular patterns (MAMPs)**: Molecular signatures that are highly conserved among microbes but are absent in the host (e.g. flagella).

**Microbiome**: Entity of microorganisms in a particular environment.

**Pattern-triggered immunity (PTI)**: Plant immunity elicited by molecular patterns associated with pathogens or cellular damage.

**Promotor profiling**: Analysis of regulatory genetic elements to predict the expression pattern and function of uncharacterized genes.

Rhizobia: Group of symbiotic nitrogen-fixing soil bacteria that infect roots of legumes.

**Rhizosphere**: The region of soil in the vicinity of plant roots in which the chemistry and microbiology is influenced by their growth, respiration and nutrient exchange.

Ribosome profiling: Technique to determine actively translated messenger RNA transcripts.

**RNAseq**: Sequencing technique revealing the presence and quantity of RNA in a biological sample at a given moment.

**Single-particle cryo-EM**: Electron microscopy of frozen specimens (e.g. proteins) that allows near-

atomic resolutions.

**Splice variant**: Alternative recombination of exons allowing one gene to code multiple proteins.

**Systemic acquired resistance (SAR)**: Enhanced immunity of the whole plant following a prior exposure to a pathogen.

**X-Ray crystallography**: Imaging of crystalline structures facilitated by analysis of diffracting X-rays.

#### 2.10 References

Alfieri, Andrea et al. (2020): The structural bases for agonist diversity in an *Arabidopsis thaliana* glutamate receptor-like channel. In: *PNAS* 117 (1), Artikel 752–760, 10.1073/pnas.1905142117. DOI: 10.1073/pnas.1905142117.

Álvarez, Consolación; Ángeles Bermúdez, M.; Romero, Luis C.; Gotor, Cecilia; García, Irene (2012): Cysteine homeostasis plays an essential role in plant immunity. In: *New Phytol.* 193 (1), S. 165–177. DOI: 10.1111/j.1469-8137.2011.03889.x.

Batista-Silva, Willian et al. (2019): The role of amino acid metabolism during abiotic stress release. In: *Plant Cell Environ.* 42 (5), S. 1630–1644. DOI: 10.1111/pce.13518.

Bauer, Sibylle et al. (2021): UGT76B1, a promiscuous hub of small molecule-based immune signaling, glucosylates N-hydroxypipecolic acid, and balances plant immunity. In: *Plant Cell* 33 (3), S. 714–734. DOI: 10.1093/plcell/koaa044.

Bell, Christopher A.; Magkourilou, Emily; Urwin, Peter E.; Field, Katie J. (2021): The influence of competing root symbionts on below-ground plant resource allocation. In: *Ecology and evolution* 11 (7), S. 2997–3003. DOI: 10.1002/ece3.7292.

Bernsdorff, Friederike; Döring, Anne-Christin; Gruner, Katrin; Schuck, Stefan; Bräutigam, Andrea; Zeier, Jürgen (2016): Pipecolic acid orchestrates plant systemic acquired resistance and defense priming via salicylic acid-dependent and -independent pathways. In: *Plant Cell* 28 (1), S. 102–129. DOI: 10.1105/tpc.15.00496.

Besnard, Julien et al. (2016): UMAMIT14 is an amino acid exporter involved in phloem unloading in *Arabidopsis* roots. In: *J. Exp. Bot.* 67 (22), S. 6385–6397. DOI: 10.1093/jxb/erw412.

Besnard, Julien et al. (2021): Increased expression of UMAMIT amino acid transporters results in activation of salicylic acid dependent stress response. In: *Front. Plant Sci.* 11, 10.3389/fpls.2020.606386. DOI: 10.3389/fpls.2020.606386.

Bjornson, Marta; Pimprikar, Priya; Nürnberger, Thorsten; Zipfel, Cyril (2021): The transcriptional landscape of *Arabidopsis thaliana* pattern-triggered immunity. In: *Nat. Plants* 7 (5), S. 579–586. DOI: 10.1038/s41477-021-00874-5.

Cai, Jianghua et al. (2021): Glycosylation of N-hydroxy-pipecolic acid equilibrates between systemic acquired resistance response and plant growth. In: *Mol. Plant* 14 (3), S. 440–455. DOI: 10.1016/j.molp.2020.12.018.

Chen, Yun-Chu et al. (2018): N-hydroxy-pipecolic acid is a mobile metabolite that induces systemic disease resistance in *Arabidopsis*. In: *PNAS* 115 (21), Artikel E4920-E4929, 10.1073/pnas.1805291115. DOI: 10.1073/pnas.1805291115.

Cheng, Xu et al. (2017): Genome-wide analysis of bacterial determinants of plant growth promotion and induced systemic resistance by *Pseudomonas fluorescens*. In: *Environ*. *Microbiol*. 19 (11), S. 4638–4656. DOI: 10.1111/1462-2920.13927.

Cheng, Yao; Zhang, Xiuxiu; Sun, Tianyang; Tian, Qiuying; Zhang, Wen-Hao (2018): Glutamate receptor homolog3.4 is involved in regulation of seed germination under salt stress in *Arabidopsis*. In: *Plant Cell Physiol*. 59 (5), S. 978–988. DOI: 10.1093/pcp/pcy034.

Cole, Benjamin J. et al. (2017): Genome-wide identification of bacterial plant colonization genes. In: *PLoS Biol.* 15 (9), 10.1371/journal.pbio.2002860. DOI: 10.1371/journal.pbio.2002860.

Corredor-Moreno, Pilar et al. (2021): The branched-chain amino acid aminotransferase TaBCAT1 modulates amino acid metabolism and positively regulates wheat rust susceptibility. In: *Plant Cell* 33 (5), S. 1728–1747. DOI: 10.1093/plcell/koab049.

Cotton, T. E. Anne et al. (2019): Metabolic regulation of the maize rhizobiome by benzoxazinoids. In: *ISME J.* 13 (7), S. 1647–1658. DOI: 10.1038/s41396-019-0375-2.

Denancé, Nicolas et al. (2013): *Arabidopsis* wat1 (walls are thin1)-mediated resistance to the bacterial vascular pathogen, *Ralstonia solanacearum*, is accompanied by cross-regulation of salicylic acid and tryptophan metabolism. In: *Plant J.* 73 (2), S. 225–239. DOI: 10.1111/tpj.12027.

Dhatterwal, Pinky; Mehrotra, Sandhya; Miller, Anthony J.; Mehrotra, Rajesh (2021): Promoter profiling of *Arabidopsis* amino acid transporters: Clues for improving crops. In: *Plant Mol. Biol.* 107 (6), S. 451–475. DOI: 10.1007/s11103-021-01193-1.

Ding, Pingtao et al. (2016): Characterization of a pipecolic acid biosynthesis pathway required for systemic acquired resistance. In: *Plant Cell* 28 (10), S. 2603–2615. DOI: 10.1105/tpc.16.00486.

Dinkeloo, Kasia; Boyd, Shelton; Pilot, Guillaume (2018): Update on amino acid transporter functions and on possible amino acid sensing mechanisms in plants. In: *Semin. Cell Dev. Biol.* 74, S. 105–113. DOI: 10.1016/j.semcdb.2017.07.010.

Dubos, Christian; Huggins, David; Grant, Guy H.; Knight, Marc R.; Campbell, Malcolm M. (2003): A role for glycine in the gating of plant NMDA-like receptors. In: *Plant J.* 35 (6), S. 800–810. DOI: 10.1046/j.1365-313X.2003.01849.x.

Fonseca, Jose Pedro et al. (2020): Iron–sulfur cluster protein NITROGEN FIXATION S-LIKE1 and its interactor FRATAXIN function in plant immunity. In: *Plant Physiol.* 184 (3), S. 1532–1548. DOI: 10.1104/pp.20.00950.

Gamas, Pascal (1996): Use of a subtractive hybridization approach to identify new *Medicago truncatula* genes induced during root nodule development. In: *MPMI* 9 (4), S. 233–242. DOI: 10.1094/mpmi-9-0233.

Glawischnig, Erich (2007): Camalexin. In: *Phytochemistry* 68 (4), S. 401–406. DOI: 10.1016/j.phytochem.2006.12.005.

Goto, Yukihisa et al. (2019): Exogenous treatment with glutamate induces immune responses in *Arabidopsis*. In: *MPMI* 33 (3), S. 474–487. DOI: 10.1094/MPMI-09-19-0262-R.

Green, Marriah N. et al. (2021): Structure of the *Arabidopsis thaliana* glutamate receptor-like channel GLR3.4. In: *Mol. Cell* 81 (15), Artikel 3216-3226.e8, 3216-3226. DOI: 10.1016/j.molcel.2021.05.025.

Harbort, Christopher J. et al. (2020): Root-secreted coumarins and the microbiota interact to improve iron nutrition in *Arabidopsis*. In: *Cell Host Microbe* 28 (6), Artikel 825-837, 825-837. DOI: 10.1016/j.chom.2020.09.006.

Hartmann, Michael et al. (2017): Biochemical principles and functional aspects of pipecolic acid biosynthesis in plant immunity. In: *Plant Physiol.* 174 (1), S. 124–153. DOI: 10.1104/pp.17.00222.

Hartmann, Michael et al. (2018): Flavin monooxygenase-generated N-hydroxypipecolic acid is a critical element of plant systemic immunity. In: *Cell* 173 (2), 456-469. DOI: 10.1016/j.cell.2018.02.049.

Hartmann, Michael; Zeier, Jürgen (2018): L-lysine metabolism to N-hydroxypipecolic acid: An integral immune-activating pathway in plants. In: *Plant J.* 96 (1), S. 5–21. DOI: 10.1111/tpj.14037.

Hartmann, Michael; Zeier, Jürgen (2019): N-hydroxypipecolic acid and salicylic acid: A metabolic duo for systemic acquired resistance. In: *Curr. Opin. Plant Biol.* 50, S. 44–57. DOI: 10.1016/j.pbi.2019.02.006.

He, Yunxia et al. (2019): The *Arabidopsis* pleiotropic drug resistance transporters PEN3 and PDR12 mediate camalexin secretion for resistance to *Botrytis cinerea*. In: *Plant Cell* 31 (9), S. 2206–2222. DOI: 10.1105/tpc.19.00239.

Heinemann, Björn; Hildebrandt, Tatjana M. (2021): The role of amino acid metabolism in signaling and metabolic adaptation to stress-induced energy deficiency in plants. In: *J. Exp. Bot.* 72 (13), S. 4634–4645. DOI: 10.1093/jxb/erab182.

Hildebrandt, Tatjana M.; Nunes Nesi, Adriano; Araújo, Wagner L.; Braun, Hans-Peter (2015): Amino acid catabolism in plants. In: *Mol. Plant* 8 (11), S. 1563–1579. DOI: 10.1016/j.molp.2015.09.005.

Holmes, Eric C.; Chen, Yun-Chu; Mudgett, Mary Beth; Sattely, Elizabeth S. (2021): *Arabidopsis* UGT76B1 glycosylates N-hydroxy-pipecolic acid and inactivates systemic acquired resistance in tomato. In: *Plant Cell* 33 (3), S. 750–765. DOI: 10.1093/plcell/koaa052.

Holmes, Eric C.; Chen Yun-Chu; Sattely Elizabeth S.; Mudgett Mary Beth (2019): An engineered pathway for N-hydroxy-pipecolic acid synthesis enhances systemic acquired resistance in tomato. In: *Sci. Signal.* 12 (604), Artikel eaay3066, doi: 10.1126/scisignal.aay3066. DOI: 10.1126/scisignal.aay3066.

Hu, Lingfei et al. (2018): Root exudate metabolites drive plant-soil feedbacks on growth and defense by shaping the rhizosphere microbiota. In: *Nat. commun.* 9 (1), Artikel 2738, 10.1038/s41467-018-05122-7. DOI: 10.1038/s41467-018-05122-7.

Huot, Bethany; Yao, Jian; Montgomery, Beronda L.; He, Sheng Yang (2014): Growth–defense tradeoffs in plants: A balancing act to optimize fitness. In: *Mol. Plant* 7 (8), S. 1267–1287. DOI: 10.1093/mp/ssu049.

Hwang, In Sun; An, Soo Hyun; Hwang, Byung Kook (2011): Pepper asparagine synthetase 1 (CaAS1) is required for plant nitrogen assimilation and defense responses to microbial pathogens. In: *Plant J.* 67 (5), S. 749–762. DOI: 10.1111/j.1365-313x.2011.04622.x.

Jacobowitz, Joseph R.; Weng, Jing-Ke (2020): Exploring uncharted territories of plant specialized metabolism in the postgenomic era. In: *Annu. Rev. Plant Bio.* 71, S. 631–658. DOI: 10.1146/annurev-arplant-081519-035634.

Jacoby, Richard P.; Chen, Li; Schwier, Melina; Koprivova, Anna; Kopriva, Stanislav (2020): Recent advances in the role of plant metabolites in shaping the root microbiome. In: *F1000Research* 9, 10.12688/f1000research.21796.1. DOI: 10.12688/f1000research.21796.1.

Jacoby, Richard P.; Koprivova, Anna; Kopriva, Stanislav (2021): Pinpointing secondary metabolites that shape the composition and function of the plant microbiome. In: *J. Exp. Bot.* 72 (1), S. 57–69. DOI: 10.1093/jxb/eraa424.

Kadotani, Naoki; Akagi, Aya; Takatsuji, Hiroshi; Miwa, Tetsuya; Igarashi, Daisuke (2016): Exogenous proteinogenic amino acids induce systemic resistance in rice. In: *BMC Plant Biol.* 16, 10.1186/s12870-016-0748-x. DOI: 10.1186/s12870-016-0748-x.

Kim, Ji-Yun; Loo, Eliza P-I; Pang, Tin Yau; Lercher, Martin; Frommer, Wolf B.; Wudick, Michael M. (2021): Cellular export of sugars and amino acids: Role in feeding other cells and organisms. In: *Plant Physiol.* 187, Artikel kiab228, S. 1893–1914. DOI: 10.1093/plphys/kiab228.

Koprivova, Anna et al. (2019): Root-specific camalexin biosynthesis controls the plant growth-promoting effects of multiple bacterial strains. In: *PNAS* 116 (31), Artikel 15735–15744, 10.1073/pnas.1818604116. DOI: 10.1073/pnas.1818604116.

Kudjordjie, Enoch Narh; Sapkota, Rumakanta; Steffensen, Stine K.; Fomsgaard, Inge S.; Nicolaisen, Mogens (2019): Maize synthesized benzoxazinoids affect the host associated microbiome. In: *Microbiome* 7 (1), Artikel 59, 10.1186/s40168-019-0677-7. DOI: 10.1186/s40168-019-0677-7.

Kwaaitaal, Mark; Huisman, Rik; Maintz, Jens; Reinstädler, Anja; Panstruga, Ralph (2011): Ionotropic glutamate receptor (iGluR)-like channels mediate MAMP-induced calcium influx in *Arabidopsis thaliana*. In: *Biochem. J.* 440 (3), S. 355–365. DOI: 10.1042/BJ20111112.

Lam, Hon-Ming et al. (1998): Glutamate-receptor genes in plants. In: *Nature* 396 (6707), S. 125–126. DOI: 10.1038/24066.

Lanfranco, Luisa; Fiorilli, Valentina; Gutjahr, Caroline (2018): Partner communication and role of nutrients in the arbuscular mycorrhizal symbiosis. In: *New Phytol* 220 (4), S. 1031–1046. DOI: 10.1111/nph.15230.

Li, Feng et al. (2013): Glutamate receptor-like channel3.3 is involved in mediating glutathione-triggered cytosolic calcium transients, transcriptional changes, and innate immunity responses in *Arabidopsis*. In: *Plant Physiol*. 162 (3), S. 1497–1509. DOI: 10.1104/pp.113.217208.

Liu, Guosheng et al. (2010): Amino acid homeostasis modulates salicylic acid-associated redox status and defense responses in *Arabidopsis*. In: *Plant Cell* 22 (11), S. 3845–3863. DOI: 10.1105/tpc.110.079392.

Lynch, Joseph H.; Dudareva, Natalia (2020): Aromatic amino acids: A complex network ripe for future exploration. In: *Trends Plant Sci.* 25 (7), S. 670–681. DOI: 10.1016/j.tplants.2020.02.005.

Maeda, Hiroshi; Dudareva, Natalia (2012): The shikimate pathway and aromatic amino acid biosynthesis in plants. In: *Annu. Rev. Plant Bio.* 63, S. 73–105. DOI: 10.1146/annurev-arplant-042811-105439.

Manzoor, Hamid et al. (2013): Involvement of the glutamate receptor AtGLR3.3 in plant defense signaling and resistance to *Hyaloperonospora arabidopsidis*. In: *Plant J.* 76 (3), S. 466–480. DOI: 10.1111/tpj.12311.

Michard Erwan et al. (2011): Glutamate receptor–like genes form Ca2+ channels in pollen tubes and are regulated by pistil d-serine. In: *Science* 332 (6028), S. 434–437. DOI: 10.1126/science.1201101.

Mohnike, Lennart et al. (2021): The glycosyltransferase UGT76B1 modulates N-hydroxy-pipecolic acid homeostasis and plant immunity. In: *Plant Cell* 33 (3), S. 735–749. DOI: 10.1093/plcell/koaa045.

Mucha, Stefanie et al. (2019): The formation of a camalexin biosynthetic metabolon. In: *Plant Cell* 31 (11), S. 2697–2710. DOI: 10.1105/tpc.19.00403.

Mur, Luis A. J.; Simpson, Catherine; Kumari, Aprajita; Gupta, Alok Kumar; Gupta, Kapuganti Jagadis (2017): Moving nitrogen to the centre of plant defence against pathogens. In: *Ann. Bot.* 119 (5), S. 703–709. DOI: 10.1093/aob/mcw179.

Návarová, Hana; Bernsdorff, Friederike; Döring, Anne-Christin; Zeier, Jürgen (2012): Pipecolic acid, an endogenous mediator of defense amplification and priming, is a critical regulator of inducible plant immunity. In: *Plant Cell* 24 (12), S. 5123–5141. DOI: 10.1105/tpc.112.103564.

Pascale, Alberto; Proietti, Silvia; Pantelides, Iakovos S.; Stringlis, Ioannis A. (2020): Modulation of the root microbiome by plant molecules: the basis for targeted disease suppression and plant growth promotion. In: *Front. Plant Sci.* 10, 10.3389/fpls.2019.01741.

Pastorczyk, Marta et al. (2020): The role of CYP71A12 monooxygenase in pathogen-triggered tryptophan metabolism and *Arabidopsis* immunity. In: *New Phytol.* 225 (1), S. 400–412. DOI: 10.1111/nph.16118.

Pratelli, Réjane; Pilot, Guillaume (2014): Regulation of amino acid metabolic enzymes and transporters in plants. In: *J. Exp. Bot.* 65 (19), S. 5535–5556. DOI: 10.1093/jxb/eru320.

Prior, Matthew J. et al. (2021): *Arabidopsis* bZIP11 is a susceptibility factor during *Pseudomonas syringae* infection. In: *MPMI* 34 (4), S. 439–447. DOI: 10.1094/MPMI-11-20-0310-R.

Qiaolin, Shao; Gao Qifei; Lhamo Dhondup; Zhang Hongsheng; Luan Sheng (2020): Two glutamate- and pH-regulated Ca2+ channels are required for systemic wound signaling in *Arabidopsis*. In: *Sci. Signal*. 13 (640), 10.1126/scisignal.aba1453. DOI: 10.1126/scisignal.aba1453.

Rajniak, Jakub; Giehl, Ricardo F. H.; Chang, Evelyn; Murgia, Irene; Wirén, Nicolaus von; Sattely, Elizabeth S. (2018): Biosynthesis of redox-active metabolites in response to iron deficiency in plants. In: *Nat. Chem. Biol.* 14 (5), S. 442–450. DOI: 10.1038/s41589-018-0019-2.

Resentini, Francesca; Ruberti, Cristina; Grenzi, Matteo; Bonza, Maria Cristina; Costa, Alex (2021): The signatures of organellar calcium. In: *Plant Physiol.* 187 (187), 1985–2004. DOI: 10.1093/plphys/kiab189.

Sasse, Joelle; Martinoia, Enrico; Northen, Trent (2018): Feed your friends: Do plant exudates shape the root microbiome? In: *Trends Plant Sci.* 23 (1), S. 25–41. DOI: 10.1016/j.tplants.2017.09.003.

Schnake, Anika et al. (2020): Inducible biosynthesis and immune function of the systemic acquired resistance inducer N-hydroxypipecolic acid in monocotyledonous and dicotyledonous plants. In: *J. Exp. Bot.* 71 (20), S. 6444–6459. DOI: 10.1093/jxb/eraa317.

Schwachtje, Jens; Fischer, Axel; Erban, Alexander; Kopka, Joachim (2018): Primed primary metabolism in systemic leaves: A functional systems analysis. In: *Sci Rep.* 8 (1), 10.1038/s41598-017-18397-5. DOI: 10.1038/s41598-017-18397-5.

Shin, Kihye et al. (2015): Genetic identification of ACC-RESISTANT2 reveals involvement of LYSINE HISTIDINE TRANSPORTER1 in the uptake of 1-aminocyclopropane-1-carboxylic acid in *Arabidopsis thaliana*. In: *Plant Cell Physiol*. 56 (3), S. 572–582. DOI: 10.1093/pcp/pcu201.

Siddique, Shahid; Coomer, Alison; Baum, Thomas; Williamson, Valerie Moroz (2022): Recognition and Response in Plant-Nematode Interactions. In: *Annual Review of Phytopathology*. DOI: 10.1146/annurev-phyto-020620-102355.

Singh, Shashi Kant; Chien, Ching-Te; Chang, Ing-Feng (2016): The *Arabidopsis* glutamate receptor-like gene GLR3.6 controls root development by repressing the Kip-related protein gene KRP4. In: *J. Exp. Bot.* 67 (6), S. 1853–1869. DOI: 10.1093/jxb/erv576.

Siwinska, Joanna et al. (2018): Scopoletin 8-hydroxylase: A novel enzyme involved in coumarin biosynthesis and iron-deficiency responses in *Arabidopsis*. In: *J. Exp. Bot*. 69 (7), S. 1735–1748. DOI: 10.1093/jxb/ery005.

Sonawala, Unnati; Dinkeloo, Kasia; Danna, Cristian H.; McDowell, John M.; Pilot, Guillaume (2018): Review: Functional linkages between amino acid transporters and plant responses to pathogens. In: *Plant Science* 277, S. 79–88. DOI: 10.1016/j.plantsci.2018.09.009.

Stepansky, A.; Less, H.; Angelovici, R.; Aharon, R.; Zhu, X.; Galili, G. (2006): Lysine catabolism, an effective versatile regulator of lysine level in plants. In: *Amino acids* 30 (2), S. 121–125. DOI: 10.1007/s00726-005-0246-1.

Stringlis, Ioannis A. et al. (2018): MYB72-dependent coumarin exudation shapes root microbiome assembly to promote plant health. In: *PNAS* 115 (22), Artikel E5213-22, 10.1073/pnas.1722335115. DOI: 10.1073/pnas.1722335115.

Stringlis, Ioannis A.; Jonge, Ronnie de; Pieterse, Corn M. J. (2019): The age of coumarins in plant–microbe interactions. In: *Plant Cell Physiol.* 60 (7), S. 1405–1419. DOI: 10.1093/pcp/pcz076.

Stuttmann, Johannes et al. (2011): Perturbation of *Arabidopsis* amino acid metabolism causes incompatibility with the adapted biotrophic pathogen *Hyaloperonospora arabidopsidis*. In: *Plant Cell* 23 (7), S. 2788–2803. DOI: 10.1105/tpc.111.087684.

Teardo, Enrico et al. (2011): Dual localization of plant glutamate receptor AtGLR3.4 to plastids and plasmamembrane. In: *Biochim. Biophys. Acta* 1807 (3), S. 359–367. DOI: 10.1016/j.bbabio.2010.11.008.

Teardo, Enrico et al. (2015): Alternative splicing-mediated targeting of the *Arabidopsis* GLUTAMATE RECEPTOR3.5 to mitochondria affects organelle morphology. In: *Plant Physiol.* 167 (1), S. 216–227. DOI: 10.1104/pp.114.242602.

Tegeder, Mechthild; Hammes, Ulrich Z. (2018): The way out and in: Phloem loading and unloading of amino acids. In: *Curr. Opin. Plant Biol.* 43, S. 16–21. DOI: 10.1016/j.pbi.2017.12.002.

Thoms, David; Liang, Yan; Haney, Cara H. (2021): Maintaining symbiotic homeostasis: How do plants engage with beneficial microorganisms while at the same time restricting pathogens? In: *MPMI* 34 (5), S. 462–469. DOI: 10.1094/MPMI-11-20-0318-FI.

Tian, Wang; Wang, Chao; Gao, Qifei; Li, Legong; Luan, Sheng (2020): Calcium spikes, waves and oscillations in plant development and biotic interactions. In: *Nat. Plants* 6 (7), S. 750–759. DOI: 10.1038/s41477-020-0667-6.

Toyota, Masatsugu et al. (2018): Glutamate triggers long-distance, calcium-based plant defense signaling. In: *Science* 361 (6407), S. 1112–1115. DOI: 10.1126/science.aat7744.

Tsai, Huei Hsuan; Schmidt, Wolfgang (2017): Mobilization of iron by plant-borne coumarins. In: *Trends Plant Sci.* 22 (6), S. 538–548. DOI: 10.1016/j.tplants.2017.03.008.

van Damme, Mireille; Zeilmaker, Tieme; Elberse, Joyce; Andel, Annemiek; Sain-van der Velden, Monique de; van den Ackerveken, Guido (2009): Downy mildew resistance in *Arabidopsis* by mutation of HOMOSERINE KINASE. In: *Plant Cell* 21 (7), S. 2179–2189. DOI: 10.1105/tpc.109.066811.

Venturi, Vittorio; Keel, Christoph (2016): Signaling in the rhizosphere. In: *Trends Plant Sci.* 21 (3), S. 187–198. DOI: 10.1016/j.tplants.2016.01.005.

Voges, Mathias J. E. E.; Bai, Yang; Schulze-Lefert, Paul; Sattely, Elizabeth S. (2019): Plant-derived coumarins shape the composition of an *Arabidopsis* synthetic root microbiome. In: *PNAS* 116 (25), Artikel 12558–12565, 10.1073/pnas.1820691116. DOI: 10.1073/pnas.1820691116.

Wudick, Michael M. et al. (2018): CORNICHON sorting and regulation of GLR channels underlie pollen tube Ca2+ homeostasis. In: *Science* 360 (6388), S. 533–536. DOI: 10.1126/science.aar6464.

Yang, Yiling et al. (2015): Relation between chemotaxis and consumption of amino acids in bacteria. In: *Mol. Microbiol.* 96 (6), S. 1272–1282. DOI: 10.1111/mmi.13006.

Yokoyama, Ryo; Oliveira, Marcos V. V. de; Kleven, Bailey; Maeda, Hiroshi A. (2021): The entry reaction of the plant shikimate pathway is subjected to highly complex metabolite-mediated regulation. In: *Plant Cell* 33 (3), S. 671–696. DOI: 10.1093/plcell/koaa042.

Yoo, Heejin et al. (2020): Translational regulation of metabolic dynamics during effector-triggered immunity. In: *Mol. Plant* 13 (1), S. 88–98. DOI: 10.1016/j.molp.2019.09.009.

Zeier, Jürgen (2021): Metabolic regulation of systemic acquired resistance. In: *Curr. Opin. Plant Biol.* 62, 10.1016/j.pbi.2021.102050. DOI: 10.1016/j.pbi.2021.102050.

Zhao, Chengsong; Pratelli, Réjane; Yu, Shi; Shelley, Brett; Collakova, Eva; Pilot, Guillaume (2021): Detailed characterization of the UMAMIT proteins provides insight into their evolution, amino acid transport properties, and role in the plant. In: *J. Exp. Bot.* 72 (18), S. 6400–6417. DOI: 10.1093/jxb/erab288.

Zhou, Feng et al. (2020): Co-incidence of damage and microbial patterns controls localized immune responses in roots. In: *Cell* 180 (3), 440-453. DOI: 10.1016/j.cell.2020.01.013.

Zhou, Jian-Min; Zhang, Yuelin (2020): Plant immunity: Danger perception and signaling. In: *Cell* 181 (5), S. 978–989. DOI: 10.1016/j.cell.2020.04.028.

## 3 Cysteine signaling in plant pathogen response

**Moormann, Jannis**; Heinemann, Björn; Angermann, Cecile; Koprivova, Anna; Armbruster, Ute; Kopriva, Stanislav; Hildebrandt, Tatjana M. (2025): Cysteine signaling in plant pathogen response. *Plant Cell Environ*. DOI: 10.1111/pce.70017.

#### 3.1 Abstract

The amino acid cysteine is the precursor for a wide range of sulfur-containing functional molecules in plants, including enzyme cofactors and defense compounds. Due to its redox active thiol group cysteine is highly reactive. Synthesis and degradation pathways are present in several subcellular compartments to adjust the intracellular cysteine concentration. However, stress conditions can lead to a transient increase in local cysteine levels. Here we investigate links between cysteine homeostasis and metabolic signaling in Arabidopsis thaliana. The systemic proteome response to cysteine feeding strongly suggests that Arabidopsis seedlings interpret accumulation of cysteine above a certain threshold as a signal for a biotic threat. Cysteine supplementation of Arabidopsis plants via the roots increases their resistance to the hemibiotrophic bacterium Pseudomonas syringae confirming the protective function of the cysteine induced defense pathways. Analysis of mutant plants reveals that the balance of cysteine synthesis between the cytosol and organelles is crucial during Arabidopsis immune response to Pseudomonas syringae. The induction profile of pathogen responsive proteins by cysteine provides insight into potential modes of action. Our results highlight the role of cysteine as a metabolic signal in the plant immune response and add evidence to the emerging concept of intracellular organelles as important players in plant stress signaling.

### 3.2 Introduction

Amino acids have multiple functions in plants. In addition to their role during protein biosynthesis, they are an integral part of several biosynthetic pathways and involved in signaling processes including plant stress responses (Heinemann & Hildebrandt 2021). Amino acids can serve as markers reflecting nutrient availability or as carbon source for alternative respiratory pathways under energy starvation (Pedrotti et al. 2018). Proline is known to function as an osmolyte during osmotic stress and as molecular chaperone preventing protein aggregation (Szabados & Savouré 2010). In addition, amino acids serve as precursors for various molecules involved in plant immunity. Perturbations in amino acid metabolism have been reported to affect plant immune responses in various ways (Moormann et al. 2022). The phloem-mobile signaling molecule N-hydroxypipecolic acid, required for establishing systemic acquired resistance, is synthesized from lysine (Gupta & Spenser 1969; Návarová et al. 2012). Aromatic amino acids are precursors for a broad range of specialized molecules that crucially shape the interaction between plants and microbes such as coumarins, phytoalexins and

indolic glucosinolates (Maeda & Dudareva 2012; Pastorczyk et al. 2020; Glawischnig 2007; Harun et al. 2020). The thiazole ring of camalexin, the characteristic phytoalexin of *Arabidopsis thaliana*, originates from the cysteine residue of glutathione (Su et al. 2011).

Among amino acids, cysteine is unique as it occupies a central position in plant sulfur metabolism. It is the precursor for a wide range of sulfur-containing molecules in the cell, including methionine, essential vitamins and cofactors such as thiamin, lipoic acid, biotin, Fe-S clusters and molybdenum cofactor (Giovanelli et al. 1985; Droux 2004; van Hoewyk et al. 2008). Furthermore, the tripeptide y-glutamyl-cysteinyl-glycine, also known as glutathione, relies on the incorporation of cysteine to function as the main determinant of cellular redox homeostasis (Foyer & Noctor 2011). Its antioxidant property is based on the redox potential of the thiol group. Next to oxidative stress protection, glutathione also acts in detoxification of heavy metals and xenobiotics as well as in the plant defense response (Noctor et al. 2024). In proteins, cysteine residues contribute to structure, stability and function. When located in the active sites of enzymes they are essential for catalysis of many enzymatic reactions as well as metal cofactor binding. Moreover, thiol groups can undergo oxidation to form covalent disulfide bridges, aiding protein folding and stability. Reversible oxidation/reduction of these disulfide bridges poses a mechanism for redox regulation of proteins (Buchanan & Balmer 2005). Another layer of regulation is added by posttranslational cysteine modifications such as glutathionylation, nitrosylation, sulfenylation and persulfidation (Moseler et al. 2024; Begara-Morales et al. 2016).

Cysteine is the product of the plant sulfur assimilatory pathway. Sulfate is taken up from the soil by specific transporters and activated by ATP sulfurylase. The resulting adenosine-5'phosphosulfate (APS) is reduced in a two-step reaction via sulfite to sulfide by APS reductase and sulfite reductase. Sulfide is incorporated into O-acetylserine (OAS) by OAS-(thiol)lyase (OASTL) to produce cysteine (Takahashi 2010; Takahashi et al. 2011). The amino acid precursor OAS is synthesized by serine acetyltransferase (SERAT) from serine and acetyl-CoA. OASTL and SERAT form a cysteine synthase complex which is required for regulating cysteine synthesis based on substrate availability (Droux 2003; Wirtz & Hell 2006). Both enzymes have isoforms localized in the cytosol (SERAT1;1, SERAT3;1, SERAT3;2, OASTL-A), plastids (SERAT2;1, OASTL-B) and mitochondria (SEART2;2, OASTL-C) enabling OAS and cysteine synthesis in different subcellular locations (Ruffet et al. 1995; Watanabe et al. 2008; Hell & Wirtz 2011). Cysteine desulfurases, which transfer sulfur to Fe-S cluster scaffold proteins, are present in plastids and mitochondria as well (Couturier et al. 2013). The cytosolic cysteine desulfurase ABA3 is required for molybdenum cofactor synthesis (Caubrière et al. 2023). Cysteine levels are tightly regulated and generally kept low within the cell requiring adequate rates of cysteine degradation (Hildebrandt et al. 2015). In the cytosol, the L-cysteine desulfhydrase DES1 deaminates cysteine resulting in pyruvate, ammonia and sulfide (Alvarez et al. 2010). In mitochondria, a four-step process catalyzing the complete oxidation of cysteine to pyruvate and thiosulfate is facilitated by an unknown aminotransferase, the 3-mercaptopyruvate sulfur transferase STR1, and the sulfur dioxygenase ETHE1 (Höfler et al. 2016). Cysteine levels vary among cellular compartments and are highest in the cytosol which is known to be the main contributor of cysteine with concentrations around 300 µM (Heeg et al. 2008; Krüger et al. 2009). Accordingly, OASTL-A together with OASTL-B were found to account for 95% of OASTL activity in Arabidopsis protein extracts, while OASTL-C contributed only 5% of the activity. However, all three major OASTL isoforms were shown to largely compensate for each other's absence in null mutant studies (Heeg et al. 2008; Birke et al. 2013).

Previous findings provide some insight into the relevance of compartment specific cysteine metabolic pathways. Cytochrome c oxidase, the last enzyme of the mitochondrial respiratory chain, is strongly inhibited by cyanide as well as by hydrogen sulfide (Cooper & Brown 2008). Biosynthesis of camalexin and the gaseous phytohormone ethylene both lead to the production of cyanide in non-cyanogenic plants such as Arabidopsis (Böttcher et al. 2009; Peiser et al. 1984). Cyanide detoxification in the mitochondria is achieved by conversion of cysteine and cyanide to hydrogen sulfide and β-cyanoalanine catalyzed by cyanoalanine synthase (CAS-C1) (Hatzfeld et al. 2000; Watanabe et al. 2008). Hydrogen sulfide in turn is detoxified via incorporation into cysteine by mitochondrial OASTL-C, creating a cyclic detoxification pathway. OASTL-C might also be involved the regulation of sulfur homeostasis since loss or decreased activity due to a single nucleotide polymorphism in Arabidopsis accessions leads to reduced sulfate uptake (Koprivova et al. 2023). In addition, cysteine synthesis was found to play a role during stomatal closure in response to drought stress. Upon soil drying, sulfate is transported to the guard cells via the xylem and is incorporated into cysteine (Ernst et al. 2010). Subsequently, cysteine mediates abscisic acid (ABA)-dependent stomatal closure in multiple ways (Heinemann & Hildebrandt 2021). It is a substrate of the MoCo-sulfurylase ABA3 involved in ABA synthesis (Caubrière et al. 2023). ABA induces the expression of DES1, which uses cysteine as a substrate to produce hydrogen sulfide in the cytosol (Chen et al. 2020). Hydrogen sulfide accumulation leads to persulfidation and activation of several proteins involved in ABAinduced stomatal closure including kinases and transcription factors (Chen et al. 2020; Shen et al. 2020; Zhou et al. 2021). These findings illustrate the wide range of functions and different modes of action of cysteine and its related metabolism. Taken together, the versatile chemical nature of cysteine and the high degree of compartmentalization of its metabolism further highlight its potential for multiple, yet unknown, regulatory functions.

In order to identify additional potential signaling functions of cysteine in Arabidopsis, we analyzed the response of seedlings to an artificial increase in cysteine levels. The proteome signature of the cysteine treated seedlings indicated perception of the disturbance in cysteine

homeostasis as a biotic threat. Thus, we further investigated the role of compartment specific cysteine metabolism in the interaction of Arabidopsis plants with the leaf pathogen *Pseudomonas syringae* pv tomato DC3000 (Pst) and identified cytosolic and mitochondrial cysteine synthesis as major contributors to pathogen resistance.

#### 3.3 Results

# 3.3.1 The seedling proteome response to increased cysteine concentrations indicates biotic stress signaling

To understand the systemic response of *Arabidopsis thaliana* to an increased cysteine content we performed a feeding experiment. Six-day-old seedlings grown in liquid culture were supplemented with 1 mM L-cysteine for 24h (Figure 3.1A, Supplementary Figure 3.1A). This treatment led to a 7.6-fold increase in the seedling cysteine content, and the glutathione content was also significantly higher (1.7 -fold) than in control seedlings (Figure 3.1B). The cysteine content in the medium continuously decreased most likely due to a combination of uptake by the plants and chemical oxidation processes in the medium and was completely depleted at the end of the 24h incubation time (Supplementary Figure 3.1B). To test, whether cysteine oxidation led to a depletion of oxygen in the medium or had an effect on seedling respiration we analyzed the oxygen content of the medium as well as seedling oxygen consumption rates, but did not detect any significant differences between cysteine treatment and control (Supplementary Figure 3.1C).

Shotgun proteome analysis revealed a distinct effect of cysteine feeding on the composition of the seedling proteome (Figure 3.1C). 479 of the 4613 detected protein groups were significantly increased and 670 significantly decreased in cysteine treated compared to control samples (Figure 3.1D). Among the strongly downregulated proteins were the transcriptional activator Hem1, kinases associated with ABA signaling, and proteins involved in sulfur assimilation whereas glutathione-S transferases (GSTs) as well as UDP-glucosyltransferases were most drastically increased (Suppl. Dataset S1). In order to systematically identify major features of the proteome response to increased cysteine levels, we performed an enrichment analysis on functional annotations of the significantly changed proteins (Suppl. Dataset S1). Enrichment of metabolic pathways was analyzed based on a modified version of the MapMan annotation system (https://mapman.gabipd.org; Figure 3.1E). The results indicated a decrease in pathways related to photosynthesis including photophosphorylation, the Calvin-Benson-Bassham cycle and also tetrapyrrole and organellar protein synthesis (Figure 3.1E, blue). In contrast, pathways required for heterotrophic energy metabolism such as carbohydrate and lipid degradation as well as cellular respiration showed increased abundance after cysteine

3.1E, The treatment (Figure red). enrichment of stress-related categories (glucosyltransferases, oxidoreductases, glutathione-S-transferases) among the significantly increased proteins prompted us to systematically probe our dataset for characteristic stress response profiles. To this end, we performed an additional enrichment analysis on the basis of published transcriptome profiles for diverse abiotic and biotic stress conditions as well as elicitor and hormone treatments focusing on the proteins significantly increased after cysteine feeding (Figure 3.1F, Suppl. Dataset S1). Strikingly, six of the seven significantly enriched categories in cysteine treated seedlings were associated with pathogen response. Enriched categories of proteins were those induced by pathogen-associated molecular patterns (PAMPs), damage-associated molecular patterns (DAMPs), systemic acquired resistance (SAR), treatment with jasmonic acid (JA) or the salicylic acid analogon benzothiadiazole (BTH) strongly suggesting a role for cysteine during biotic stress signaling (Figure 3.1F). Indeed, the concentration of the phytoalexin camalexin was significantly (4.5-fold) increased in the cysteine-treated seedlings indicating a similarity to an active pathogen response (Figure 3.1G).

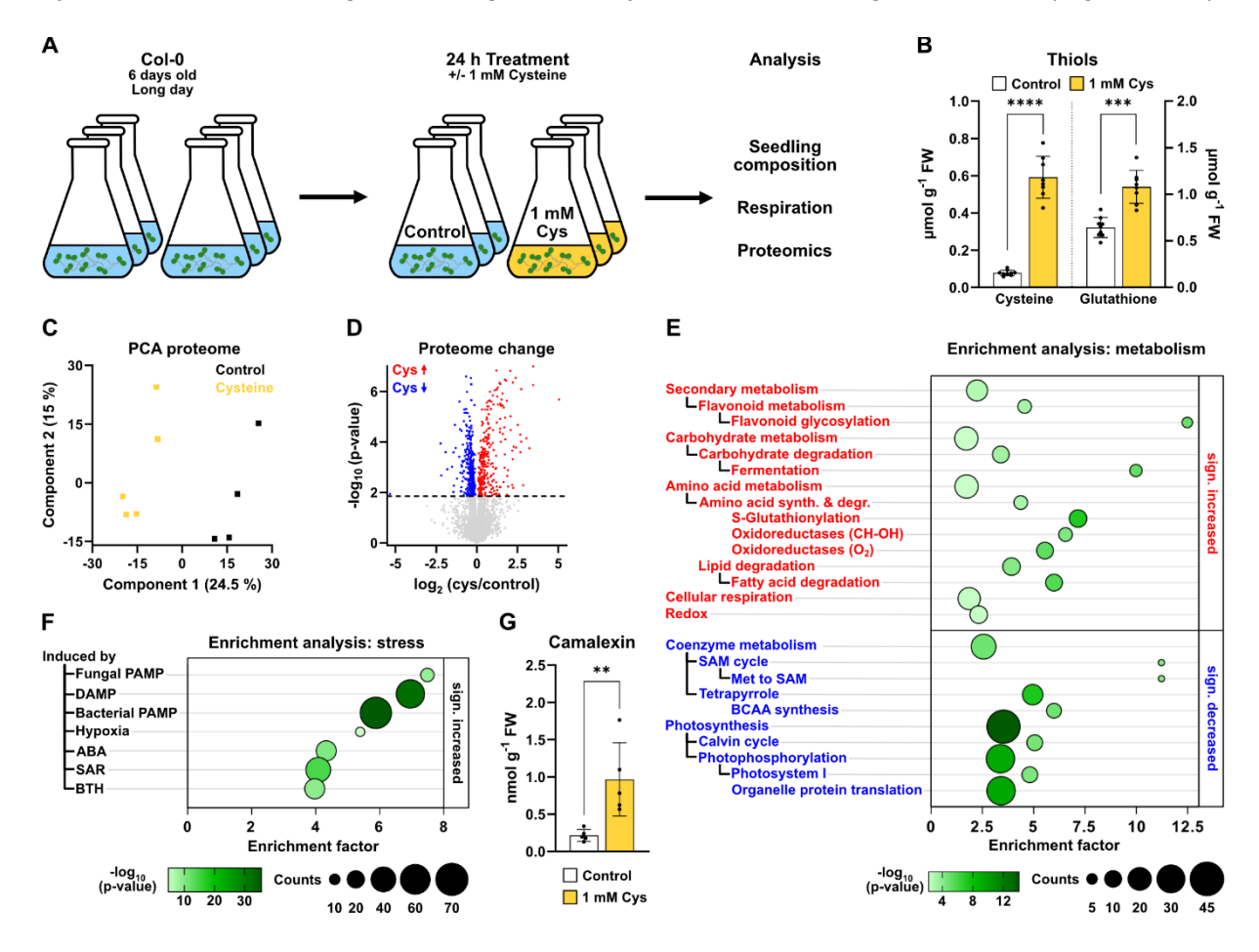


Figure 3.1: Seedling proteome response to cysteine treatment

**A**. An A. thaliana seedling culture was supplemented with 1 mM L-cysteine for 24 hours before harvest. **B**. Seedling content of L-cysteine and reduced glutathione (GSH) [µmol · g fresh weight <sup>-1</sup>] (n = 8-9). **C**. Principal component analysis of shotgun proteomics dataset with control (black) and cysteine-treated (yellow) seedlings. **D**. Volcano plot illustrating differences in the proteome of cysteine treated seedlings vs. controls. Proteins of significantly higher or lower abundance after cysteine feeding are marked in red and blue, respectively (t-test, FDR < 0.05). **E**. Enrichment of functional categories in proteins that are significantly increased (top, red) or decreased (bottom, blue) in the

presence of cysteine. **F**. Enrichment of stress induced categories among proteins that are significantly increased in the presence of cysteine. ABA, abscisic acid; BCAA, branched-chain amino acid; BTH, benzothiadiazole, DAMP, damage-associated molecular pattern; JA, jasmonic acid; PAMP, pathogen-associated molecular pattern; SAM, S-adenosylmethionine; SAR, systemic acquired resistance. The complete proteomics dataset including the enrichment analysis is provided as Suppl. Dataset S1. **G**. Seedling camalexin content [nmol·g fresh weight¹] (n = 5). Mean (bars) and individual (dots) values  $\pm$  SD are shown. Asterisks indicate statistically significant differences compared with control seedlings following students t-test (\*\* P < 0.01 > 0.001; \*\*\* P < 0,001 > 0,0001; \*\*\*\* P < 0,0001). Raw data is provided in Suppl. Dataset S4.

## 3.3.2 Cysteine treatment induces pathogen resistance

To test the physiological relevance of the observed induction of pathogen response pathways by cysteine feeding under physiological conditions we watered six-week-old *A. thaliana* plants grown on soil with 10 mM cysteine 24 hours before performing a pathogen assay using the hemibiotrophic bacterium *Pseudomonas syringae* pv. tomato DC3000 (Pst) (Figure 3.2A). Quantification of thiols confirmed that cysteine was taken up by the plants and transported to the leaves (Figure 3.2B). Cysteine accumulated in the rosette leaves to a similar extent as in the seedling culture in treated compared to control plants (7-fold). The cysteine treated plants were significantly less susceptible to Pst indicated by reduced bacterial growth and less chlorosis after three days of infection (Figure 3.2C,D).

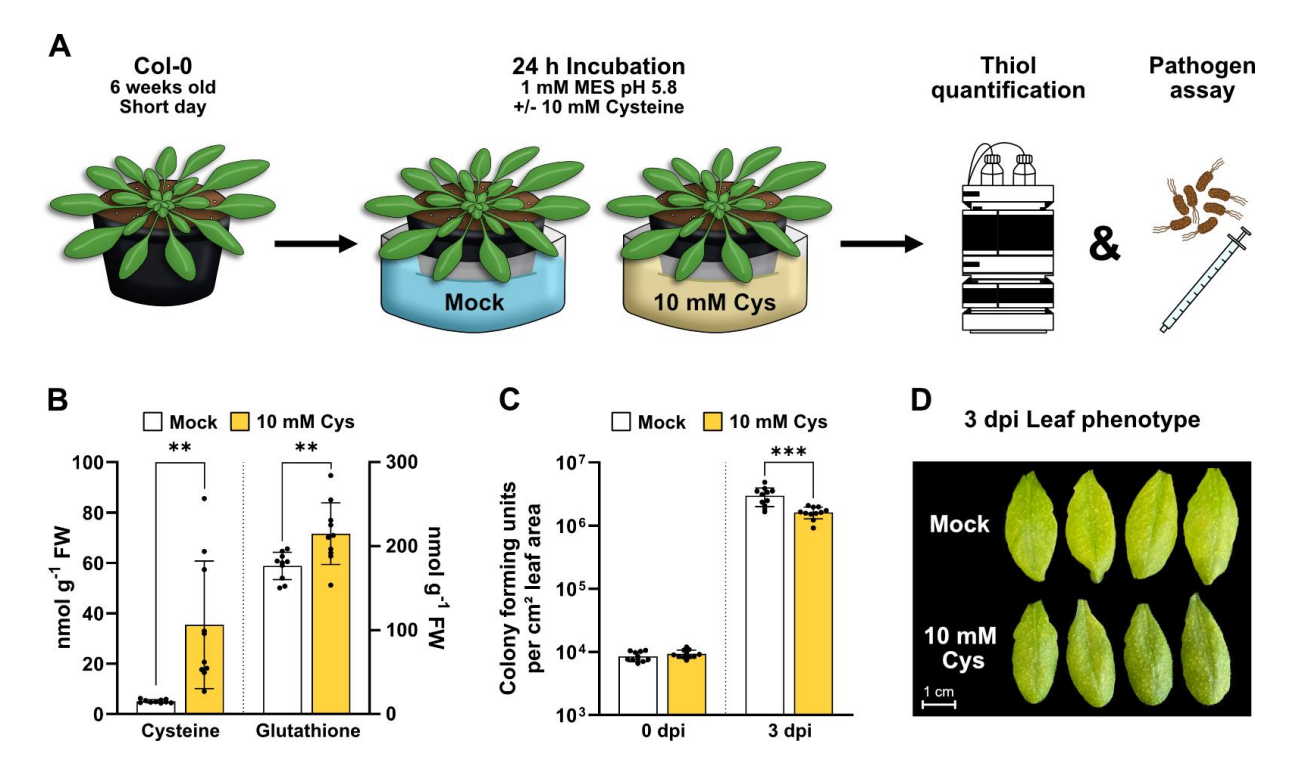


Figure 3.2: Cysteine treatment induces resistance to the virulent pathogen Pseudomonas syringae

**A**. Schematic representation of the workflow: A. thaliana plants were grown for 6 weeks under short-day conditions and incubated in 10 mM L-cysteine for 24 h before further analysis. **B**. Content of L-cysteine and reduced glutathione (GSH) [nmol  $\cdot$  g fresh weight<sup>-1</sup>] in the rosette leaves of mock treated (white bars) and cysteine treated (yellow bars) plants (n = 10). **C**. Pst infection assay: Four leaves per plant were infiltrated with *P. syringae* DC3000 solution including 5 × 10<sup>5</sup> colony forming units (CFU) per ml using a needleless syringe and sampled at 0 and 3 days past infection (dpi) to quantify CFU per cm leaf area (n = 11). **D**. Phenotype of four representative leaves per treatment at three days after inoculation. Mean (bars) and individual (dots) values  $\pm$  SD are shown. Asterisks indicate

# 3.3.3 Pathogen attack induces cysteine synthesis, and proteome responses to cysteine treatment and pathogen interaction overlap

To investigate the function of cysteine during plant-pathogen interaction, we quantified thiols in Arabidopsis leaves infected with Pst. Cysteine levels were significantly increased already 12 hours post infection (hpi), peaked at 24 hpi at 6.6-fold level of the mock treated controls and remained constantly high until 48 hpi (Figure 3.3A). The proteome of the infected leaves showed clear differences to the mock treated samples (Figure 3.3B; Suppl. Dataset S2). The pattern of changes in individual protein abundances was highly consistent between the two timepoints analyzed with a stronger response at 48 hpi (Suppl. Dataset S3; Supplementary Figure 3.2). 697 proteins were significantly increased and 582 proteins significantly decreased at both timepoints. Highlighting proteins with significant changes in the cysteine-treated seedlings in the Pst infection dataset illustrates that there is also a strong overlap between the Arabidopsis proteome response to increased cysteine contents and pathogen attack (Figure 3.3C; Supplementary Figure 3.2; Suppl. Dataset S3). 174 proteins were significantly increased and 268 proteins significantly decreased after cysteine feeding as well as after pathogen attack. Among the consistently highly induced proteins in both responses were several glutathione-S-transferases, UDP-glucosyltransferases, and ALTERNATIVE OXIDASE 1A (Suppl. Dataset S3). Enrichment analysis of functional annotations identifies a repression of photosynthesis related pathways, coenzyme metabolism as well as organellar protein translation (Figure 3.3D, blue) and an induction of lipid catabolism (Figure 3.3D, red) as common effects of both treatments.

We performed additional experiments to validate these cysteine responses with potential relevance in immune signaling (Supplementary Figure 3.3). The chlorophyll content of the cysteine treated seedlings was significantly decreased by 10% compared to the control, which is in line with the repression of photosynthesis indicated by the proteome data (Supplementary Figure 3.3A). However, we did not detect any significant effect of cysteine supplementation via the roots on the photosynthetic performance of the leaves as determined by chlorophyll a fluorescence analysis (Supplementary Figure 3.3B). The overall seedling composition with respect to carbohydrates, lipids and proteins remained unchanged (Supplementary Figure 3.3C). The induction of several glutathione-S-transferases (GSTs) in response to cysteine treatment led to a 1.6-fold increase in total GST abundance, which was also reflected in a 1.7-fold higher GST activity (Supplementary Figure 3.3D). To evaluate, whether the trigger for the induction of GSTs and other stress related proteins such as alternative oxidase might be an accumulation of reactive oxygen species we performed DAB staining with the seedlings

(Supplementary Figure 3.3E). The results revealed that hydrogen peroxide levels in the cysteine treated seedlings were even lower than in the controls indicating that other signaling processes are involved.

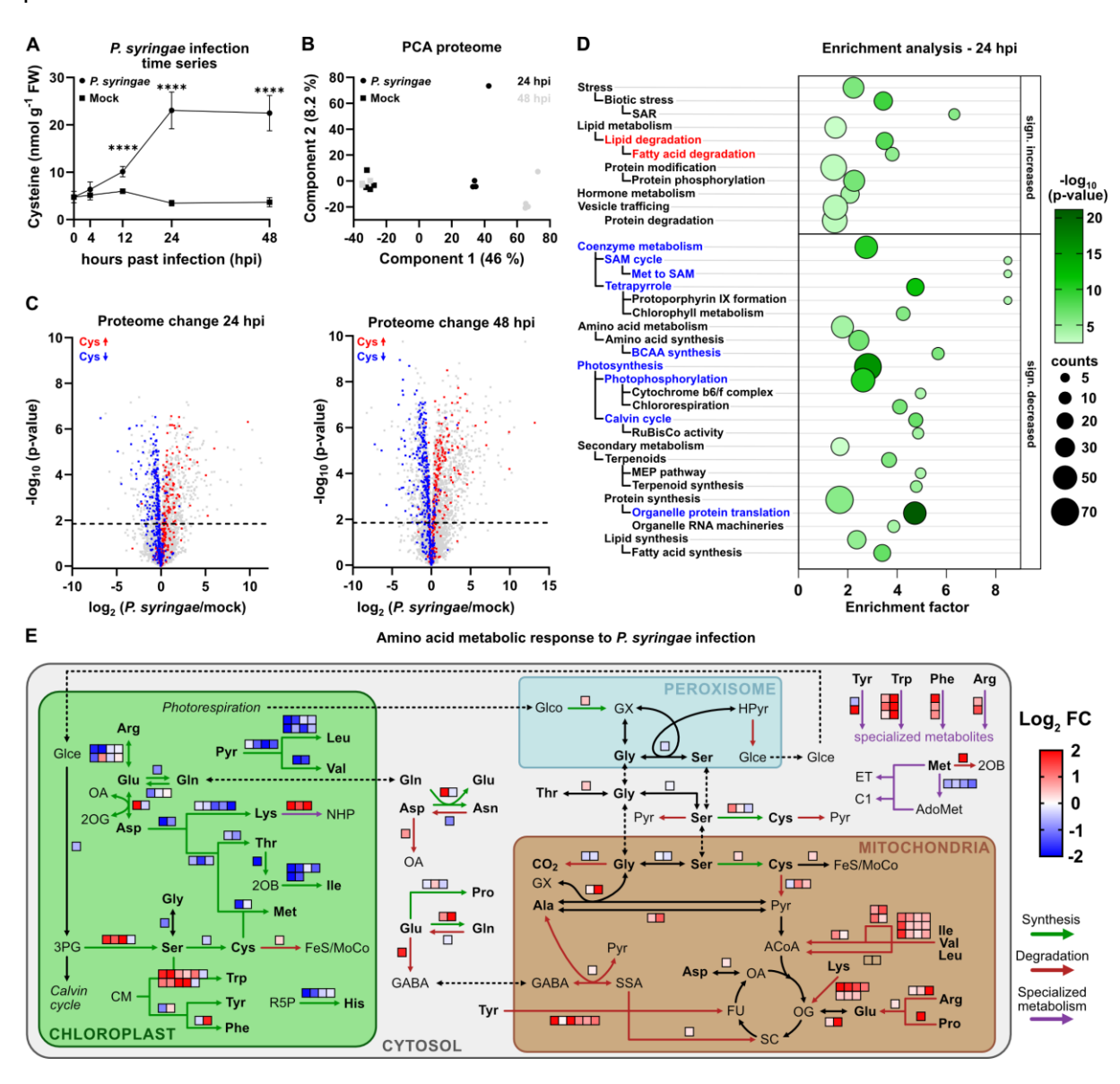


Figure 3.3: Cysteine accumulation and proteome response during pathogen interaction

Six weeks old A. thaliana plants were infiltrated with P. syringae DC3000 (Pst) (2.5 × 10<sup>6</sup> colony forming units per ml). Six leaves per plant were sampled at the indicated time points. A. Content of L-cysteine [nmol · g fresh weight] 1] in infected vs. mock treated leaves (n = 4-9). Mean values ± SD are shown. Asterisks indicate statistically significant differences compared with mock-treated plants (\*\*\*\* P < 0,0001), B. Principal component analysis of the proteome of Pst- and mock-infected leaves (circles and squares, respectively) at 24 and 48 h after inoculation (black and grey, respectively) C. Volcano plots illustrating differences in the proteome of Pst- vs. mock-infected plants at 24 and 48 hpi. Proteins of significantly higher or lower abundance after treatment with 1 mM L-cysteine (Fig. 3.1C) are highlighted in red and blue, respectively. D. Enrichment of functional categories in proteins that are significantly increased (top) or decreased (bottom) at 24 hpi with Pst. Red and blue fonts indicate significantly increased or decreased categories, respectively, that were also enriched after cysteine treatment (Fig. 3.1E). E. Effect of Pst infection on amino acid metabolic pathways. Relative protein abundances in infected vs. mock treated leaves at 48 hours after inoculation Pst. Proteins significantly increasing or decreasing in abundance are indicated by red or blue squares, respectively. 2-OB, 2-oxobutyrate; 2-OG, 2-oxoglutarate; 3PG, 3-phosphoglycerate; ACoA, Acetyl-CoA; AdoMet, S-Adenosylmethionin; C1, C1-metabolism; CM, chorismate; ET, ethylene; FeS, iron-sulfur cluster; FU, fumarate; GABA, γ-aminobutyric acid; Glce, glycerate; Glco, glycolate; GX, glyoxylate; Hpyr, Hydroxypyruvate; MoCo, molybdenum cofactor; NHP, N-hydroxypipecolic acid; OA, oxaloacetic acid; Pyr, pyruvate; R5P, ribose-5phosphate; SSA, succinic semialdehyde. The complete proteomics dataset including the enrichment analysis is provided in Suppl. Dataset S2. Additional raw data is provided in Suppl. Dataset S4.

Several aspects of the proteome response to Pst interaction such as a decrease in terpenoid synthesis and an increase in hormone metabolism or vesicle trafficking did not become apparent during cysteine feeding and thus might be unrelated to cysteine signaling. The general effect on amino acid metabolism included an increase in the catabolic pathways mainly localized in the mitochondria and a decrease in plastidic synthesis pathways. A clear exception were the synthesis pathway of serine and the aromatic amino acids, which were strongly induced together with downstream pathways required for their conversion to specialized metabolites (Figure 3.3E).

# 3.3.4 Compartment specific cysteine synthesis is required for pathogen resistance

A focus on the proteins involved in cysteine metabolism illustrates that the cytosolic and the mitochondrial pathway for cysteine synthesis as well as plastidic GSH production increased in abundance after pathogen attack whereas sulfate reduction and cysteine synthesis in the chloroplasts decreased (Figure 3.4A). In order to estimate the contributions of the individual compartments to cellular cysteine production we compared the total abundance of O-acetyl serine lyase (OASTL) isoforms catalyzing the last step in cysteine synthesis in the leaf proteome (Figure 3.4B). The cytosolic and plastidic isoforms OASTL-A and OASTL-B were of similar abundance, but OASTL-C localized in the mitochondria represented only about 5% of the total OASTL leaf content. During pathogen interaction OASTL-A and OASTL-C significantly increased in abundance whereas OASTL-B significantly decreased (Figure 3.4A). Next, we tested the response of knockout mutant lines for the individual OASTL isoforms during interaction with Pst (Figure 3.4C-G). The oastl-c (mitochondrial) mutant was significantly more susceptible to Pst infection compared to the wild type and the oastl-b (chloroplast) mutant (Figure 3.4C). The stronger infection was also visible in the phenotype of the infected leaves, which were shriveled up with necrotic tips (Figure 3.4D). The cytosolic oastl-a mutant showed an intermediate level of bacterial growth rates between the wild type and oastl-c (Figure 3.4C). We detected a significant decrease in leaf camalexin levels at 24 hpi in oastl-a and b and the same tendency in oastl-c. (Figure 3.4E). Total leaf cysteine levels were lower than in the wild type already under control conditions in oastl-a (deficient in cytosolic cysteine synthesis) and also the cysteine increase during infection lagged behind in this line but not in the others (Figure 3.4F, grey bars). Glutathione levels showed a similar trend (Figure 3.4G).

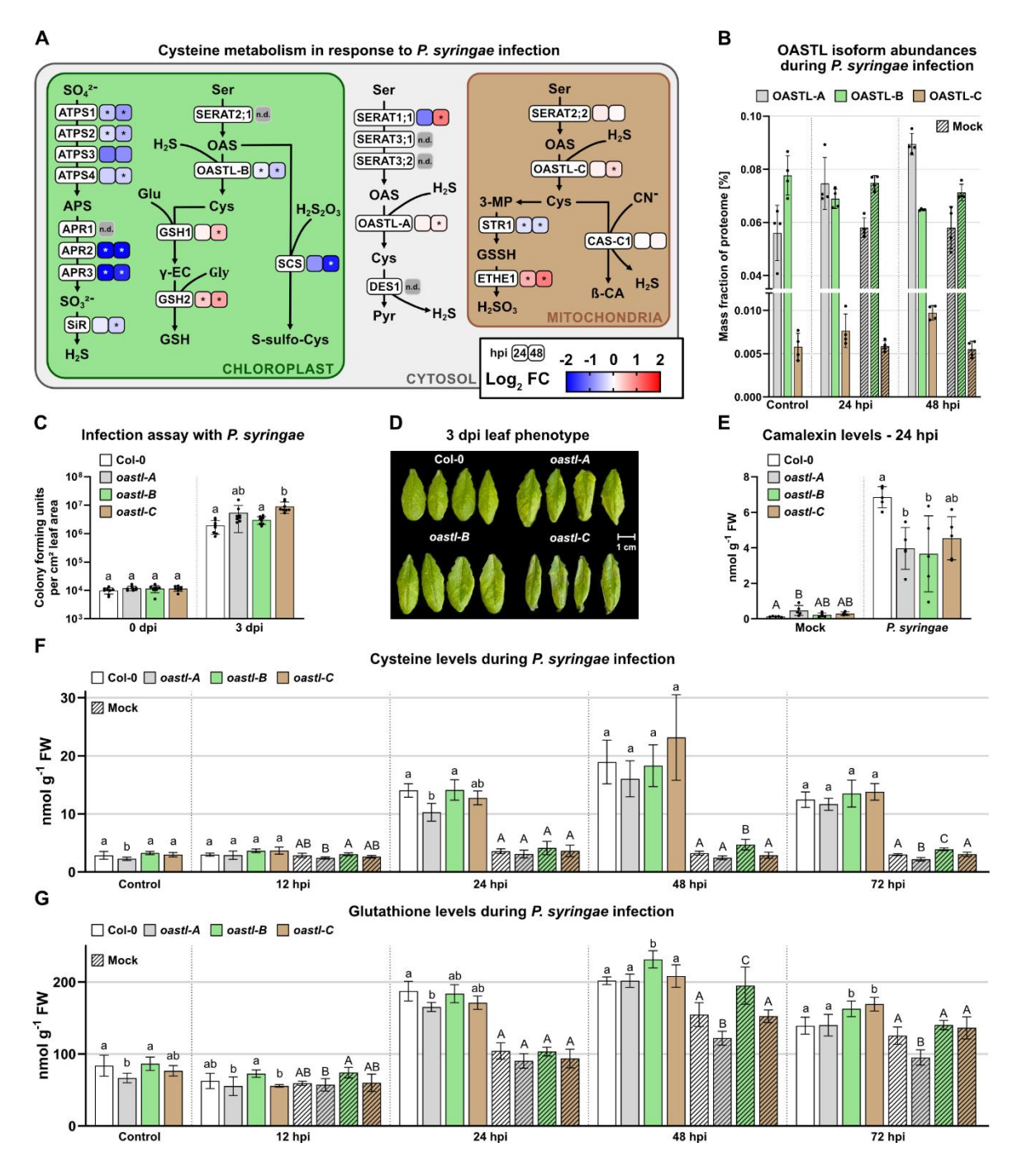


Figure 3.4: Compartmentalization of cysteine synthesis in pathogen resistance

**A**. Effect of Pst infection on cysteine metabolic pathways: Relative protein abundances in infected vs. mock treated leaves at 24 and 48 hours after inoculation with *P. syringae* DC3000 (Pst) (2.5 ×  $10^6$  colony forming units (CFU) per ml). Proteins increasing or decreasing in abundance are indicated by red or blue squares, respectively (n.d., undetected proteins). Asterisks indicate statistically significant differences compared with mock treated plants following students t-test (\*P < 0.05). APS, adenosine 5'-phophosulfate; ATPS, ATP sulfhydrase; APR, APS reductase; SiR, sulfite reductase; SERAT, serine acetyltransferase; OAS, O-acetylserine; OAS-A, O-acetylserin(thiol)lyase; GSH, glutathione; GSH1, γ-glutamyl-cysteine synthetase; GSH2, GSH syntethase; SCS, S-sulfocysteine synthase; DES1, L-cysteine desulfhydrase; Pyr, Pyruvate; 3-MP, 3-mercaptopyruvate; STR1, 3-MP sulfurtransferase; GSSH, GSH-persulfide; ETHE1, sulfur dioxygenase; β-CA, β-cyanoalanine; CAS-C1, CAS synthase. **B**. Total abundance of O-acetylserin(thiol)lyase isoforms in control, mock treated and Pst infected leaves of wild type *A. thaliana* plants calculated from quantitative iBAQ-values (n = 4). **C**. Pst infection assay: Four leaves per plant were infiltrated with *P. syringae* DC3000 solution including 5 ×  $10^5$  colony forming units (CFU) per ml using a needleless syringe and sampled at 0 and 3 days past infection (dpi) to quantify CFU per cm leaf area. (n = 8). **D**. Phenotype of four representative leaves per treatment at three days after inoculation. **E**. Camalexin content [nmol

 $\cdot$  g fresh weight<sup>-1</sup>] in mock treated and Pst infected leaves of wild type *A. thaliana* plants and OASTL-deficient mutant lines (n = 4-5). **F.** Cysteine and **G.** Glutathione content [nmol  $\cdot$  g fresh weight<sup>-1</sup>] in control, mock treated, and Pst infected leaves of wild type *A. thaliana* plants and OASTL-deficient mutant lines (n = 5-10). Mean (bars) and individual (dots) values  $\pm$  SD are shown. Letters indicate statistically significant differences following ANOVA with Tukey's test ( $\alpha$  = 0.05). Raw data is provided in Suppl. Dataset S4.

#### 3.4 Discussion

### 3.4.1 Links of cysteine homeostasis to plant immune signaling

The systemic proteome response to cysteine treatment strongly suggests that Arabidopsis seedlings interpret accumulation of cysteine above a certain threshold as a signal for a biotic threat. In accordance with these results, artificially increasing the intracellular cysteine concentration in mature plants renders them significantly less susceptible to infection by the hemibiotrophic bacterium *Pseudomonas syringae*, confirming the protective function of the defense pathways activated in response to cysteine treatment. Cysteine strongly accumulated within the first 24h of infection in control plants that had not been treated prior to inoculation showing that a disturbance in cysteine homeostasis is an integral feature of the interaction between plant and pathogen. These findings indicate that the results obtained using the artificial but also highly reproducible and homogenous seedling culture approach can provide valuable insight into physiologically relevant processes. Effects observed consistently in seedling cultures and in the plants grown on soil despite the differences in age, tissues, and cultivation style have the potential to reveal fundamental aspects of metabolic immune signaling.

Several proteins were strongly induced by both, cysteine feeding as well as infection with Pst and thus might provide some insight into potential links between cysteine homeostasis and immune signaling. The functional category with the strongest enrichment in cysteine induced proteins consisted of UDP-glucosyltransferases (UGTs) of the 73B subfamily annotated as flavonoid glycosidases. Several additional UGTs responded similarly to Pst infection and cysteine treatment, and among them UGT71C5, UGT74F2, and UGT87A2 showed the strongest consistent induction (Suppl. Dataset S3). The multigene family of uridine diphosphate-dependent glucosyltransferases catalyzes the covalent addition of sugars from nucleotide UDP sugar donors to functional groups on a variety of compounds which can increase the solubility of lipophilic metabolites or inactivate hormones and signaling molecules (Lairson et al. 2008). A number of UGTs have already been linked to plant immunity. UGT74F2 and UGT76B1 glycosylate and thereby inactivate immune signals including salicylic acid (SA) and N-hydroxypipecolic acid. Knockout lines develop an autoimmune phenotype indicating that this function is required for balancing and containing immune responses (Lim et al. 2002; Bauer et al. 2021). UGT71C5 uses the phytohormone abscisic acid (ABA) as a substrate and is

involved in regulating ABA homeostasis (Liu et al. 2015). ABA mediates abiotic stress responses and acts antagonistically to SA induced immune signaling (Torres-Zabala et al. 2007; Torres Zabala et al. 2009). The induction of UGT71C5 by cysteine will therefore amplify the plant pathogen response by suppressing antagonistic signals. A modeling approach recently suggested that UGT71C5 is activated by persulfidation of a cysteine residue at the active site, which would add an additional post-translational layer to sulfur signaling in pathogen response (Li et al. 2024). The strongly cysteine-responsive UGTs of the 73B subfamily also seem to have a positive regulatory role in immune signaling since Arabidopsis mutant plants lacking functional UGT73B3 or UGT73B5 showed increased susceptibility to Pst avrRpm1 (Langlois-Meurinne et al. 2005). However, the relevant substrate(s) and the mechanism behind this effect have not been identified yet.

Among the group of proteins accumulating in response to cysteine treatment as well as during pathogen infection were also several glutathione-S-transferases (GSTs) of the plant-specific phi (GSTF) and tau (GSTU) classes. GSTs catalyze the conjugation of glutathione to various substrates, mostly for detoxification purposes, and several of them are induced by pathogen infection and SA (Cummins et al. 2011; Lieberherr et al. 2003; Sappl et al. 2004). An accumulation during pathogen response has also been found in previous proteome studies (Jones et al. 2006; Maldonado-Alconada et al. 2011). However, very limited information is available on endogenous substrates or the exact metabolic functions of disease-induced GST isoenzymes. GSTF2, GSTF8, GSTF10 and GSTF11 were shown to bind to SA, though the biological implications remain unclear (Tian et al. 2012). Also, GSTF2 interacts with camalexin and was suggested to translocate plant defense compounds (Dixon et al. 2011).

Alternative oxidase (AOX) is induced by Pst infection and has been proposed to modulate reactive oxygen species (ROS) signaling in the mitochondria (Simons et al. 1999; Maxwell et al. 1999; Colombatti et al. 2014). The balance between AOX and manganese superoxide dismutase activities seems to be relevant for the specificity of ROS signaling by either confining the signal to the mitochondrial matrix  $(O_2^-)$  or spreading it to the rest of the cell  $(H_2O_2)$  (Cvetkoska & Vanlerberghe 2012). Our results indicate that induction of AOX can be triggered in response to cysteine accumulation prior to or independently of a pathogen-induced ROS burst.

The general response of the Arabidopsis leaf proteome to pathogen attack revealed that microbe interaction induces profound changes in organelle metabolism. Mitochondria strongly increase their oxidative phosphorylation capacity and use amino acids as alternative respiratory substrates. In contrast, chloroplasts decrease most of their functions including photosynthesis as well as amino acid synthesis and focus on the production of precursors for specialized metabolites and immune signals. This general metabolic shift from growth to

defense is also clearly visible in the proteome response of cysteine treated seedlings, which in addition had a slightly decreased chlorophyll content compared to the control. However, the macromolecular composition and respiration rate of the seedlings as well as the photosynthetic performance of the plants was unaffected 24h after cysteine treatment indicating that the systemic induction of defense pathways was able to protect the plant without causing major growth restrictions at this stage.

Interestingly, the protein most decreased in response to cysteine was HEM1, which has recently been reported to act as a translational regulator involved in the attenuation of the immune response during effector-triggered immunity (Zhou et al. 2023). The loss of HEM1 caused exaggerated cell death and restricted bacterial growth. Thus, a major aspect of cysteine signaling during pathogen response might be the repression of antagonistic signals.

# 3.4.2 Compartment specific functions of cysteine synthesis in immune signaling

While most amino acid anabolic pathways are localized in the chloroplasts, cysteine can be synthesized in different subcellular compartments (Heeg et al. 2008; Watanabe et al. 2008). The total leaf cysteine content after pathogen attack was reduced only in oastl-A mutant plants defective in cytosolic cysteine synthesis, but not in oastl-B or oastl-C indicating that the remaining isoforms can at least partially compensate for the defect. These finding confirm the quantitatively dominant role of the cytosol in cysteine production reported before (Heeg et al. 2008; Krüger et al. 2009). A previous study with a focus on cytosolic cysteine homeostasis had already demonstrated an increased susceptibility of oastl-A plants to Botrytis cinerea and Pst in contrast to a constitutive systemic immune response with high resistance to biotrophic and necrotrophic pathogens in des1 mutants, which accumulate cysteine due to defects in the cytosolic degradation pathway (Álvarez et al. 2012). Our results are in good agreement with these finding. In addition, they clearly show that cysteine synthesis in the mitochondria is also crucial for Arabidopsis pathogen resistance. Lack of mitochondrial OASTL-C, despite constituting only about 5% of the total OASTL leaf content, had the strongest impact on pathogen response as indicated by the highest bacterial colony counts and leaf chlorosis after infection with Pst. Mitochondria require cysteine as a precursor for the synthesis of iron-sulfur clusters and the cofactors biotin and lipoate as well as for cyanide detoxification. It was previously reported that overexpression of the mitochondrial cysteine desulfurase NFS1, which provides inorganic sulfur for FeS-cluster synthesis, results in constitutive upregulation of defense-related genes and increased resistance against Pst (Fonseca et al. 2020). The mechanism behind this response is currently unknown and could be related to regulatory functions of FeS proteins. However, increased cysteine desulfurase activity would also

potentially lead to an increase in the product sulfane sulfur, which, if produced in excess, can be reduced to hydrogen sulfide in the presence of a reductant like GSH (Frazzon et al. 2007). Hydrogen sulfide production by the mitochondrial β-cyanoalanine synthase CAS-C1 in turn has recently been shown to be crucial for stomatal closure in response to the pathogen-associated molecular pattern flagellin (Pantaleno et al. 2025). NFS1 was significantly induced by cysteine treatment and during Pst infection. Thus, an increase in compartment specific cysteine production as well as additional downstream metabolic processes seem to be involved in cysteine signaling during pathogen response.

Sulfate metabolism in plants branches at the level of adenosine 5'-phosphosulfate (APS), which can either be reduced to sulfide and incorporated into cysteine or phosphorylated by APS kinase (APK) and used for sulfation reactions. Blocking the sulfatation branch leads to an increased flux through the reductive branch of the pathway resulting in 4-fold increased leaf cysteine contents in *apk1xapk2* double knockout mutant plants compared to the wild type (Mugford et al. 2009). Re-evaluation of published datasets reveals that the expression profile of the *apk1xapk2* mutant strongly overlaps with the characteristic transcriptional response of Arabidopsis plants to bacterial pathogens, which would be in line with cysteine acting as a metabolic signal (Supplementary Figure 3.4). Since the cytosolic and mitochondrial but not the plastidic isoform of OASTL were induced in the APK deficient plants, compartment specific effects might again be relevant.

## 3.4.3 Potential mechanisms of cysteine immune signaling

Signaling events can be mediated by receptor proteins coupled to either kinase cascades or ion channels, allosteric protein regulation or post-translational modifications. Previous proteomic studies have already demonstrated an effect of *Pseudomonas syringae* infection on post-translational modifications such as S-nitrosylation in Arabidopsis leaves (Jones et al. 2006; Maldonado-Alconada et al. 2011). However, the mechanism of cysteine sensing and signaling during pathogen response remains poorly understood. Emerging evidence suggests possible modes of action that warrant further investigation. Glutamate receptor-like calcium channels (GLRs) are involved in long-distance plant defense signaling in response to wounding (Toyota et al. 2018). GLR3.3 is activated by GSH and several amino acids and responds to L-cysteine in physiologically relevant micromolar concentrations (Alfieri et al. 2020; Grenzi et al. 2023). Treatment of the leaves with GSH or cysteine suppressed Pst propagation in wild type but not *glr3.3* mutant plants indicating that induction of pathogen response in reaction to extracellular cysteine is associated with this signaling pathway (Li et al. 2013). Based on a detailed transcriptome study and subsequent experimental confirmation clade 2 GLRs have also been linked to immune signaling (Bjornson et al. 2021). Since GLRs

are mostly localized in the plasma membrane, they can detect extracellular changes in cysteine and other amino acids due to cell damage or release by pathogens but are unlikely to be involved in intracellular signaling. The induction of proteins associated with a DAMP-response in the cysteine treated seedlings indicates that extracellular receptors might be relevant.

Persulfidation of protein cysteine residues has been established as a post-translational modification involved in ABA signaling during drought response (Chen et al. 2020; Shen et al. 2020). A function in plant microbe interactions has not been demonstrated yet. However, in Aspergillus fumigatus, a human fungal pathogen causing severe pulmonary infections, persulfidation levels have been linked to both, the pathogenic potential of the fungus as well as the antifungal potency of alveolar macrophages and epithelial cells of the host (Sueiro-Olivares et al. 2021). Although the mechanisms of protein persulfidation and de-persulfidation is not entirely clear yet, cysteine most likely serves as the sulfur donor either via desulfhydration producing hydrogen sulfide or via transamination to 3-mercaptopyruvate and subsequent transsulfuration (Shen et al. 2020; Pedre et al. 2023). Thus, an increase in cysteine content might be translated to persulfidation signals. The cysteine desulfhydrase DES1 (AT5G28030), which has been previously associated with protein persulfidation in Arabidopsis (Aroca et al. 2017; Shen et al. 2020; Zhou et al. 2021), is not included in our proteomics dataset and 3-mercaptopyruvate sulfurtransferase (AT1G79230), the Arabidopsis ortholog of a yeast protein persulfidase (Pedre et al. 2023), was slightly decreased during Pst infection (Suppl. Dataset S2). Thus, there is currently no clear evidence for a role of protein persulfidation in cysteine signaling and this aspect requires further investigation. Another potential mechanism of cysteine signaling would be via protein cysteinylation, which has been demonstrated in animals (Martí-Andrés et al. 2024). Downstream effects can include transcriptional or posttranslational regulation. According to our results, the modulation of phytohormones and defense compounds as well as the alteration of immune gene translation pose potential hubs for cysteine-induced biotic stress signaling.

In conclusion, cysteine, an important precursor for defense compounds, was shown to elicit plant immune signaling and thus serve as an infochemical during plant microbe interactions. Compartmental cysteine synthesis appears to be vital for properly mounting a pathogen response. The specific signaling pathways still need to be identified including potential intracellular cysteine receptors as well as connections to hormonal crosstalk during stress response. A potential role in hypoxic signaling indicated by proteomics also deserves further investigation.

#### 3.5 Materials and Methods

### 3.5.1 Plant Material and growth conditions

All experiments were performed with *Arabidopsis thaliana* ecotype Col-0 as wild type control. All mutants are T-DNA insertion lines deficient (knockout) of the respective genes and were derived from Col-0. Homozygous seeds of *oastl-A* (At4g14880; N572213; SALK\_072213; aka *oastl-a1.1*; characterized in (López-Martín et al. 2008)) and *oastl-B* (At2g43750; N521183; SALK\_021183; characterized in (Heeg et al. 2008)) as well as of *oastl-C* (At3g59760, N500860; SALK\_000860; characterized in (Heeg et al. 2008)) were kindly provided by Stanislav Kopriva and Andreas Meyer, respectively. Stratified seeds were sown in pots containing soil and grown in a climate chamber under short-day conditions with 8h of light (120  $\mu$ mol·m-2·s-1). The temperature during the day and night changed from 22 to 18 °C. Soil-grown plants were kept under these conditions for 6 weeks until experiments were performed.

For seedling cultures, seeds were incubated in 100% (v/v) ethanol for 2 min followed by two consecutive incubation steps in 6% (v/v) sodium hypochlorite (Carl Roth, Germany) for 2 min each. Afterwards, seeds were washed five times using sterile  $ddH_2O$  and transferred to liquid growth media containing 0.43% (w/v) Murashige & Skoog salt mixture (Merck, Germany), 3 mM MES; and 0.5% (w/v) sucrose at pH 5.8. Individual cultures consisting of approximately 3 mg seeds in 50 ml liquid growth media were cultivated under long day conditions with 16 h of light (120 µmol · m<sup>-2</sup> · s<sup>-1</sup>) shaking at 100 rpm. The temperature during the day and night changed from 22 to 18 °C. Seedlings cultures were kept under these conditions for 6 days until treatment.

## 3.5.2 Cysteine treatment

For seedling cultures, 1 mM L-cysteine (Merck, Germany) was supplemented after 6 days of growth. The cysteine content in the medium decreased to low  $\mu M$  concentrations within the 24h treatment.

Conditions for cysteine feeding of plants grown on soil were optimized in preliminary experiments to achieve a similar increase in tissue cysteine levels as in the experiments performed with seedling culture. Pots were soaked in 1 mM MES pH 5.8 with or without 10 mM L-cysteine (Merck, Germany) for 24 hours starting at the beginning of the light period. Afterwards, plants were either harvested and flash frozen in liquid nitrogen immediately or follow-up experiments were performed.

### 3.5.3 Quantification of total lipids

The total lipid content was determined using the sulpho-phospho-vanillin method described in (Park et al., 2016). Absorbance was measured at 530 nm using a spectrophotometer (Multiscan Sykhigh, Thermo Fisher Scientific, Germany).

### 3.5.4 Quantification of total carbohydrates

The total carbohydrate content was determined using the phenol-sulphuric acid method described by. (Tamboli et al., 2020). 5 mg of lyophilised plant powder was dissolved in 1 ml of 2.5 N HCl and incubated for 3 h at 95 °C, shaking. The extracts were diluted (1:50) with demineralized water and 10 µl phenol and 1 ml concentrated sulphuric acid were added. After incubation (10 min, 95 °C, shaking) the absorbance was measured at 490 nm with a spectrophotometer (Multiskan Skyhigh, Thermo Fisher Scientific, Germany).

### 3.5.5 Extraction and quantification of total protein

5 mg lyophilized seedling powder was dissolved in 700 μl methanol (100% (v/v)) and incubated for 20 min shaking at 80 °C. After centrifugation (10 min, 4 °C, 18,800 xg) the pellet was washed twice in 1 ml ethanol (70% (v/v)) and resuspended in 400 μl NaOH (0.1 M). The solution was incubated for 1h shaking at 95 °C and centrifuged again. The protein content of the supernatant was quantified using Ready-to-use Coomassie Blue G-250 Protein Assay Reagent (Thermo Fisher Scientific, Germany) and Albumin Standard 23209 (Thermo Fisher Scientific, Germany).

#### 3.5.6 Quantification of chlorophyll

The quantification of chlorophyll was carried out according to a modified version of the method described by (Lichtenthaler 1987). 5 mg plant powder was dissolved in 700 ml methanol (100% (v/v)) and incubated for 20 min at 80 °C with shaking. After centrifugation (10 min, 4 °C, 18,800 xg), the chlorophyll content of the supernatant was quantified with a spectrophotometer (Multiskan Skyhigh, Thermo Fisher Scientific, Germany) (wavelengths: 470 nm, 653 nm and 666 nm).

## 3.5.7 Analysis of seedling respiration

Respiration rates were measured at ambient conditions using a Clark type oxygen electrode (model DW1, Hansatech Instruments Ltd, United Kingdom). Measurements were performed on control seedlings and seedlings fed 1 mM L-cysteine for 24 h in fresh, air-saturated liquid growth medium under constant stirring. After equilibration, 1 mM L-cysteine (Merck, Germany) was added. After respiration measurements, seedlings were lyophilized and oxygen consumption rates were calculated on the basis of dry weight.

### 3.5.8 Reactive oxygen species staining

Seedlings were rinsed with distilled water and transferred to the staining solution. For 3,3'-diaminobenzidine (DAB; Merck, Germany) staining, seedlings were incubated in DAB staining solution (50 mM sodium phosphate buffer pH 7.5; DAB 0.1% (w/v); Tween 20 0.05% (v/v)) for 7 h at 10 rpm. Afterwards, seedlings were rinsed with distilled water and incubated in destaining solution (ethanol 60% (v/v), glycerol 20% (v/v), acetic acid 20% (v/v) for 15 min at 95 °C to remove chlorophyll for proper visualization of the stain. Stained seedlings were scanned using the Epson Perfection V850 Pro (Epson, Germany).

## 3.5.9 Glutathione-S-transferase activity assay

Glutathione-S-transferase (GST) activity in crude extracts of seedlings was determined using a 1-chloro-2,4-dinitrobenzene (CDNB)-based photometric assay and performed as stated in (Koschmieder et al. 2022) if not mentioned otherwise. In short, 150 µl of cold extraction buffer (50 mM Tris-HCl, pH 8, 50 mM NaCl, 1 mM EDTA and 1% (w/v) PVPP) was added to 50 mg of seedlings ground in liquid nitrogen. Samples were resuspended thoroughly, kept on ice for 5 min and centrifuged at 18,000 xg for 15 min at 4 °C to obtain crude extracts. Protein concentration was determined using Bradford assay and 10-15 µg of enzyme was added to 200 µl GST assay (2 mM GSH, 1 mM CDNB in modified PBS). The increase in absorbance at 340 nm was monitored every 5 s for 10 min at room temperature and GST activity was calculated.

## 3.5.10 Analysis of photosynthetic performance

For ChI a fluorescence analyses, the HEXAGON IMAGING-PAM (Walz, Effeltrich, Germany) was used on whole rosettes. Saturation light pulses of 0.5 s were applied after 30 min dark treatment to determine Fm and Fm' during the illumination with increasing actinic light intensities. Non-photochemical quenching (NPQ) was calculated as (Fm – Fm')/Fm' and ΦPSII as (Fm' – F')/Fm (Baker 2008).

### 3.5.11 Pseudomonas syringae infection assays

For bacterial growth curves and thiol quantification, *Pseudomonas syringea* pv. tomato DC3000 (Pst), grown on Kings-B Agar (KB) plates containing 50  $\mu$ g · ml<sup>-1</sup> Rifampicin, were resuspended in 10 mM MgCl<sub>2</sub> to a final concentration of 5 × 10<sup>5</sup> colony forming units (cfu) ml<sup>-1</sup> (OD<sub>600</sub> 0.001). For shot-gun proteomics analysis, 2.5 × 10<sup>6</sup> cfu · ml-1 (OD<sub>600</sub> 0.005) Pst DC3000 was prepared as described. Five to seven of the youngest, fully matured leaves per plant were hand-infiltrated with the bacterial suspension using a needless syringe. For bacterial growth curves, leaf discs were cut from infected leaves 0 days past infection (dpi) and 3 dpi and ground in 200  $\mu$ l sterile MilliQ water using a tissue lyser (Mill Retsch MM400, Retsch GmbH, Haan, Germany). Dilution series were plated on KB plates containing 50  $\mu$ g · ml<sup>-1</sup>

Rifampicin and 50  $\mu$ g · ml<sup>-1</sup> Cycloheximide, and colony forming units were counted after two days of growth at 28 °C. Students t-tests were performed with 8 biological replicates per time point and genotype or treatment from two independent experiments showing similar results. For thiol quantification and shot-gun proteomics, all infected leaves were harvested, flash frozen in liquid nitrogen and ground for further procedures.

#### 3.5.12 Quantification of sulfur metabolites

Sulfur compounds in plant samples were derivatized using bromobimane and quantified by reverse phase high performance liquid chromatography (HPLC). Samples were solved in derivatization buffer (1.5 mM bromobimane (Merck, Darmstadt, Germany); 32% (v/v) acetonitrile; 10.3 mM EDTA and 103 mM HEPES pH 8) and incubated at 1400 rpm for 30 min in darkness. Afterwards, 15.9 mM methanesulfonic acid was added, cell debris pelleted at 18,000 xg for 5 min and the supernatant filtered using Corning Costar Spin-X (0.22 µm) centrifuge filter tubes (Merck, Darmstadt, Germany). Samples were diluted and measured using an Agilent 1260 Infinity II HPLC (Agilent Technologies, Waldbronn, Germany) by fluorescence detection (ex. 380 nm; em. 480 nm). Peaks were evaluated and quantified using OpenLabCDS software (Agilent, Santa Clara, United States).

#### 3.5.13 Quantification of camalexin

Camalexin was determined by HPLC as described in (Koprivova et al. 2019). In short, approximately 50 mg plant material were extracted in 150  $\mu$ l of dimethlysulfoxide (DMSO) for 20 min with shaking and centrifuged. 20  $\mu$ l of extracts were injected into a HPLC system with a Spherisorb ODS-2 column (250 mm x 4.6 mm, 5  $\mu$ m) and resolved using a gradient of acetonitrile in 0.01% (v/v) formic acid. Camalexin was detected by a FLD detector with an excitation at 318 nm and emission at 368 nm as described in (Bednarek et al. 2011). For the quantification of camalexin external standards were used ranging from 1 pg to 1 ng per  $\mu$ l.

# 3.5.14 Protein extraction, digestion and sample preparation for proteome analysis via mass spectrometry

Protein extraction, purification and digestion was performed with an adapted single-pot solid-phase-enhanced sample preparations (SP3) protocol from (Mikulášek et al. 2021) which originates from (Hughes et al. 2019). In short, 5 mg of lyophilized plant powder were solved in 500 µl SDT buffer (4% sodium dodecyl sulfate, 0.1 M dithiothreitol, 0.1 M Tris pH 7.6) and incubated at 60 °C for 30 min. Thirty microliters of the supernatants were mixed with 7.5 µl iodoacetamide (0.1 M) and incubated for 30 min in the dark. Then 2 µl dithiothreitol (0.1 M) was added. Equal shares (v/v) of hydrophobic and hydrophilic carboxylate-modified magnetic beads (Sera-Mag: No. 441521050250, No. 241521050250, GE Healthcare) were prepared for protein binding. Here, 600 µg beads were used per sample. Washing steps with ethanol (80%)

were performed on a magnetic rack as described in (Mikulášek et al. 2021). The bound proteins were digested for 18 h at 37 °C with 0.5 µg trypsin (MS grade, Promega) per sample. The peptide-containing supernatants were collected in tubes with low peptide binding properties. The beads were rinsed in 60 µl ammonium bicarbonate (50 mM) to recover the remaining peptides. The eluates were acidified with formic acid and desalted on 50 mg Sep-Pak tC18 columns (Waters). Peptide concentrations were quantified using the Pierce Quantitative Colorimetric Peptide Assay Kit (Thermo Fisher Scientific) and adjusted to the same concentration in 0.1% formic acid.

## 3.5.15 Shotgun proteomics by ion mobility mass spectrometry (IMS-MS/MS)

For proteome profiling of the cysteine treated seedlings, 200 ng of peptides were injected via a nanoElute 1 (Bruker Daltonic, Bremen, Germany), separated on an analytical reversed-phase C18 column (Aurora Ultimate 25 cm×75 µm, 1.6 µm, 120 Å; IonOpticks) and analyzed with a timsTOF Pro 2 mass spectrometer. Using a multi-staged linear gradient (Eluent A: MS grade water containing 0.1% formic acid, Eluent B: acetonitrile containing 0.1% formic acid, gradient: 0 min, 2%; 54 min, 25%; 60 min, 37%; 62 min, 95%; 70 min, 95% eluent B), peptides were eluted and ionized by a CaptiveSpray 1 ion source with a flow of 300 nl min-1. The ionized peptides were analyzed with a standard data-dependent acquisition parallel accumulation—serial fragmentation application method (DDA-PASEF) with the following settings: Ion mobility window: 0.6–1.6 V·s/cm², 10 PASEF ramps, target intensity of 20,000 (threshold 2,500), and a cycle time of ~1.1 s.

For proteome analysis of plants infected with *Pseudomonas syringae* 400 ng of peptides were injected via a nanoElute 2 UHPLC (Bruker Daltonic) and separated on the same type of analytical column with the same multi-staged gradient as above. Here, the eluting peptides were ionized by a CaptiveSpray 2 source and analyzed with a timsTOF-HT mass spectrometer. It was programmed with the following DDA-PASEF method parameters: Ion mobility window of 0.7–1.5 V·s/cm², 4 PASEF ramps, target intensity 14,500 (threshold 1,200), and a cycle time of ~0.53 s.

## 3.5.16 Data Processing and Evaluation

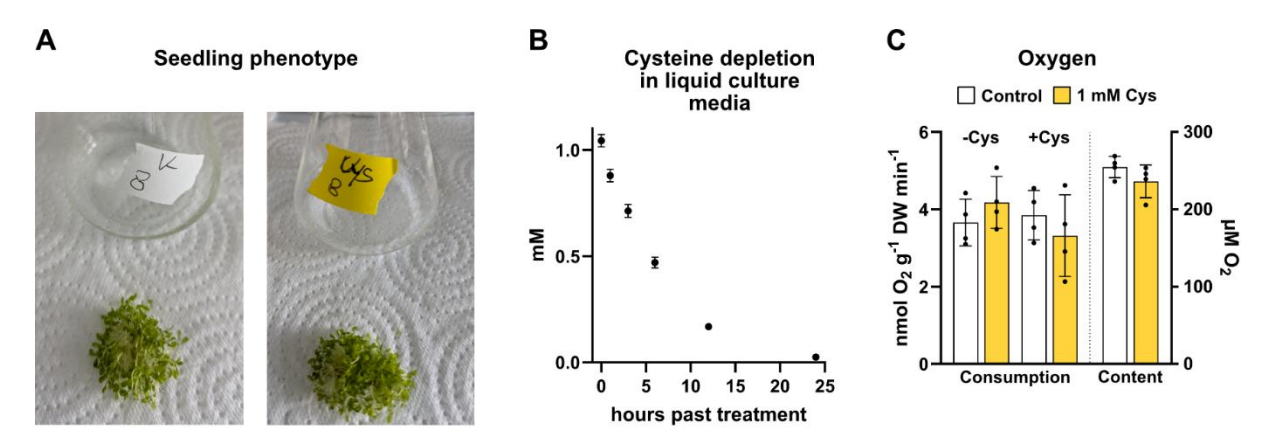
The ion mobility spectrometry (IMS-MS/MS) spectra from both experiments were analyzed with MaxQuant software (Cox & Mann 2008) using default search parameters and TAIR10 (Arabidopsis.org) as database for protein identification. The calculation of label-free quantification (LFQ) values and intensity-based absolute quantification (iBAQ) values were both enabled. Data evaluation was performed using Perseus software (Tyanova et al. 2016). Proteins were excluded from further analysis if they were not detected in at least n-1 biological replicates in at least one of the sample groups. Subsequently, missing values were replaced with randomly chosen low values from a normal distribution. Significant changes were

calculated from the LFQ values using Student's t-tests (p = 0.05). Fisher exact tests were performed in Perseus to identify significantly enriched or depleted metabolic pathways as well as environmental response patterns. The metabolic pathway categories were based on a modified version of MapMan (see Suppl. Datasets S1 and S2; mapman.gabipd.org). Several RNA-seq datasets were used to annotate proteins that showed a response to different stimuli, including fungal PAMPs, DAMPs, bacterial PAMPs (Bjornson et al. 2021), hypoxia (Klecker et al. 2014), ABA treatment, JA treatment (Goda et al. 2008), BTH treatment (Wang et al. 2006), or systemic acquired resistance (Gruner et al. 2013). Transcriptomics datasets for additional abiotic stress conditions (heat, cold, drought, salt, darkness) were used as summarized in (Hildebrandt 2018).

## 3.5.17 Data availability

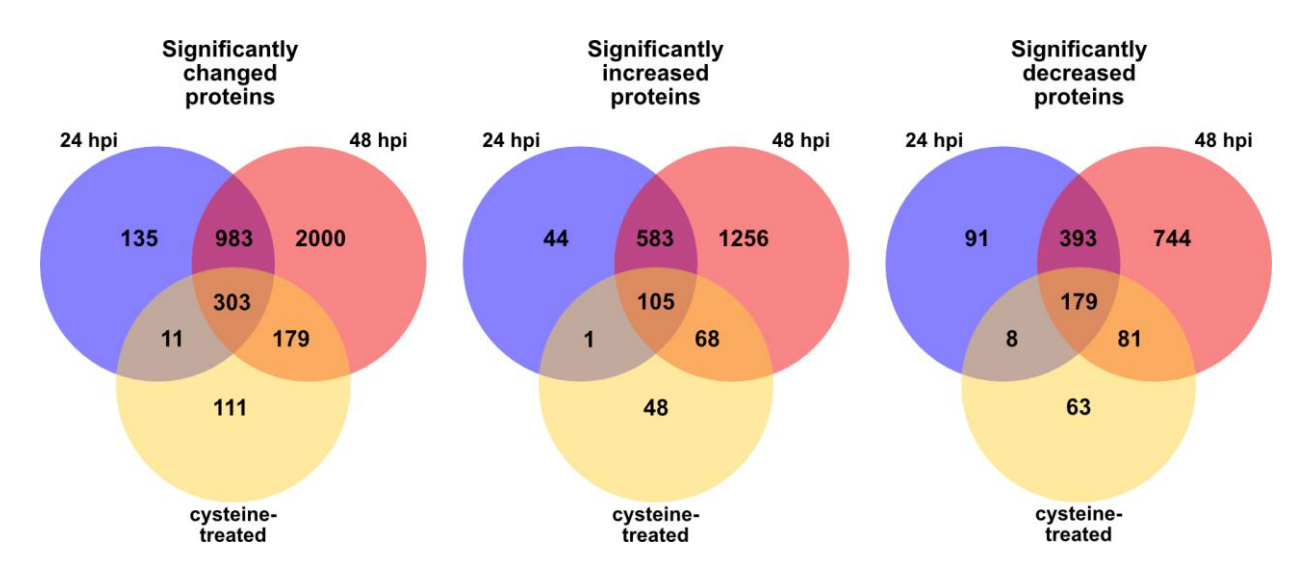
The mass spectrometry proteomics data have been deposited to the ProteomeXchange Consortium (http://proteomecentral.proteomexchange.org) via the PRIDE partner repository (Perez-Riverol et al. 2022) with the dataset identifier PXD054723.

### 3.6 Supplementary Figures



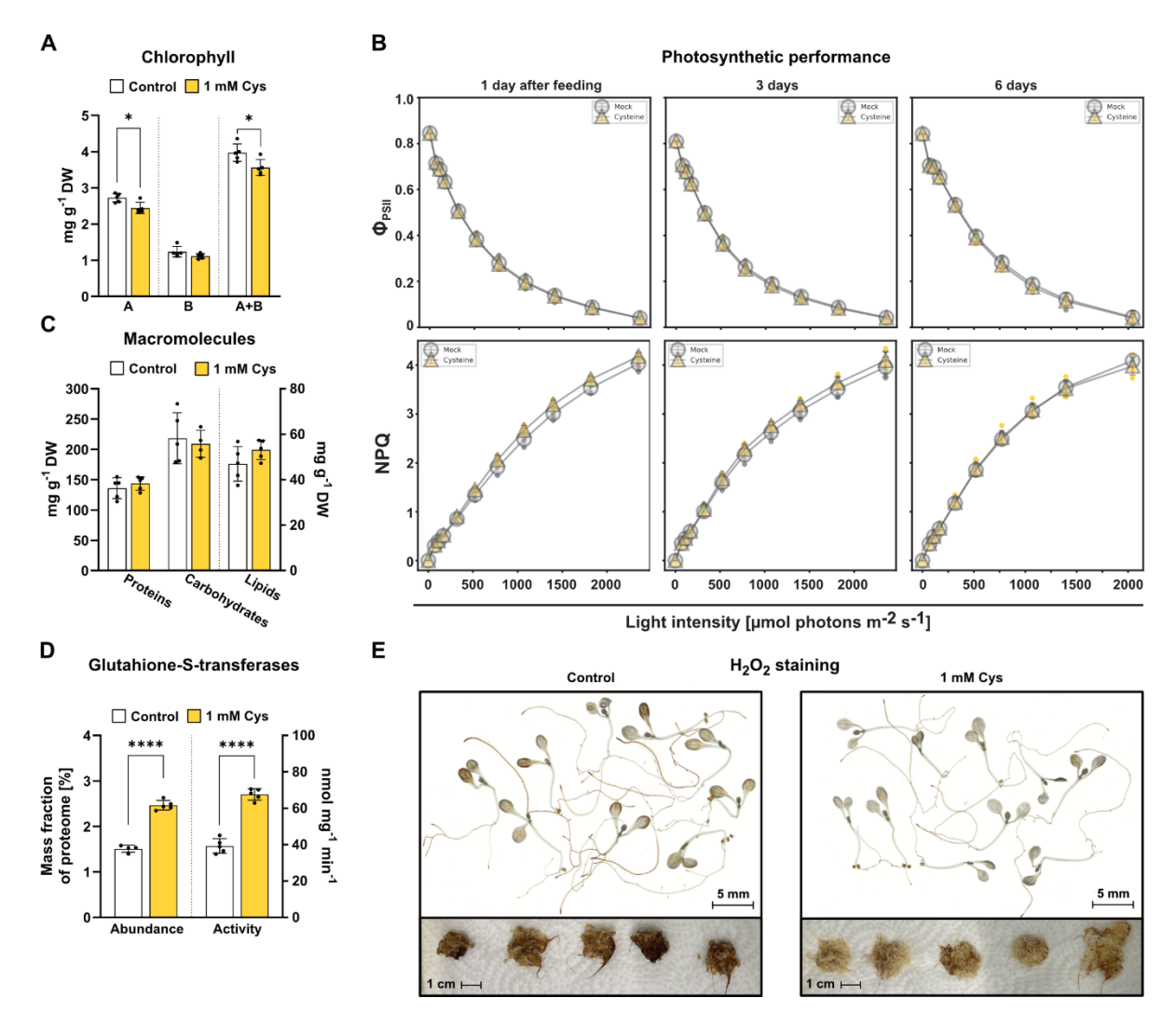
Supplementary Figure 3.1: Seedling culture - dynamics and effects of cysteine treatment.

An *Arabidopsis thaliana* seedling culture was supplemented with 1 mM L-cysteine for 24 hours before harvest. **A**. Pictures of representative control (left) and cysteine supplemented (right) seedling cultures. **B**. The cysteine concentration [mM] of media containing 6 days old seedlings was determined 0, 1, 3, 6, 12 and 24 hours after addition of 1 mM cysteine. Mean values (dots)  $\pm$  SD are shown (n = 5). **C**. Oxygen consumption rates [nmol O<sub>2</sub> · g dry weight<sup>-1</sup> · min<sup>-1</sup>] of control seedlings (white bars) and seedlings fed with 1 mM L-cysteine for 24h (yellow bars) in the presence (+Cys) or absence (-Cys) of 1 mM L-cysteine in the respiration buffer (left axis, n = 5). The seedlings were lyophilized after respiration measurements and oxygen consumption rates were calculated based on dry weight. Oxygen content [µM] of control medium (white bar) and medium supplemented with 1 mM cysteine for 24h (yellow bar) (right axis, n = 4). Mean (bars) and individual (dots) values  $\pm$  SD are shown.



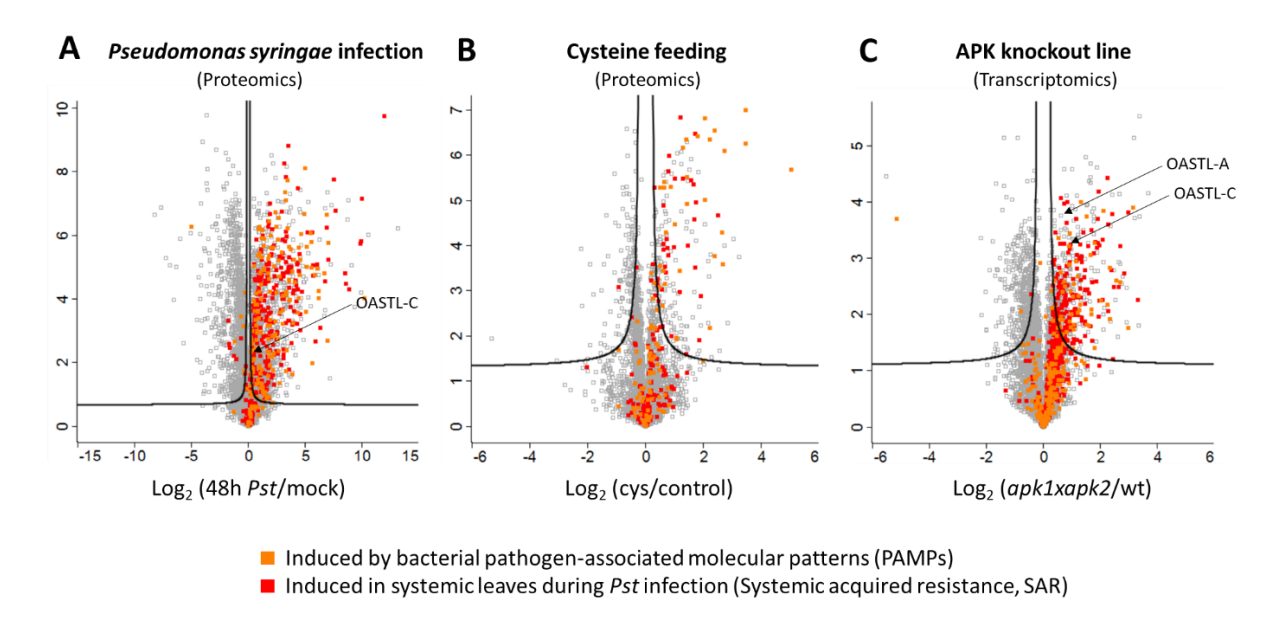
Supplementary Figure 3.2 Overlap between the Arabidopsis proteome responses to pathogen interaction and cysteine treatment.

A. thaliana plants were infiltrated with P. syringae DC3000 (Pst) (2.5 x 10<sup>6</sup> colony forming units per ml). Six leaves per plant were sampled at 24 and 48 hours after inoculation and used for shotgun proteome analysis (24 hpi and 48 hpi). In addition, an A. thaliana seedling culture was supplemented with 1 mM L-cysteine for 24 hours before harvest and proteome analysis (cysteine-treated). The sum of significantly increased (middle) and decreased (right) proteins in a compared subset does not necessarily equal the respective total amount of significantly changed proteins in that subset (left) due to proteins that are increased in one but decreased in the other condition or vice versa.



Supplementary Figure 3.3 Arabidopsis response to cysteine treatment.

**A**. Seedling contents of chlorophyll A and B [mg  $\cdot$  g dry weight<sup>-1</sup>] (n = 5). **B**. Photosynthetic performance of rosette leaves determined via chlorophyll a fluorescence. **C**. Seedling contents of proteins, carbohydrates, and lipids [mg  $\cdot$  g dry weight<sup>-1</sup>] (n = 5). **D**. Seedling abundance [mass fraction of proteome in %] and activity [nmol  $\cdot$  mg<sup>-1</sup>  $\cdot$  min<sup>-1</sup>] of glutathione-S-transferases (n = 4-5). Mean (bars) and individual (dots) values  $\pm$  SD are shown. Asterisks indicate statistically significant differences compared with control seedlings following students t-test (\* P < 0.05; \*\*\*\* P < 0.001). **E**. Seedlings following H<sub>2</sub>O<sub>2</sub> staining using 3,3'-diaminobenzidine with scans of representative seedlings (top) and pictures of whole seedling cultures (bottom). **A**, **C**, **D**, **E**: An *A. thaliana* seedling culture was supplemented with 1 mM L-cysteine for 24 hours before harvest. **B**: A. thaliana plants were grown for 6 weeks under short-day conditions and watered with 10 mM L-cysteine for 24 h before analysis.



Supplementary Figure 3.4: Overlap between proteome and transcriptome responses to bacterial pathogens and cysteine accumulation.

**A.** *A.* thaliana plants were infiltrated with *P.* syringae DC3000 (Pst) ( $2.5 \times 10^6$  colony forming units per ml). Six leaves per plant were sampled 48 hours after inoculation and used for shotgun proteome analysis. Infected leaves had 6.6-fold increased cysteine contents compared to mock-infected leaves. **B.** An *A.* thaliana seedling culture was supplemented with 1 mM L-cysteine for 24 hours before harvest and proteome analysis. Cysteine treated seedlings had 7.6fold increased cysteine contents compared to the control. **C.** Transcriptome analysis of rosette leaves of adenosine 5'-phosphosulfate kinase deficient Arabidopsis mutants compared to wild type plants. Mutant plants had 4-fold increased cysteine contents compared to the wild type. Data are taken from (Mugford et al. 2009). In all three volcano plots genes with significantly induced expression ( $\log_2 FC \ge 1.5$ ) in response to bacterial PAMP treatment (Bjornson et al. 2021) or during systemic acquired resistance (Gruner et al. 2013) are highlighted in orange and red, respectively. OASTL-A: Cytosolic O-acetylserine (thiol) lyase (AT4G14880), OASTL-C: Mitochondrial O-acetylserine (thiol) lyase (AT3G59760).

#### 3.7 References

Alfieri, Andrea et al. (2020): The structural bases for agonist diversity in an Arabidopsis thaliana glutamate receptor-like channel. In: *Proceedings of the National Academy of Sciences of the United States of America* 117 (1), S. 752–760. DOI: 10.1073/pnas.1905142117.

Alvarez, Consolacion; Calo, Leticia; Romero, Luis C.; Garcia, Irene; Gotor, Cecilia (2010): An O-Acetylserine(thiol)lyase Homolog with I-Cysteine Desulfhydrase Activity Regulates Cysteine Homeostasis in Arabidopsis. In: *Plant Physiol* 152 (2), S. 656–669. DOI: 10.1104/pp.109.147975.

Álvarez, Consolación; Ángeles Bermúdez, M.; Romero, Luis C.; Gotor, Cecilia; García, Irene (2012): Cysteine homeostasis plays an essential role in plant immunity. In: *New Phytologist* 193 (1), S. 165–177. DOI: 10.1111/j.1469-8137.2011.03889.x.

Aroca, Angeles; Benito, Juan M.; Gotor, Cecilia; Romero, Luis C. (2017): Persulfidation proteome reveals the regulation of protein function by hydrogen sulfide in diverse biological processes in Arabidopsis. In: *J Exp Bot* 68 (17), S. 4915–4927. DOI: 10.1093/jxb/erx294.

Baker, Neil R. (2008): Chlorophyll Fluorescence: A Probe of Photosynthesis In Vivo. In: *Annual review of plant biology* 59 (Volume 59, 2008), S. 89–113. DOI: 10.1146/annurev.arplant.59.032607.092759.

Bauer, Sibylle et al. (2021): UGT76B1, a promiscuous hub of small molecule-based immune signaling, glucosylates N-hydroxypipecolic acid, and balances plant immunity. In: *Plant Cell* 33 (3), S. 714–734. DOI: 10.1093/plcell/koaa044.

Bednarek, Paweł; Piślewska-Bednarek, Mariola; Ver Loren Themaat, Emiel; Maddula, Ravi Kumar; Svatoš, Aleš; Schulze-Lefert, Paul (2011): Conservation and clade-specific diversification of pathogen-inducible tryptophan and indole glucosinolate metabolism in Arabidopsis thaliana relatives. In: *New Phytologist* 192 (3), S. 713–726. DOI: 10.1111/j.1469-8137.2011.03824.x.

Begara-Morales, J. C. et al. (2016): Protein S-Nitrosylation and S-Glutathionylation as Regulators of Redox Homeostasis During Abiotic Stress Response. In: Dharmendra K. Gupta, José M. Palma und Francisco J. Corpas (Hg.): Redox State as a Central Regulator of Plant-Cell Stress Responses. Cham: Springer International Publishing, S. 365–386.

Birke, Hannah; Heeg, Corinna; Wirtz, Markus; Hell, Rüdiger (2013): Successful Fertilization Requires the Presence of at Least One Major O-Acetylserine(thiol)lyase for Cysteine Synthesis in Pollen of Arabidopsis. In: *Plant Physiol* 163 (2), S. 959–972. DOI: 10.1104/pp.113.221200.

Bjornson, Marta; Pimprikar, Priya; Nürnberger, Thorsten; Zipfel, Cyril (2021): The transcriptional landscape of Arabidopsis thaliana pattern-triggered immunity. In: *Nature Plants* 7 (5), S. 579–586. DOI: 10.1038/s41477-021-00874-5.

Böttcher, Christoph; Westphal, Lore; Schmotz, Constanze; Prade, Elke; Scheel, Dierk; Glawischnig, Erich (2009): The Multifunctional Enzyme CYP71B15 (PHYTOALEXIN DEFICIENT3) Converts Cysteine-Indole-3-Acetonitrile to Camalexin in the Indole-3-Acetonitrile Metabolic Network of Arabidopsis thaliana. In: *Plant Cell* 21 (6), S. 1830–1845. DOI: 10.1105/tpc.109.066670.

Buchanan, Bob B.; Balmer, Yves (2005): REDOX REGULATION: A Broadening Horizon. In: *Annual review of plant biology* 56 (Volume 56, 2005), S. 187–220. DOI: 10.1146/annurev.arplant.56.032604.144246.

Caubrière, Damien; Moseler, Anna; Rouhier, Nicolas; Couturier, Jérémy (2023): Diversity and roles of cysteine desulfurases in photosynthetic organisms. In: *J Exp Bot* 74 (11), S. 3345–3360. DOI: 10.1093/jxb/erad065.

Chen, Sisi et al. (2020): Hydrogen Sulfide Positively Regulates Abscisic Acid Signaling through Persulfidation of SnRK2.6 in Guard Cells. In: *Molecular Plant* 13 (5), S. 732–744. DOI: 10.1016/j.molp.2020.01.004.

Colombatti, Francisco; Gonzalez, Daniel H.; Welchen, Elina (2014): Plant mitochondria under pathogen attack: A sigh of relief or a last breath? In: *Mitochondrion* 19, S. 238–244. DOI: 10.1016/j.mito.2014.03.006.

Cooper, Chris E.; Brown, Guy C. (2008): The inhibition of mitochondrial cytochrome oxidase by the gases carbon monoxide, nitric oxide, hydrogen cyanide and hydrogen sulfide: chemical mechanism and physiological significance. In: *Journal of Bioenergetics and Biomembranes* 40 (5), S. 533–539. DOI: 10.1007/s10863-008-9166-6.

Couturier, Jérémy; Touraine, Brigitte; Briat, Jean-Francois; Gaymard, Frédéric; Rouhier, Nicolas (2013): The iron-sulfur cluster assembly machineries in plants: current knowledge and open questions. In: *Frontiers in Plant Science* 4. Online verfügbar unter https://www.frontiersin.org/journals/plant-science/articles/10.3389/fpls.2013.00259.

Cox, Jürgen; Mann, Matthias (2008): MaxQuant enables high peptide identification rates, individualized p.p.b.-range mass accuracies and proteome-wide protein quantification. In: *Nature Biotechnology* 26 (12), S. 1367–1372. DOI: 10.1038/nbt.1511.

Cummins, Ian; Dixon, David P.; Freitag-Pohl, Stefanie; Skipsey, Mark; Edwards, Robert (2011): Multiple roles for plant glutathione transferases in xenobiotic detoxification. In: *Drug Metabolism Reviews* 43 (2), S. 266–280. DOI: 10.3109/03602532.2011.552910.

Cvetkoska, Marina; Vanlerberghe, Greg C. (2012): Coordination of a mitochondrial superoxide burst during the hypersensitive response to bacterial pathogen in Nicotiana tabacum. In: *Plant, cell & environment* 35 (6), S. 1121–1136. DOI: 10.1111/j.1365-3040.2011.02477.x.

Dixon, David P.; Sellars, Jonathan D.; Edwards, Robert (2011): The Arabidopsis phi class glutathione transferase AtGSTF2: binding and regulation by biologically active heterocyclic ligands. In: *Biochem J* 438 (1), S. 63–70. DOI: 10.1042/BJ20101884.

Droux, Michel (2003): Plant serine acetyltransferase: new insights for regulation of sulphur metabolism in plant cells. In: *Plant Physiology and Biochemistry* 41 (6), S. 619–627. DOI: 10.1016/S0981-9428(03)00083-4.

Droux, Michel (2004): Sulfur Assimilation and the Role of Sulfur in Plant Metabolism: A Survey. In: *Photosynthesis Research* 79 (3), S. 331–348. DOI: 10.1023/B:PRES.0000017196.95499.11.

Ernst, Laura et al. (2010): Sulphate as a xylem-borne chemical signal precedes the expression of ABA biosynthetic genes in maize roots. In: *J Exp Bot* 61 (12), S. 3395–3405. DOI: 10.1093/jxb/erg160.

Fonseca, Jose Pedro et al. (2020): Iron–Sulfur Cluster Protein NITROGEN FIXATION S-LIKE1 and Its Interactor FRATAXIN Function in Plant Immunity. In: *Plant Physiol* 184 (3), S. 1532–1548. DOI: 10.1104/pp.20.00950.

Foyer, Christine Helen; Noctor, Graham (2011): Ascorbate and Glutathione: The Heart of the Redox Hub. In: *Plant Physiol* 155 (1), S. 2–18. DOI: 10.1104/pp.110.167569.

Frazzon, Ana Paula Guedes et al. (2007): Functional analysis of Arabidopsis genes involved in mitochondrial iron–sulfur cluster assembly. In: *Plant Molecular Biology* 64 (3), S. 225–240. DOI: 10.1007/s11103-007-9147-x.

Giovanelli, John; Mudd, S. Harvey; Datko, Anne H. (1985): Quantitative Analysis of Pathways of Methionine Metabolism and Their Regulation in Lemna. In: *Plant Physiol* 78 (3), S. 555–560. DOI: 10.1104/pp.78.3.555.

Glawischnig, Erich (2007): Camalexin. In: *Phytochemistry* 68 (4), S. 401–406. DOI: 10.1016/j.phytochem.2006.12.005.

Goda, Hideki et al. (2008): The AtGenExpress hormone and chemical treatment data set: experimental design, data evaluation, model data analysis and data access. In: *Plant J* 55 (3), S. 526–542. DOI: 10.1111/j.1365-313X.2008.03510.x.

Grenzi, Matteo et al. (2023): Long-distance turgor pressure changes induce local activation of plant glutamate receptor-like channels. In: *Current biology : CB* 33 (6), 1019-1035.e8. DOI: 10.1016/j.cub.2023.01.042.

Gruner, Katrin; Griebel, Thomas; Návarová, Hana; Attaran, Elham; Zeier, Jürgen (2013): Reprogramming of plants during systemic acquired resistance. In: *Frontiers in Plant Science* 4. DOI: 10.3389/fpls.2013.00252.

Gupta, R. N.; Spenser, I. D. (1969): Biosynthesis of the Piperidine Nucleus: The mode of incorporation of lysine into pipecolic acid and into piperidine alkaloids. In: *Journal of Biological Chemistry* 244 (1), S. 88–94. DOI: 10.1016/S0021-9258(19)78195-2.

Harun, Sarahani; Abdullah-Zawawi, Muhammad-Redha; Goh, Hoe-Han; Mohamed-Hussein, Zeti-Azura (2020): A Comprehensive Gene Inventory for Glucosinolate Biosynthetic Pathway in Arabidopsis thaliana. In: *Journal of Agricultural and Food Chemistry* 68 (28), S. 7281–7297. DOI: 10.1021/acs.jafc.0c01916.

Hatzfeld, Yves; Maruyama, Akiko; Schmidt, Ahlert; Noji, Masaaki; Ishizawa, Kimiharu; Saito, Kazuki (2000): β-Cyanoalanine Synthase Is a Mitochondrial Cysteine Synthase-Like Protein in Spinach and Arabidopsis1. In: *Plant Physiol* 123 (3), S. 1163–1172. DOI: 10.1104/pp.123.3.1163.

Heeg, Corinna et al. (2008): Analysis of the Arabidopsis O-Acetylserine(thiol)lyase Gene Family Demonstrates Compartment-Specific Differences in the Regulation of Cysteine Synthesis. In: *Plant Cell* 20 (1), S. 168–185. DOI: 10.1105/tpc.107.056747.

Heinemann, Björn; Hildebrandt, Tatjana M. (2021): The role of amino acid metabolism in signaling and metabolic adaptation to stress-induced energy deficiency in plants. In: *J Exp Bot* 72 (13), S. 4634–4645. DOI: 10.1093/jxb/erab182.

Hell, Rüdiger; Wirtz, Markus (2011): Molecular Biology, Biochemistry and Cellular Physiology of Cysteine Metabolism in *Arabidopsis thaliana*. In: *The Arabidopsis Book* 2011 (9). DOI: 10.1199/tab.0154.

Hildebrandt, Tatjana M. (2018): Synthesis versus degradation: directions of amino acid metabolism during Arabidopsis abiotic stress response. In: *Plant Molecular Biology* 98 (1), S. 121–135. DOI: 10.1007/s11103-018-0767-0.

Hildebrandt, Tatjana M.; Nunes Nesi, Adriano; Araújo, Wagner L.; Braun, Hans-Peter (2015): Amino Acid Catabolism in Plants. In: *Molecular Plant* 8 (11), S. 1563–1579. DOI: 10.1016/j.molp.2015.09.005.

Höfler, Saskia et al. (2016): Dealing with the sulfur part of cysteine: four enzymatic steps degrade I-cysteine to pyruvate and thiosulfate in Arabidopsis mitochondria. In: *Physiologia Plantarum* 157 (3), S. 352–366. DOI: 10.1111/ppl.12454.

Hughes, Christopher S.; Moggridge, Sophie; Müller, Torsten; Sorensen, Poul H.; Morin, Gregg B.; Krijgsveld, Jeroen (2019): Single-pot, solid-phase-enhanced sample preparation for

proteomics experiments. In: *Nature Protocols* 14 (1), S. 68–85. DOI: 10.1038/s41596-018-0082-x.

Jones, Alexandra M. E.; Thomas, Vincent; Bennett, Mark H.; Mansfield, John; Grant, Murray (2006): Modifications to the Arabidopsis defense proteome occur prior to significant transcriptional change in response to inoculation with Pseudomonas syringae. In: *Plant Physiol* 142 (4), S. 1603–1620. DOI: 10.1104/pp.106.086231.

Klecker, Maria et al. (2014): A Shoot-Specific Hypoxic Response of Arabidopsis Sheds Light on the Role of the Phosphate-Responsive Transcription Factor PHOSPHATE STARVATION RESPONSE1. In: *Plant Physiol* 165 (2), S. 774–790. DOI: 10.1104/pp.114.237990.

Koprivova, Anna et al. (2019): Root-specific camalexin biosynthesis controls the plant growth-promoting effects of multiple bacterial strains. In: *Proceedings of the National Academy of Sciences* 116 (31), S. 15735–15744. DOI: 10.1073/pnas.1818604116.

Koprivova, Anna et al. (2023): Natural Variation in OASC Gene for Mitochondrial O-Acetylserine Thiollyase Affects Sulfate Levels in Arabidopsis. In: *Plants* 12 (1). DOI: 10.3390/plants12010035.

Koschmieder, Julian et al. (2022): Color recycling: metabolization of apocarotenoid degradation products suggests carbon regeneration via primary metabolic pathways. In: *Plant cell reports* 41 (4), S. 961–977. DOI: 10.1007/s00299-022-02831-8.

Krüger, Stephan et al. (2009): Analysis of cytosolic and plastidic serine acetyltransferase mutants and subcellular metabolite distributions suggests interplay of the cellular compartments for cysteine biosynthesis in Arabidopsis. In: *Plant, cell & environment* 32 (4), S. 349–367. DOI: 10.1111/j.1365-3040.2009.01928.x.

Lairson, L. L.; Henrissat, B.; Davies, G. J.; Withers, S. G. (2008): Glycosyltransferases: Structures, Functions, and Mechanisms. In: *Annual Review of Biochemistry* 77 (Volume 77, 2008), S. 521–555. DOI: 10.1146/annurev.biochem.76.061005.092322.

Langlois-Meurinne, Mathilde; Gachon, Claire M.M.; Saindrenan, Patrick (2005): Pathogen-Responsive Expression of Glycosyltransferase Genes UGT73B3 and UGT73B5 Is Necessary for Resistance to Pseudomonas syringae pv tomato in Arabidopsis. In: *Plant Physiol* 139 (4), S. 1890–1901. DOI: 10.1104/pp.105.067223.

Li, Feng et al. (2013): Glutamate Receptor-Like Channel3.3 Is Involved in Mediating Glutathione-Triggered Cytosolic Calcium Transients, Transcriptional Changes, and Innate Immunity Responses in Arabidopsis. In: *Plant Physiol* 162 (3), S. 1497–1509. DOI: 10.1104/pp.113.217208.

Li, Miaomiao et al. (2024): Insights from Structure-Based Simulations into the Persulfidation of Uridine Diphosphate-Glycosyltransferase71c5 Facilitating the Reversible Inactivation of Abscisic Acid. In: *International journal of molecular sciences* 25 (17). DOI: 10.3390/ijms25179679.

Lichtenthaler, Hartmut K. (1987): [34] Chlorophylls and carotenoids: Pigments of photosynthetic biomembranes. In: Plant Cell Membranes, Bd. 148: Elsevier (Methods in Enzymology), S. 350–382.

Lieberherr, Damien; Wagner, Ulrich; Dubuis, Pierre-Henri; Métraux, Jean-Pierre; Mauch, Felix (2003): The Rapid Induction of Glutathione S-Transferases AtGSTF2 and AtGSTF6 by Avirulent Pseudomonas syringae is the Result of Combined Salicylic Acid and Ethylene Signaling. In: *Plant Cell Physiol* 44 (7), S. 750–757. DOI: 10.1093/pcp/pcg093.

Lim, Eng-Kiat et al. (2002): The Activity of ArabidopsisGlycosyltransferases toward Salicylic Acid, 4-Hydroxybenzoic Acid, and Other Benzoates\*. In: *Journal of Biological Chemistry* 277 (1), S. 586–592. DOI: 10.1074/jbc.M109287200.

Liu, Zhen et al. (2015): UDP-Glucosyltransferase71C5, a Major Glucosyltransferase, Mediates Abscisic Acid Homeostasis in Arabidopsis. In: *Plant Physiol* 167 (4), S. 1659–1670. DOI: 10.1104/pp.15.00053.

López-Martín, M. Carmen; Becana, Manuel; Romero, Luis C.; Gotor, Cecilia (2008): Knocking Out Cytosolic Cysteine Synthesis Compromises the Antioxidant Capacity of the Cytosol to Maintain Discrete Concentrations of Hydrogen Peroxide in Arabidopsis. In: *Plant Physiol* 147 (2), S. 562–572. DOI: 10.1104/pp.108.117408.

Maeda, Hiroshi; Dudareva, Natalia (2012): The Shikimate Pathway and Aromatic Amino Acid Biosynthesis in Plants. In: *Annual review of plant biology* 63 (Volume 63, 2012), S. 73–105. DOI: 10.1146/annurev-arplant-042811-105439.

Maldonado-Alconada, Ana M.; Echevarría-Zomeño, Sira; Lindermayr, Christian; Redondo-López, Inmaculada; Durner, Jörg; Jorrín-Novo, Jesús V. (2011): Proteomic analysis of Arabidopsis protein S-nitrosylation in response to inoculation with Pseudomonas syringae. In: *Acta Physiol Plant* 33 (4), S. 1493–1514. DOI: 10.1007/s11738-010-0688-2.

Martí-Andrés, Pablo et al. (2024): TRP14 is the rate-limiting enzyme for intracellular cystine reduction and regulates proteome cysteinylation. In: *The EMBO Journal* 43 (13), S. 2789–2812. DOI: 10.1038/s44318-024-00117-1.

Maxwell, Denis P.; Wang, Yong; McIntosh, Lee (1999): The alternative oxidase lowers mitochondrial reactive oxygen production in plant cells. In: *Proceedings of the National Academy of Sciences* 96 (14), S. 8271–8276. DOI: 10.1073/pnas.96.14.8271.

Mikulášek, Kamil; Konečná, Hana; Potěšil, David; Holánková, Renata; Havliš, Jan; Zdráhal, Zbyněk (2021): SP3 Protocol for Proteomic Plant Sample Preparation Prior LC-MS/MS. In: *Frontiers in Plant Science* 12. Online verfügbar unter https://www.frontiersin.org/journals/plant-science/articles/10.3389/fpls.2021.635550.

Moormann, Jannis; Heinemann, Björn; Hildebrandt, Tatjana M. (2022): News about amino acid metabolism in plant–microbe interactions. In: *Trends in Biochemical Sciences* 47 (10), S. 839–850. DOI: 10.1016/j.tibs.2022.07.001.

Moseler, Anna; Wagner, Stephan; Meyer, Andreas J. (2024): Protein persulfidation in plants: mechanisms and functions beyond a simple stress response. In: *Biological Chemistry* 405 (9-10), S. 547–566. DOI: 10.1515/hsz-2024-0038.

Mugford, Sarah G. et al. (2009): Disruption of Adenosine-5'-Phosphosulfate Kinase in Arabidopsis Reduces Levels of Sulfated Secondary Metabolites. In: *Plant Cell* 21 (3), S. 910–927. DOI: 10.1105/tpc.109.065581.

Návarová, Hana; Bernsdorff, Friederike; Döring, Anne-Christin; Zeier, Jürgen (2012): Pipecolic Acid, an Endogenous Mediator of Defense Amplification and Priming, Is a Critical Regulator of Inducible Plant Immunity. In: *Plant Cell* 24 (12), S. 5123–5141. DOI: 10.1105/tpc.112.103564.

Noctor, Graham; Cohen, Mathias; Trémulot, Lug; Châtel-Innocenti, Gilles; van Breusegem, Frank; Mhamdi, Amna (2024): Glutathione: a key modulator of plant defence and metabolism through multiple mechanisms. In: *J Exp Bot* 75 (15), S. 4549–4572. DOI: 10.1093/jxb/erae194.

Pantaleno, Rosario; Scuffi, Denise; Schiel, Paula; Schwarzländer, Markus; Costa, Alex; García-Mata, Carlos (2025): Mitochondrial ß-Cyanoalanine Synthase Participates in flg22-Induced Stomatal Immunity. In: *Plant Cell Environ* 48 (1), S. 537–552. DOI: 10.1111/pce.15155.

Pastorczyk, Marta et al. (2020): The role of CYP71A12 monooxygenase in pathogen-triggered tryptophan metabolism and Arabidopsis immunity. In: *New Phytologist* 225 (1), S. 400–412. DOI: 10.1111/nph.16118.

Pedre, Brandán et al. (2023): 3-Mercaptopyruvate sulfur transferase is a protein persulfidase. In: *Nature chemical biology* 19 (4), S. 507–517. DOI: 10.1038/s41589-022-01244-8.

Pedrotti, Lorenzo et al. (2018): Snf1-RELATED KINASE1-Controlled C/S1-bZIP Signaling Activates Alternative Mitochondrial Metabolic Pathways to Ensure Plant Survival in Extended Darkness. In: *Plant Cell* 30 (2), S. 495–509. DOI: 10.1105/tpc.17.00414.

Peiser, Galen D.; Wang, Tsu-Tsuen; Hoffman, Neil E.; Yang, Shang Fa; Liu, Hung-wen; Walsh, Christopher T. (1984): Formation of cyanide from carbon 1 of 1-aminocyclopropane-1-carboxylic acid during its conversion to ethylene. In: *Proceedings of the National Academy of Sciences* 81 (10), S. 3059–3063. DOI: 10.1073/pnas.81.10.3059.

Perez-Riverol, Yasset et al. (2022): The PRIDE database resources in 2022: a hub for mass spectrometry-based proteomics evidences. In: *Nucleic Acids Res* 50 (D1), D543-D552. DOI: 10.1093/nar/gkab1038.

Ruffet, Marie-Line; Lebrun, Michel; Droux, Michel; Douce, Roland (1995): Subcellular Distribution of Serine Acetyltransferase from Pisum sativum and Characterization of an Arabidopsis thaliana Putative Cytosolic Isoform. In: *European Journal of Biochemistry* 227 (1-2), S. 500–509. DOI: 10.1111/j.1432-1033.1995.tb20416.x.

Sappl, Pia G.; Oñate-Sánchez, Luis; Singh, Karam B.; Millar, A. Harvey (2004): Proteomic Analysis of Glutathione S-Transferases of Arabidopsis thaliana Reveals Differential Salicylic Acid-Induced Expression of the Plant-Specific Phi and Tau Classes. In: *Plant Molecular Biology* 54 (2), S. 205–219. DOI: 10.1023/B:PLAN.0000028786.57439.b3.

Shen, Jie et al. (2020): Persulfidation-based Modification of Cysteine Desulfhydrase and the NADPH Oxidase RBOHD Controls Guard Cell Abscisic Acid Signaling. In: *Plant Cell* 32 (4), S. 1000–1017. DOI: 10.1105/tpc.19.00826.

Simons, Bert H.; Millenaar, Frank F.; Mulder, Lonneke; van Loon, Leendert C.; Lambers, Hans (1999): Enhanced Expression and Activation of the Alternative Oxidase during Infection of Arabidopsis withPseudomonas syringae pv tomato1. In: *Plant Physiol* 120 (2), S. 529–538. DOI: 10.1104/pp.120.2.529.

Su, Tongbing et al. (2011): Glutathione-Indole-3-Acetonitrile Is Required for Camalexin Biosynthesis in Arabidopsis thaliana. In: *Plant Cell* 23 (1), S. 364–380. DOI: 10.1105/tpc.110.079145.

Sueiro-Olivares, Monica et al. (2021): Fungal and host protein persulfidation are functionally correlated and modulate both virulence and antifungal response. In: *PLOS Biology* 19 (6), e3001247. DOI: 10.1371/journal.pbio.3001247.

Szabados, László; Savouré, Arnould (2010): Proline: a multifunctional amino acid. In: *Trends in Plant Science* 15 (2), S. 89–97. DOI: 10.1016/j.tplants.2009.11.009.

Takahashi, Hideki (2010): Chapter 4 - Regulation of Sulfate Transport and Assimilation in Plants. In: Kwang W. Jeon (Hg.): International Review of Cell and Molecular Biology, Bd. 281: Academic Press, S. 129–159. Online verfügbar unter https://www.sciencedirect.com/science/article/pii/S1937644810810044.

Takahashi, Hideki; Kopriva, Stanislav; Giordano, Mario; Saito, Kazuki; Hell, Rüdiger (2011): Sulfur Assimilation in Photosynthetic Organisms: Molecular Functions and Regulations of Transporters and Assimilatory Enzymes. In: *Annual review of plant biology* 62 (Volume 62, 2011), S. 157–184. DOI: 10.1146/annurev-arplant-042110-103921.

Tian, Miaoying; Dahl, Caroline C. von; Liu, Po-Pu; Friso, Giulia; van Wijk, Klaas J.; Klessig, Daniel F. (2012): The combined use of photoaffinity labeling and surface plasmon resonance-based technology identifies multiple salicylic acid-binding proteins. In: *Plant J* 72 (6), S. 1027–1038. DOI: 10.1111/tpj.12016.

Torres Zabala, Marta de; Bennett, Mark H.; Truman, William H.; Grant, Murray R. (2009): Antagonism between salicylic and abscisic acid reflects early host–pathogen conflict and moulds plant defence responses. In: *Plant J* 59 (3), S. 375–386. DOI: 10.1111/j.1365-313X.2009.03875.x.

Torres-Zabala, Marta de et al. (2007): *Pseudomonas syringae* pv. *tomato* hijacks the *Arabidopsis* abscisic acid signalling pathway to cause disease. In: *The EMBO Journal* 26 (5), 1434-1443. DOI: 10.1038/sj.emboj.7601575.

Toyota, Masatsugu et al. (2018): Glutamate triggers long-distance, calcium-based plant defense signaling. In: *Science* 361 (6407), S. 1112–1115. DOI: 10.1126/science.aat7744.

Tyanova, Stefka et al. (2016): The Perseus computational platform for comprehensive analysis of (prote)omics data. In: *Nature Methods* 13 (9), S. 731–740. DOI: 10.1038/nmeth.3901.

van Hoewyk, Doug; Pilon, Marinus; Pilon-Smits, Elizabeth A.H. (2008): The functions of NifS-like proteins in plant sulfur and selenium metabolism. In: *Plant Science* 174 (2), S. 117–123. DOI: 10.1016/j.plantsci.2007.10.004.

Wang, Dong; Amornsiripanitch, Nita; Dong, Xinnian (2006): A Genomic Approach to Identify Regulatory Nodes in the Transcriptional Network of Systemic Acquired Resistance in Plants. In: *PLOS Pathogens* 2 (11), e123. DOI: 10.1371/journal.ppat.0020123.

Watanabe, Mutsumi; Kusano, Miyako; Oikawa, Akira; Fukushima, Atsushi; Noji, Masaaki; Saito, Kazuki (2008): Physiological Roles of the β-Substituted Alanine Synthase Gene Family in Arabidopsis. In: *Plant Physiol* 146 (1), S. 310–320. DOI: 10.1104/pp.107.106831.

Wirtz, Markus; Hell, Rüdiger (2006): Functional analysis of the cysteine synthase protein complex from plants: Structural, biochemical and regulatory properties. In: *Journal of plant physiology* 163 (3), S. 273–286. DOI: 10.1016/j.jplph.2005.11.013.

Zhou, Mingjian et al. (2021): Hydrogen sulfide-linked persulfidation of ABI4 controls ABA responses through the transactivation of MAPKKK18 in Arabidopsis. In: *Molecular Plant* 14 (6), S. 921–936. DOI: 10.1016/j.molp.2021.03.007.

Zhou, Yulu et al. (2023): Plant HEM1 specifies a condensation domain to control immune gene translation. In: *Nature Plants* 9 (2), S. 289–301. DOI: 10.1038/s41477-023-01355-7.

# 4 Thermal proteome profiling identifies mitochondrial aminotransferases involved in cysteine catabolism via persulfides in plants

Heinemann, Björn; **Moormann, Jannis**; Bady, Shivsam; Angermann, Cecile; Schrader, Andrea; Hildebrandt, Tatjana M. (2025): Thermal proteome profiling identifies mitochondrial aminotransferases involved in cysteine catabolism via persulfides in plants. *BioRxiv*. DOI: 10.1101/2025.05.23.655777

#### 4.1 Abstract

Cysteine is a central metabolite in plant sulfur metabolism, with key roles in biosynthesis, redox regulation, and stress responses. While a mitochondrial cysteine degradation pathway has been described, the enzyme catalyzing its initial transamination step remained unidentified. Here, we applied thermal proteome profiling (TPP) to Arabidopsis mitochondria to uncover cysteine-interacting proteins. TPP successfully detected known cysteine-utilizing enzymes, validating its utility in plant metabolic research. Among newly identified targets were two aminotransferases annotated as alanine and aspartate aminotransferases that catalyze the transamination of cysteine to 3-mercaptopyruvate in vitro. These enzymes, together with the sulfurtransferase STR1 and the persulfide dioxygenase ETHE1, reconstituted a complete mitochondrial cysteine catabolic pathway. Kinetic data indicate that alanine aminotransferase, in particular, may function in vivo under physiological cysteine levels. Additionally, GABA aminotransferase was inhibited by cysteine, suggesting a regulatory role in stress metabolism. Beyond enzyme identification, the dataset provides a resource for exploring cysteine-mediated regulation of transporters, RNA-editing factors, and respiratory components. Given cysteine's emerging role as a metabolic signal in stress responses, and the importance of allosteric regulation in amino acid metabolism, these findings highlight the broader regulatory potential of cysteine-protein interactions in plants. This study demonstrates the utility of TPP for elucidating metabolite-protein networks and advancing our understanding of plant mitochondrial metabolism.

#### 4.2 Introduction

The amino acid cysteine holds a central position in plant sulfur metabolism, serving as the entry point of reduced sulfur into organic molecules. It is a precursor for a wide range of sulfurcontaining compounds including methionine, cofactors such as thiamin, lipoic acid, biotin, Fe-S clusters, and the molybdenum cofactor (Droux 2004; Giovanelli et al. 1985; van Hoewyk et al. 2008). The tripeptide glutathione (y-glutamyl-cysteinyl-glycine) represents a major antioxidant and redox buffer in plants, protecting cells from oxidative damage and regulating cellular signaling pathways. Its antioxidant function is rooted in the redox potential of the thiol group (Foyer & Noctor 2011). In addition to its role in oxidative stress protection, glutathione contributes to heavy metal and xenobiotic detoxification, as well as to defense responses against pathogens (Noctor et al. 2024). Phytochelatins, synthesized from glutathione-derived cysteine, play a crucial role in heavy metal detoxification by chelating toxic metals and facilitating their sequestration in vacuoles (Cobbett & Goldsbrough 2002). Cysteine also serves as a precursor for the biosynthesis of various secondary metabolites, such as glucosinolates and camalexin, which play important roles in plant defense against herbivores and pathogens (Halkier & Gershenzon 2006; Su et al. 2011). Cysteine residues in proteins support structure, catalysis, and redox regulation through disulfide bond formation as well as reversible thiol modifications such as glutathionylation, nitrosylation, and persulfidation (Buchanan & Balmer 2005; Begara-Morales et al. 2016; Moseler et al. 2024).

Cysteine is synthesized via the sulfur assimilation pathway. Sulfate taken up from the soil is activated by ATP sulfurylase and reduced via sulfite to sulfide by APS reductase and sulfite reductase, respectively. O-acetylserine (OAS), synthesized from serine and acetyl-CoA by serine acetyltransferase (SERAT), serves as the carbon skeleton for cysteine biosynthesis. The final step, incorporation of sulfide into OAS to form cysteine, is catalyzed by OAS-(thiol)lyase (OASTL) (Takahashi 2010; Takahashi et al. 2011). SERAT and OASTL form a regulatory cysteine synthase complex that adjusts synthesis in response to substrate availability (Droux 2003; Wirtz & Hell 2006). Isoforms of both enzymes are present in the cytosol (SERAT1;1, SERAT3;1, SERAT3;2; OASTL-A), plastids (SERAT2;1; OASTL-B), and mitochondria (SERAT2;2; OASTL-C), enabling localized cysteine synthesis across compartments (Hell & Wirtz 2011; Ruffet et al. 1995; Watanabe et al. 2008). The cytosol and plastids account for 95% of total OASTL activity and null mutant analyses suggest a certain degree of functional redundancy among the major isoforms (Birke et al. 2013; Heeg et al. 2008; Krüger et al. 2009). However, evidence is accumulating for the functional relevance of compartment-specific cysteine metabolism.

Mitochondrial cysteine synthesis provides substrates for the production of cysteinyl-tRNA during translation of mitochondrial-encoded proteins but also supports other compartment-

specific functions (Figure 4.1). Cysteine serves as a sulfur donor for the formation of Fe-S clusters, which are critical cofactors for several mitochondrial enzymes, required for the biosynthesis of lipoic acid and biotin and can also be exported to the cytosol (Couturier et al. 2013). The capacity for cysteine synthesis in the mitochondrial matrix is also necessary for local detoxification of the potent cytochrome c oxidase inhibitors cyanide and hydrogen sulfide. Cyanide, a byproduct of ethylene and camalexin biosynthesis in Arabidopsis, is detoxified by cyanoalanine synthase (CAS-C1), which uses cysteine as a substrate to convert cyanide into β-cyanoalanine and hydrogen sulfide (Hatzfeld et al. 2000; Watanabe et al. 2008; Böttcher et al. 2009; Peiser et al. 1984). Accumulating hydrogen sulfide is then re-assimilated into cysteine by OASTL-C, completing a local detoxification cycle. Thus, mitochondrial cysteine metabolism is essential for maintaining electron transport chain activity (Cooper & Brown 2008). Beyond detoxification and biosynthesis, cysteine participates in regulatory processes with compartment specific mechanisms and functions. Recent work has demonstrated that cysteine triggers defense responses in Arabidopsis and enhances resistance to Pseudomonas syringae, suggesting a signaling function beyond metabolic necessity. The balance between cytosolic and organellar cysteine synthesis appears critical for proper immune function (Moormann et al. 2025). Post-translational modifications, such as disulfide bond formation and glutathionylation, nitrosylation, and persulfidation, mediate signaling processes by regulating protein function and activity (Buchanan & Balmer 2005; Begara-Morales et al. 2016; Moseler et al. 2024). The mechanism of protein persulfidation and de-persulfidation in the different subcellular compartments is largely unknown and the physiological relevance of this posttranslational modification in plant mitochondria has not been established yet (Moseler et al. 2024). It might well be linked to the mitochondrial cysteine degradation pathway, which produces persulfides as intermediates (Figure 4.1, (Höfler et al. 2016). Cysteine catabolism in the mitochondria starts with a transamination step to 3-mercaptopyruvate, which then transfers its thiol group to glutathione catalyzed by mercaptopyruvate sulfurtransferase (STR1, AT1G79230) producing glutathione persulfide. Yeast mercaptopyruvate sulfurtransferase has recently been shown to act as a protein persulfidase, and it is tempting to speculate that this function might also be present and relevant in plant mitochondria (Pedre et al. 2023). To complete the cysteine catabolic pathway, glutathione persulfide can be oxidized to sulfite by the persulfide dioxygenase ETHE1 (AT1G53580) and converted to thiosulfate via addition of a second persulfide group by STR1 (Krüßel et al. 2014; Höfler et al. 2016). For more than 10 years after initial identification of the mitochondrial cysteine degradation pathway in plants the aminotransferase catalyzing the initial step has remained enigmatic.

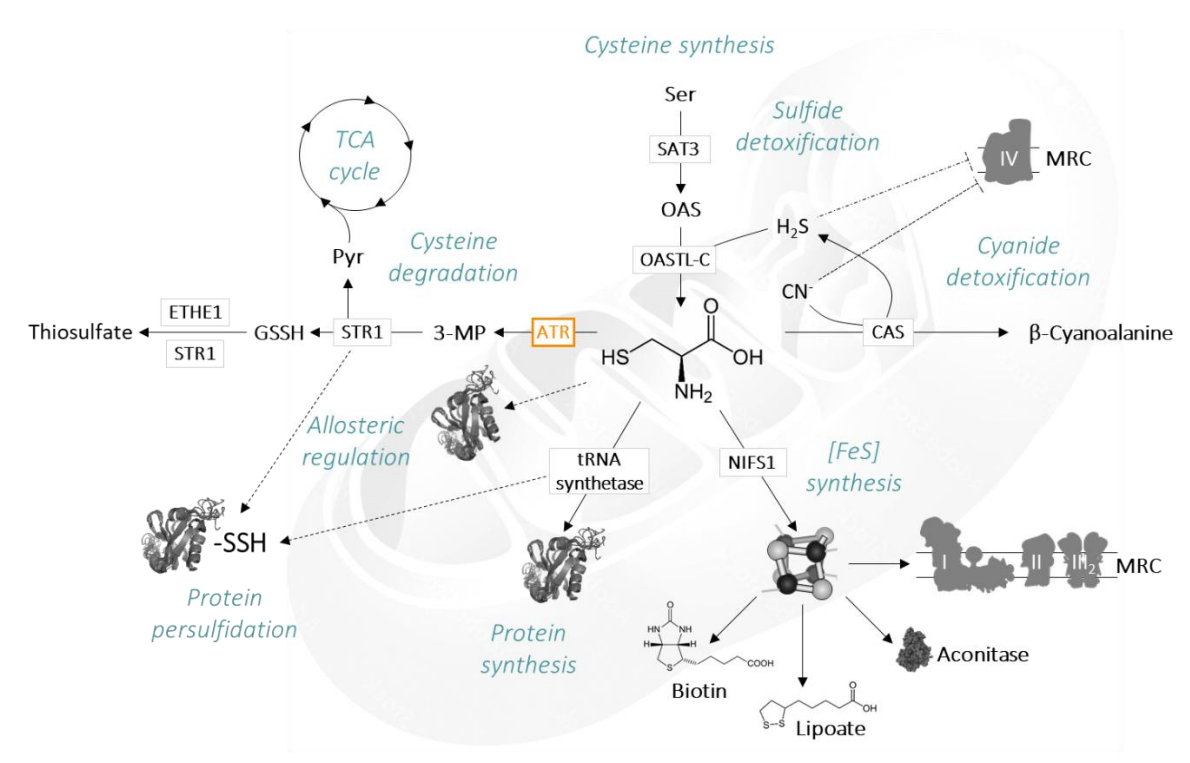


Figure 4.1: Mitochondrial cysteine metabolism

Plant mitochondria contain the enzymes required for cysteine synthesis and for the production of cysteinyl-tRNA for protein synthesis. In addition, cysteine serves as a sulfur donor during the synthesis of iron-sulfur clusters, which are required as cofactors for several mitochondrial enzymes and provide the sulfur for the cofactors biotin and lipoate. Cysteine is also involved in the detoxification of two different inhibitors of cytochrome c oxidase. It is a substrate of  $\beta$ -cyanoalanine synthase catalyzing cyanide detoxification, and cysteine synthesis detoxifies accumulating hydrogen sulfide. Regulatory functions can be mediated either by post-translational protein modification or allosteric effects. Mitochondrial cysteine catabolism proceeds via transamination to 3-mercaptopyruvate, subsequent transfer of the thiol group to glutathione by mercaptopyruvate sulfurtransferase, and oxidation to sulfite by the persulfide dioxygenase ETHE1 followed by transfer of an additional thiol group to produce thiosulfate. Mitochondrial aminotransferases catalyzing the first step of this cysteine degradation pathway have been identified in the frame of this study. ATR, aminotransferase; CAS,  $\beta$ -cyanoalanine synthase; ETHE1, persulfide dioxygenase; MRC, mitochondrial respiratory chain; NIFS1, cysteine desulfurase; OASTL-C, O-actylserine(thiol)lyase C; SAT3, serine acetyltransferase 3; STR1, mercaptopyruvate sulfurtransferase; TCA cycle, tricarboxylic acid cycle.

We here explore the potential of thermal proteome profiling (TPP) as a new powerful tool to screen for mitochondrial cysteine metabolic enzymes. TPP is based on the principle that ligand binding affects the thermostability of proteins. Depending on the nature of the interaction proteins can be stabilized but also destabilized during interaction with small molecules. TPP identifies these changes in the melting temperatures of proteins that are able to bind a metabolite of interest. Aliquots of a protein extract are heated to different temperatures in the presence and absence of potential ligands. Afterwards, precipitated proteins are removed by centrifugation, and the relative abundance of each protein in the remaining non-denatured fraction is determined by mass spectrometry (Figure 4.2). While originally developed for drug target discovery in biomedical research (Savitski et al. 2014), the application of TPP in plant systems remains largely unexplored. Here, we demonstrate its effectiveness in uncovering a metabolic enzyme involved in plant primary metabolism, a mitochondrial cysteine aminotransferase. We identify two mitochondrial aminotransferases, previously annotated as

aspartate and alanine aminotransferases, that use cysteine as an amino donor and 3-mercaptopyruvate as a keto acid acceptor *in vitro*, placing them as functional components of the mitochondrial cysteine oxidation pathway. TPP thus proved successful in filling a critical gap in our understanding of mitochondrial sulfur catabolism and its integration into cellular metabolism and signaling. Beyond this, the dataset reveals a broader set of cysteine-binding proteins, providing a resource for further exploration of cysteine metabolism and its regulatory roles in plant mitochondria.

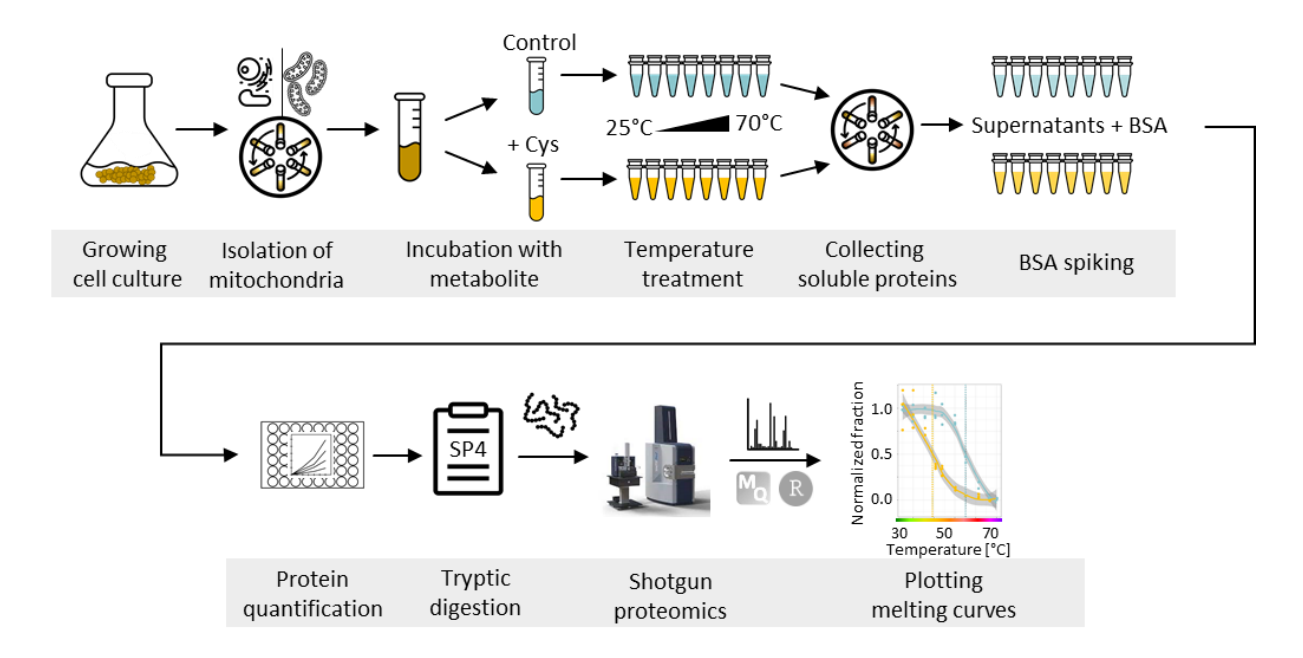


Figure 4.2: Thermal proteome profiling (TPP) workflow

Mitochondria were isolated from *Arabidopsis thaliana* cell culture via differential and density gradient centrifugation. The mitochondrial extract was split and either incubated with L-cysteine or water. The treated extracts were then aliquoted for the temperature treatment (n=3). Treated aliquots were centrifuged and supernatants were collected. BSA was added as internal standard to preserve the information of differences in protein concentrations. Protein concentrations were then adjusted to 1  $\mu$ g  $\mu$ l<sup>-1</sup> to ensure equal conditions during tryptic digestion. The resultant peptides were quantified using shotgun mass spectrometry, MaxQuant software and a custom R-script.

#### 4.3 Results

# 4.3.1 Thermal proteome profiling of the Arabidopsis thaliana mitochondrial proteome

Thermal mitochondrial-proteome profiling requires protein samples with sufficient coverage and concentration of the target proteome to allow reliable melting curve generation. To this end, mitochondria were isolated from *Arabidopsis thaliana* cell suspension cultures, yielding a protein fraction highly enriched in mitochondrial proteins (88%). Aliquots of this fraction were subjected to a temperature gradient from 25°C to 70°C in the presence or absence of 1 mM L-

cysteine, each in triplicate. Soluble proteins were identified and quantified via shotgun proteomics (Figure 4.2), resulting in the detection of 3903 protein groups.

Principal component analysis (PCA) clearly separated the samples along the temperature gradient, reflecting progressive thermal denaturation of individual proteins (Figure 4.3A). Correspondingly, the average normalized abundance of mitochondrial proteins decreased gradually with increasing temperature (Figure 4.3B). Melting curves were generated from normalized abundance data using a custom R script (see Methods). We applied stringent filters to exclude proteins detected in fewer than two replicates at 25°C, non-mitochondrial proteins, and proteins with inconsistent melting curves due to high variability within the dataset (see Supplementary Figure 4.1 for filtering workflow).

After filtering, high-confidence melting curves were obtained for 716 mitochondrial proteins (Suppl. Dataset S1). Calculated melting temperatures (Tm) ranged from 31.7°C to 68.7°C, with most proteins denaturing around 40°C (Figure 4.3C). Notably, a subset of proteins displayed exceptional thermal stability: 12.2% had Tm values between 50°C and 60°C, and 4.2% above 60°C. The thermotolerant fraction (Tm = 50–60°C) was significantly enriched in enzymes of the tricarboxylic acid (TCA) cycle and amino acid metabolism (Figure 4.3D), while the extremely heat-stable proteins (Tm > 60°C) included additional enzymes of amino acid metabolism and a group of heat shock proteins. Mean thermostability also varied significantly across the major mitochondrial pathways (Figure 4.3E). Proteins involved in amino acid metabolism and the TCA cycle were generally more heat-stable, whereas RNA editing factors exhibited low melting temperatures and were absent from the thermotolerant fractions.

# 4.3.2 Cysteine-induced thermal stability shifts in the Arabidopsis thaliana mitochondrial proteome

In this study, we applied TPP to identify mitochondrial proteins that interact with L-cysteine. Comparison of melting curves between cysteine-treated and control samples revealed significant thermal stability shifts for 146 mitochondrial proteins ( Figure 4.3F). Among these were three enzymes known to utilize L-cysteine as a substrate ( Figure 4.1), the cysteine desulfurase NifS1 (AT5G65720,  $\Delta$ Tm = -2.9°C), O-actylserine-(thiol)lyase C (OASTL-C; AT3G59760;  $\Delta$ Tm = -4.1°C), and cysteinyl-tRNA synthetase (AT2G31170,  $\Delta$ Tm = 6.1°C) (Suppl. Dataset S1). These findings serve as a positive control, validating the suitability of TPP for identifying metabolic enzymes that use a specific compound of interest as a substrate. In addition, our dataset offers a resource for identifying potential targets of cysteine-mediated metabolic regulation including transporters, RNA editing factors, and respiratory chain components (Suppl. Dataset S1).

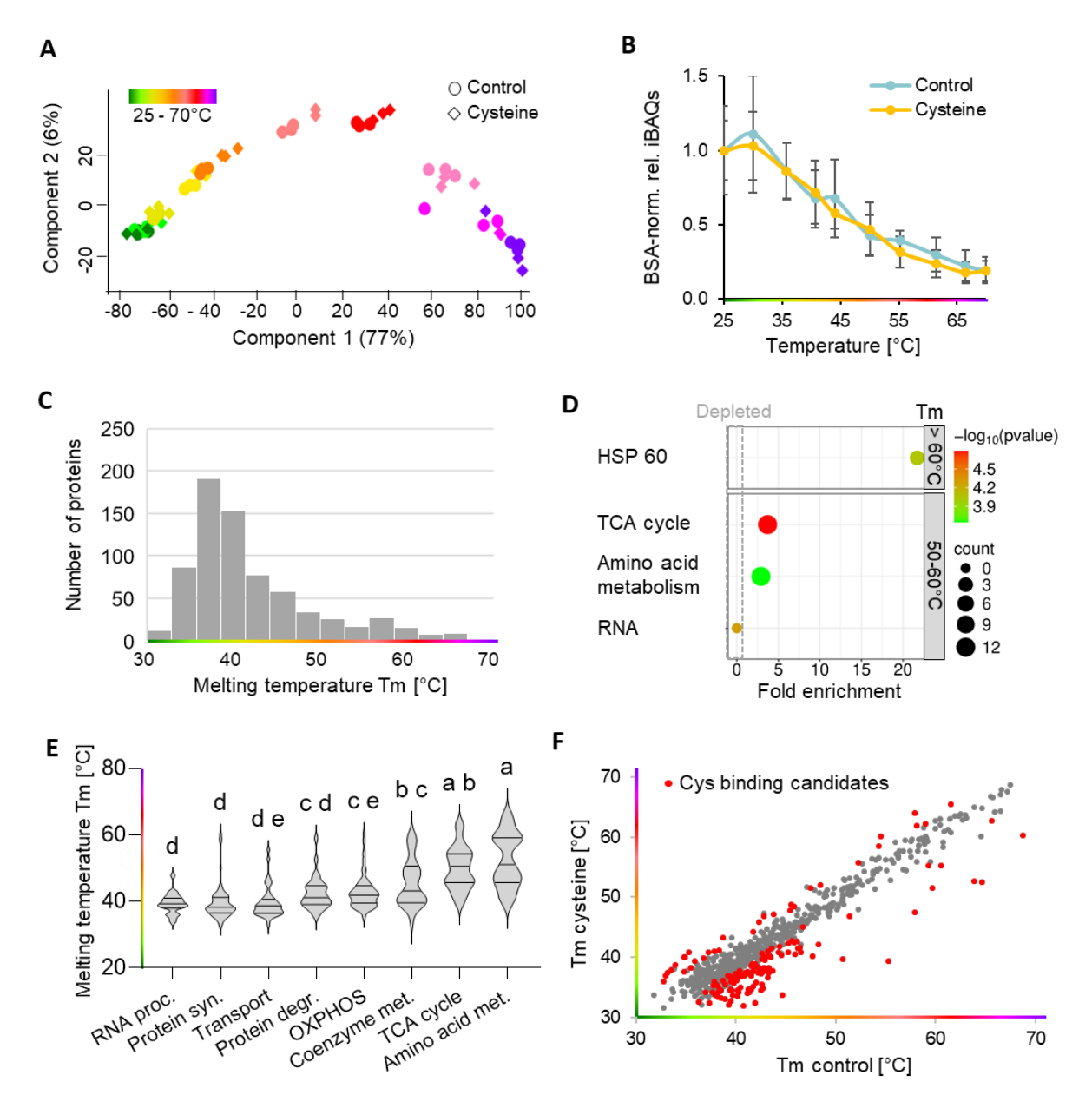


Figure 4.3: Thermal proteome profiling of the Arabidopsis thaliana mitochondrial proteome

**A**. iBAQ-based principal component analysis of the proteomics dataset. **B**. Mean normalized soluble fractions of all quantified mitochondrial proteins (BSA-normalized and relative to 25°C). **C**. Histogram illustrating the distribution of melting temperatures in the mitochondrial proteome. **D**. Enrichment analysis of highly and extremely heat stable mitochondrial protein fractions. **E**. Mean thermostability of proteins involved in major mitochondrial pathways. **F**. Melting temperatures (Tm) of the 716 mitochondrial proteins with high-quality melting curves. Candidates for cysteine-interacting proteins (= 146 proteins showing melting point shifts in the presence of 5 mM cysteine) are highlighted in red.

# 4.3.3 Identification and biochemical characterization of mitochondrial cysteine aminotransferase candidates

Among the cysteine-interacting mitochondrial proteins five were annotated as aminotransferases (Figure 4.4, Suppl. Dataset S1). Depending on the site and nature of interaction this could either be candidates for a mitochondrial cysteine aminotransferase

catalyzing transamination of cysteine to 3-mercaptopyruvate or enzymes regulated by cysteine. The candidate aminotransferases were annotated as gamma-aminobutyric acid (GABA) aminotransferase (GABA-AT, AT3G22200,  $\Delta$ Tm = -10.9°C), aspartate aminotransferase (Asp-AT, AT2G30970,  $\Delta$ Tm = -8.2°C), alanine-glyoxylate aminotransferase (AT4G39660,  $\Delta$ Tm = -11.2°C), and alanine aminotransferases (Ala-AT, AT1G17290,  $\Delta$ Tm = 3.2°C; AT1G72330,  $\Delta$ Tm = 3.5°C). The first three candidates were strongly destabilized in the presence of cysteine whereas the alanine aminotransferases were stabilized (Figure 4.4).

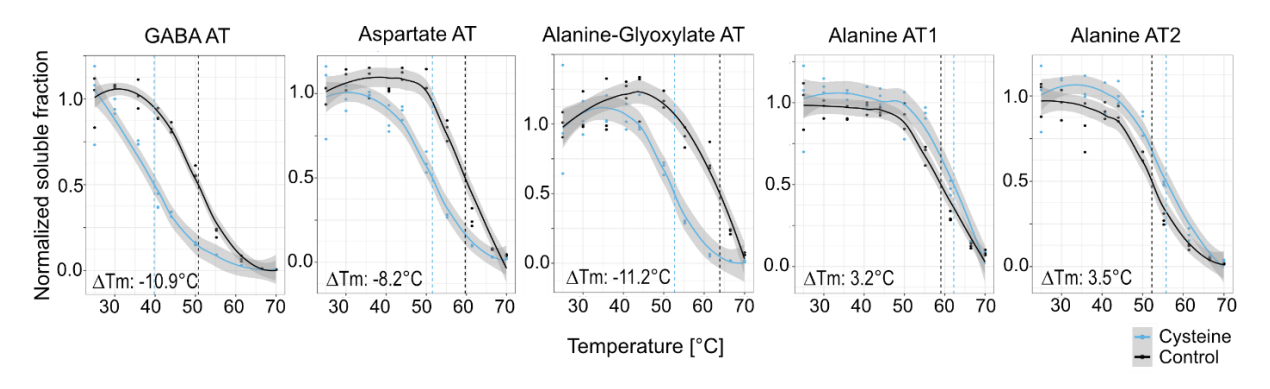


Figure 4.4: Candidates for a mitochondrial cysteine aminotransferase identified by thermal proteome profiling

Melting curves of the five mitochondrial aminotransferases (AT) showing a shift in the melting point (marked by dotted lines) in the presence of 5 mM cysteine. Grey shadows: Locally estimated scatterplot smoothing (LOESS); GABA aminotransferase (AT3G22200), Aspartate aminotransferase 1 (AT2G30970), Alanine-glyoxylate aminotransferase 2 (AT4G39660), Alanine aminotransferase 1 (AT1G17290), Alanine aminotransferase 2 (AT1G72330).

For functional analysis and biochemical characterization, the genes (excluding predicted mitochondrial targeting sequences) were expressed in *Escherichia coli*, and the His-tagged proteins were purified via Ni-NTA affinity and size-exclusion chromatography (Supplementary Figure 4.2 & Supplementary Figure 4.3). Despite repeated attempts to optimize the protocol, active alanine-glyoxylate aminotransferase could not be obtained, consistent with previous reports (Liepman & Olsen 2003). In contrast, GABA-AT, Asp-AT, and Ala-AT were successfully expressed and purified, with Ala-AT1 (AT1G17290) selected as the representative isoform for further analysis.

Enzyme assays confirmed that the purified aminotransferases were catalytically active with their canonical substrates and the kinetic parameters were in the expected range (Figure 4.5; Table 4.1; Supplementary Figure 4.4). Ala-AT and Asp-AT also accepted L-cysteine as an amino acid substrate, albeit with reduced catalytic efficiency. (Figure 4.5A, B; Table 4.1). However, kinetic analysis of Ala-AT revealed a  $K_m$ -value of  $0.77 \pm 0.10$  mM for L-Cys compared to  $2.51 \pm 0.18$  mM for L-Ala indicating a higher affinity of the enzyme for cysteine as an amino group donor (Figure 4.5A, Table 4.1). In contrast, Asp-AT showed a higher affinity for its established substrate with  $K_m$ -values of  $3.33 \pm 0.06$  mM for L-Asp vs.  $15.14 \pm 0.64$  mM for L-

Cys (Figure 4.5B, Table 4.1). GABA-AT did not metabolize cysteine in our experimental setup but was inhibited by it. Kinetic evaluation suggested a competitive mode of inhibition with a  $K_i$  of 0.42 mM Cys for transamination of GABA and 0.18 mM Cys for the reverse reaction using Ala as an amino group donor (Figure 4.5C).

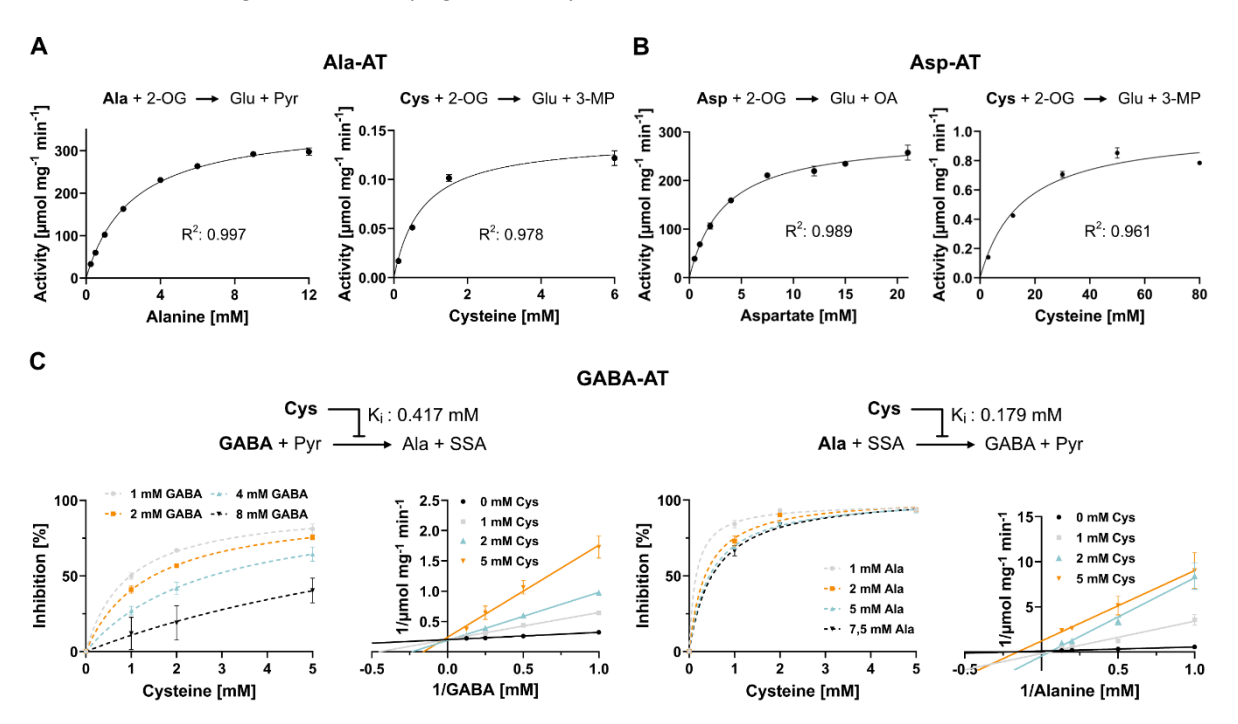


Figure 4.5: Biochemical characterization of mitochondrial cysteine aminotransferase candidates

**A.** Michaelis Menten kinetics for alanine aminotransferase 1 (AT1G17290) with L-Ala and L-Cys as a variable substrate. **B.** Michaelis Menten kinetics for aspartate aminotransferase 1 (AT2G30970) with L-Asp and L-Cys as a variable substrate. **C.** Inhibition kinetics for GABA aminotransferase 1 (AT3G22200) by L-Cys for both directions of the reaction. 2-OG, 2-oxoglutarate; 3-MP, 3-mercaptopyruvate; GABA, gamma-aminobutyric acid; OA, oxaloacetate; Pyr, pyruvate; SSA, succinic semialdehyde.

Table 4.1: Kinetic parameters for the purified recombinant Ala-AT, Asp-AT and GABA-AT

Protein	Varied Substrate	Fixed substarte	K <sub>m</sub> (mM)	V <sub>max</sub> (µmol mg <sup>-1</sup> min <sup>-1</sup> )	k <sub>cat</sub> (s <sup>-1</sup> )	k <sub>cat</sub> /K <sub>m</sub> (s <sup>-1</sup> mM <sup>-1</sup> )
Ala-AT	2-Oxoglutarate	Alanine	0.18±0.01	263.7±11.68	262.91	1460.63
	Alanine	2-Oxoglutarate	2.51±0.18	368.8±9.1	367.69	146.49
	Cysteine	2-Oxoglutarate	0.77±0.1	0.14±0.001	0.14	0.18
Asp-AT	2-Oxoglutarate	Aspartate	0.46±0.02	226.9±3.74	180.60	392.62
	Aspartate	2-Oxoglutarate	3.33±0.06	291.8±8.49	232.26	69.75
	Cysteine	2-Oxoglutarate	15.14±0.64	1.02±0.02	0.81	0.05
GABA- AT	GABA	Pyruvate	0.59±0.2	4.97±0.3	4.97	7.75
	Alanine	Succinic semialdehyde	4.37±0.2	9.91±0.75	9.11	2.08

# 4.3.4 Reconstruction of the complete plant mitochondrial cysteine catabolic pathway

We next tested, whether the candidate aminotransferases could support the proposed mitochondrial cysteine catabolic pathway. The pathway involves four enzymatic steps catalyzed by three enzymes: transamination of L-cysteine to 3-mercaptopyruvate, conversion to glutathione persulfide by STR1 (AT1G79230), oxidation to sulfite by the persulfide dioxygenase ETHE1 (AT1G53580), and transfer of an additional persulfide to sulfite by STR1 producing the final product thiosulfate (Figure 4.6A). All components were heterologously expressed in and purified from E. coli. (Supplementary Figure 4.5). ETHE1 activity was measured by oxygen consumption and confirmed via HPLC-based sulfite quantification (Figure 4.6A, F). In the presence of STR1, ETHE1-dependent oxygen consumption could be triggered using 3-mercaptopyruvate as substrate, leading to equimolar thiosulfate production (Figure 4.6C, G). The complete three-enzyme system successfully catalyzed the oxidation of Lcysteine to thiosulfate when either Asp-AT or Ala-AT was included (Figure 4.6D, E, H, I). Pathway activity nearly matched that of isolated ETHE1 when the aminotransferase and STR1 were provided in excess. Protein abundance estimates from the mitochondrial fraction revealed that Ala-AT, Asp-AT, and STR1 were present at about 10-fold higher levels than ETHE1, supporting the pathway's feasibility in vivo (Suppl. Dataset S1). This is further supported by the higher spatial proximity of the enzymes in the mitochondrial matrix compared to the in vitro system. Consistent with its lack of cysteine-metabolizing activity, GABA-AT did not support ETHE1-mediated oxygen consumption from cysteine.

To get a first impression about the metabolic integration of the three aminotransferases in mitochondrial sulfur metabolism as well as the physiological context of these networks we compared co-expression profiles available on ATTED (<a href="https://atted.ip/">https://atted.ip/</a>). There was a strong overlap of 43 genes between the top 100 co-expressed genes for STR1 and Asp-AT, and those were mainly involved in the mitochondrial housekeeping functions TCA cycle and oxidative phosphorylation (Supplementary Figure 4.6, Suppl. Dataset S2). The co-expression profile of ETHE1 was most similar to that of GABA-AT with 31 common genes in the top 100 (Supplementary Figure 4.6B). In this case the group of overlapping genes was dominated by enzymes involved in lipid catabolism as well as amino acid transport and degradation, placing these enzymes (ETHE1 and GABA-AT) into the context of energy deficiency stress (Suppl. Dataset S2).

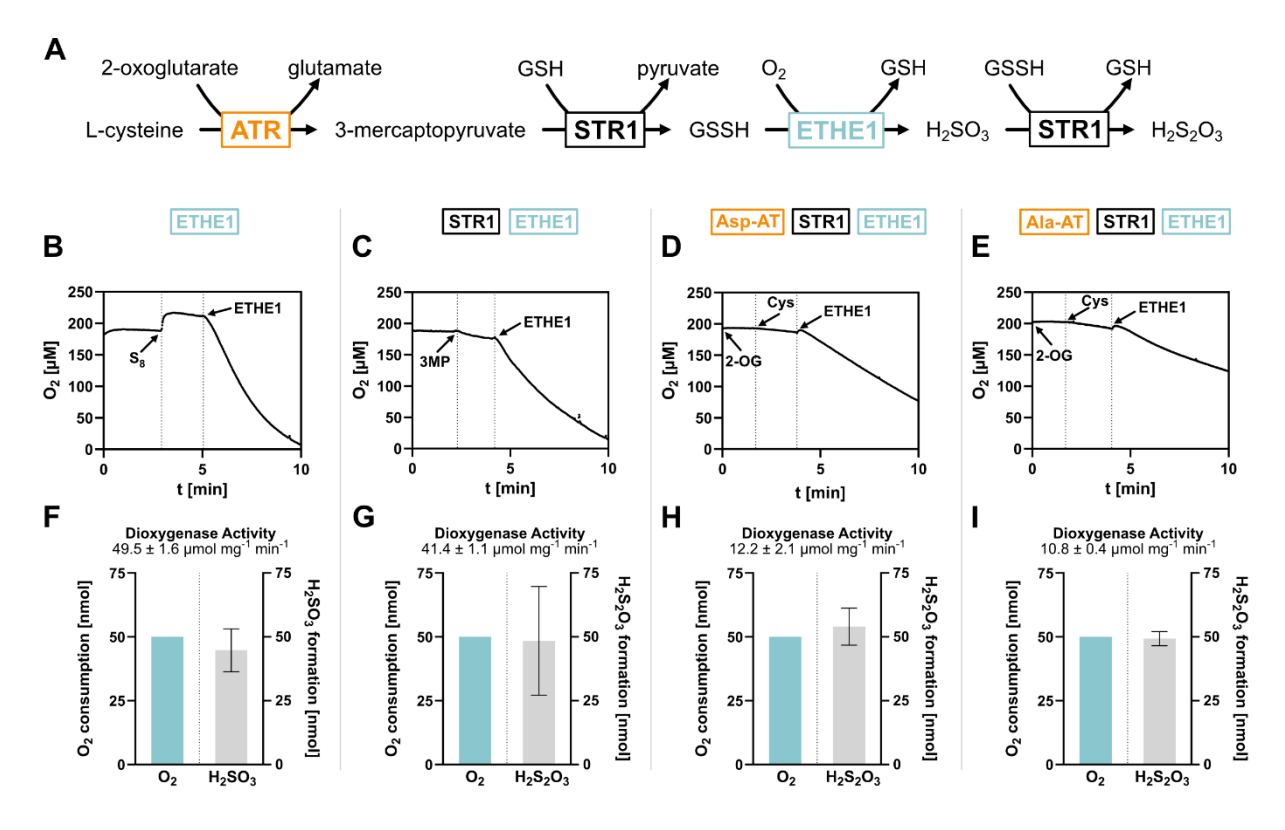


Figure 4.6: Reconstruction of the complete plant mitochondrial cysteine catabolic pathway in vitro

**A.** Reaction scheme of the mitochondrial cysteine catabolic pathway. **B-E.** Original traces of oxygen electrode measurements illustrating pathway activity based on oxygen consumption by the persulfide dioxygenase (ETHE1) step. The reactions contained GSH as well as the enzymes listed above, except for ETHE1, which was added at the indicated timepoint. Substrates were supplied as noted in the graph **F-I.** Stoichiometry between oxygen consumption and product accumulation. Samples were taken from the reaction mix after exactly 50 nmol O<sub>2</sub> had been consumed and thiol contents were analyzed by HPLC (**B,F**) Activity of the persulfide dioxygenase ETHE1 with GSSH (non-enzymatically produced from GSH plus elemental sulfur) as a substrate. (**C,G**) Activity of the partial cysteine catabolic pathway consisting of the sulfurtransferase STR1 plus ETHE1 with 3-mercaptopyruvate (3MP) as a substrate. (**D,H**) Activity of the complete cysteine catabolic pathway consisting of aspartate aminotransferase 1, STR1 and ETHE1 with cysteine as a substrate. (**E,I**) Activity of the complete cysteine catabolic pathway consisting of alanine aminotransferase 1, STR1 and ETHE1 with cysteine as a substrate.

#### 4.4 Discussion

### 4.4.1 Thermostability of plant mitochondrial proteins

Our thermal profiling of the *Arabidopsis thaliana* mitochondrial proteome revealed marked differences in the average thermostability of distinct functional categories. Notably, enzymes of the tricarboxylic acid (TCA) cycle and amino acid catabolism exhibited high melting temperatures, suggesting an intrinsic robustness that may be critical under conditions of energy limitation. During episodes of heat stress often coinciding with drought, plants frequently experience compromised photosynthesis and ATP depletion. Under such constraints, the persistence of a thermo-stable core of TCA cycle enzymes would help sustain mitochondrial ATP production when alternative energy-generating pathways falter. Similarly, the high thermal stability of amino acid catabolic enzymes likely reflects their central role in

maintaining metabolic flexibility under stress. Amino acids act as alternative respiratory substrates, contributing intermediates to the TCA cycle and, in some cases, directly donating electrons to the mitochondrial electron transport chain via the ubiquinone pool (Hildebrandt et al. 2015). This catabolic route becomes especially critical during carbohydrate starvation, as demonstrated by the compromised stress tolerance and shortened survival of mutants deficient in key steps of amino acid degradation (Ishizaki et al. 2005; Ishizaki et al. 2006; Araújo et al. 2010; Peng et al. 2015; Hirota et al. 2018). The induction of these pathways is regulated by SnRK1 signaling, which activates a broader energy conservation program in response to carbon limitation (Dietrich et al. 2011; Pedrotti et al. 2018). These findings underscore the physiological importance of maintaining a robust, thermo-stable core of mitochondrial enzymes to support respiratory metabolism during abiotic stress.

In contrast, Pentatricopeptide Repeat (PPR) proteins involved in mitochondrial RNA editing consistently displayed low melting temperatures and were largely absent from the high-stability fractions. PPR proteins bind specific mitochondrial transcripts, and their stability *in vitro* may depend on the presence of substrate RNA. We therefore hypothesize that, *in vivo*, PPR proteins are stabilized upon mRNA binding and may be targeted for degradation when editing demand is low. Under hyperthermic or severe stress conditions that exceed the stability of unbound PPR proteins, a decline in RNA editing could lead to the accumulation of unedited respiratory complex subunits. Such defective subunits may fail to assemble properly, triggering reactive oxygen species (ROS) production and amplifying stress-responsive signaling cascades (Waltz et al. 2020).

Our findings are well in line with the results of a recent study on the thermal tolerance of the Arabidopsis proteome using CESTA (cellular thermal shift assay; (Lyu et al. 2023)). While for our approach we isolated mitochondrial proteins to focus on interactions with cysteine as a ligand, CESTA works with intact cells preserving the diverse protein-protein and proteinmetabolite interactions in the native cellular context. Both studies detected high thermal stability in mitochondrial dehydrogenases involved in the TCA cycle and amino acid metabolism. The extraordinary thermal vulnerability of mitochondrial RNA editing factors we observed in the protein extract also became apparent in the cellular context. Several PPR proteins were included in the 10% of the proteins with the lowest Tm within the CESTA study. In general, the proteostasis network, including aminoacyl-tRNA biosynthesis, protein translation initiation, and protein folding, was among the most vulnerable targets of heat stress in cells, and a suppression of protein synthesis by heat stress could be experimentally verified (Lyu et al. 2023). Overall, the comparison underscores that TPP on isolated mitochondrial proteins can provide valuable insights into intrinsic protein stability, even though in vivo, individual enzymes might be stabilized due to metabolon formation and protein-metabolite interactions that enhance thermal resilience.

# 4.4.2 Thermal proteome profiling identifies mitochondrial cysteine aminotransferases

This study demonstrates that thermal proteome profiling, which was originally developed for drug target and off-target discovery in biomedical research (Savitski et al. 2014), is a powerful tool to identify plant enzymes metabolizing a compound of interest. By monitoring shifts in thermal stability upon L-cysteine treatment, we successfully re-identified three known mitochondrial cysteine-metabolizing enzymes, validating our approach as an effective screening tool. Encouraged by these positive controls, we targeted the long-hypothesized aminotransferase catalyzing the initial transamination of cysteine to 3-mercaptopyruvate (Höfler et al. 2016). Indeed, we could experimentally validate the interaction of cysteine with three mitochondrial aminotransferases showing a melting point shift in TPP. Activity tests confirmed that Asp-AT and Ala-AT can use cysteine as a substrate and catalyze the first step of the mitochondrial cysteine catabolic pathway. These results suggest that a dedicated cysteine aminotransferase is not required, but endogenous promiscuous aminotransferases can accommodate cysteine. This finding aligns with observations in mammalian mitochondria, where aspartate aminotransferase has similarly been implicated in cysteine transamination (Miyamoto et al. 2014). To our knowledge, no enzyme exclusively dedicated to cysteine transamination has been described in eukaryotes to date.

Beyond identifying candidate enzymes, the melting curves provided by TPP could potentially reveal some additional information on the mode of the enzyme-metabolite interactions. Aminotransferases require pyridoxal phosphate (PLP) as a cofactor. In the resting state, PLP is covalently linked to the enzyme via a Schiff base linkage formed by the condensation of its aldehyde group with the  $\varepsilon$ -amino group of a lysine residue at the active site (Kirsch et al. 1984). Upon substrate binding this internal aldimine is replaced by an external aldimine bond resulting in pyridoxamine-5'-phosphate (PMP), which is no longer covalently linked to the enzyme. In the absence of the second substrate the cofactor will eventually defuse off compromising the enzyme structure. The pronounced destabilization of Asp-AT, GABA-AT, and alanineglyoxylate aminotransferase in the presence of cysteine likely reflects this cofactor release upon formation of a stalled external aldimine. In the case of GABA-AT we did not detect any cysteine aminotransferase activity, so the mechanism of inhibition might involve binding of cysteine at the active site without catalysis. Our data indicate a competitive character of the inhibition which would be in line with this mode of action. Conversely, Ala-AT's stabilization by cysteine hints at an unusually strong non-covalent affinity for its cofactor-substrate complex, meriting further structural and spectroscopic investigation (Figure 4.4).

## 4.4.3 Metabolic integration of mitochondrial cysteine aminotransferases

Our study identified two mitochondrial aminotransferases able to use cysteine as an alternative substrate. Kinetic parameters place Ala-AT in a physiologically relevant role. Its  $K_m$  for cysteine (0.77 mM) is three-fold lower than for alanine and close to the physiological range of cysteine concentrations reported under normal and stress conditions (Watanabe et al. 2008; Heeg et al. 2008; Moormann et al. 2025). Moreover, both mitochondrial Ala-AT isoforms are upregulated by cysteine feeding in Arabidopsis seedlings, supporting their *in vivo* function in cysteine catabolism (Moormann et al. 2025). For Asp-AT we determined a comparatively high  $K_m$  of 15 mM with cysteine indicating that *in vivo* its activity will strongly depend on the cysteine concentration in the mitochondrial matrix.

Although aminotransferase activities with cysteine were lower than with canonical substrates, this may reflect metabolic flux distributions: alanine and aspartate are directly linked to central carbon metabolism via transamination to pyruvate and oxaloacetate, respectively. In contrast, cysteine catabolism via 3-mercaptopyruvate might be relevant for protein persulfidation (Pedre et al. 2023) and for the removal of accumulating cysteine during stress, while otherwise alternative branches in mitochondrial cysteine metabolism such as FeS synthesis or cyanide detoxification (Figure 4.1) are most likely quantitatively more relevant. There could also be some presently unknown regulatory mechanism shifting the substrate preferences and catalytic efficiencies of the aminotransferases *in vivo*.

Co-expression profiles provide some first hints on the metabolic and physiological context of the different steps and variants of the mitochondrial cysteine catabolic pathway. Asp-AT and STR1 share an expression profile with core mitochondrial pathways, the TCA cycle and the respiratory chain, and are thus universally expressed. It is tempting to speculate that these two enzymes might also participate in functions of general importance, which could be related to the production of persulfides for signaling. In contrast, ETHE1 and GABA-AT are clearly stress responsive. Their expression profiles overlap with several enzymes from lysine and branchedchain amino acid catabolism that are also localized in the mitochondria and typically strongly induced by energy deficiency stress via SnRK1 signaling (Heinemann & Hildebrandt 2021). In these stress conditions massive protein degradation releases high amounts of all proteinogenic amino acids so that the intracellular concentrations of those amino acids that are normally low abundant massively accumulate in the free pool (Heinemann et al. 2021). Cysteine belongs to this group of low abundant amino acids together with lysine and the branched-chain amino acids indicating that their catabolism might be regulated in a concerted fashion. The mitochondrial cysteine catabolic pathway we reconstruct here represents the only known route in plants that oxidizes the thiol moiety of cysteine instead of releasing hydrogen sulfide, a potent and potentially damaging gasotransmitter (Cooper & Brown 2008). Thus, a

physiological role in mitigating toxic amino acid accumulation during stress seems reasonable. The non-protein amino acid GABA also rapidly accumulates in plant tissues in response to biotic and abiotic stress. It enhances stress tolerance by regulating osmotic balance, improving antioxidant defense, and serving as a signaling molecule (Clark et al. 2009; Kinnersley & Turano 2000). Our findings demonstrate that GABA-AT binds cysteine, most likely at the active site, without catalyzing its transamination. This is in line with a previous report that had tested cysteine and several other amino acids as substrates for GABA-AT (Clark et al. 2009). Instead, cysteine acts as an inhibitor of GABA-AT and thus its accumulation might serve as a regulatory brake on GABA turnover during acute stress. A high abundance of GABA-AT allows rapid removal of GABA after stress release providing significant amounts of anaplerotic carbon to the TCA cycle via the GABA shunt (Kinnersley & Turano 2000).

#### 4.5 Conclusion

This study establishes thermal proteome profiling (TPP) as a valuable tool for identifying plant enzymes metabolizing a specific substrate of interest. By applying TPP to Arabidopsis mitochondrial proteins, we identified aminotransferases capable of initiating cysteine catabolism through transamination to 3-mercaptopyruvate. These findings enabled the reconstitution of a complete mitochondrial cysteine degradation pathway in vitro. The enzymatic properties and expression patterns of alanine aminotransferase and aspartate aminotransferase suggest distinct regulatory and physiological roles under stress conditions. Furthermore, cysteine's inhibitory effect on GABA aminotransferase points to a potential regulatory interaction during metabolic adaptation. Beyond that, the TPP dataset represents a valuable resource for identifying potential targets of cysteine-mediated metabolic regulation, including transporters, RNA editing factors, and respiratory chain components. This aspect is especially relevant in the context of stress signaling, as cysteine has been implicated as a metabolic signal during both abiotic and biotic interactions (Moormann et al. 2025; Heinemann & Hildebrandt 2021; Romero et al. 2014). Given the prevalence of allosteric regulation in amino acid biosynthetic pathways, our findings highlight the potential for cysteine to modulate enzyme activity through direct binding. Together, these insights deepen our understanding of mitochondrial sulfur metabolism and its potential integration into plant stress responses and metabolic signaling.

#### 4.6 Materials & Methods

### 4.6.1 Plant material and protein extraction

Mitochondria were isolated from an *Arabidopsis thaliana* Col-0 cell suspension culture according to the procedure published in (Werhahn et al. 2001). The mitochondrial pellets were resuspended in 1 ml homogenization buffer (50 mM Tris (pH 7.5), 10 mM KCl, 3 mM EGTA, 0.4% NP-40) per 0.1 g pellet. The mild detergent NP-40 was included to extract membrane-bound proteins (e.g. receptors, (Reinhard et al. 2015). The mitochondrial fractions were incubated on ice for 30 min, ruptured in a Potter homogenizer, frozen at -20°C and stored until the thermal treatment experiment.

# 4.6.2 Temperature gradient precipitation

We used approx. 10 ml of mitochondrial protein extract (~1 μg μl<sup>-1</sup>) to perform a thermal proteome profiling experiment. With this amount we could cover three replicates for ten different temperatures of a control and an L-cysteine treated variant. In detail, the mitochondrial extract was split in half and was either incubated with 5 mM L-cysteine or water for 10 min on a shaker at room temperature. The treated extracts were then aliquoted (150 μl) into PCR-tubes for the temperature treatment in a thermocycler. Three aliquots per treatment and temperature were prepared and incubated for 10 min at either 25°C, 30°C, 35.8°C, 40.7°C, 44°C, 50°C, 55.2°C, 61.4°C, 66°C or 70°C. The treated and heated extracts were then transferred into 1.5 mL reaction tubes and centrifuged at 20,000 x g for 20 min to pelletize the potentially denatured proteins. Supernatants were collected and protein concentrations were quantified via Bradford assay (Thermo Fisher Scientific). Subsequently, 1 μg bovine serum albumin (BSA) was added to each sample as internal standard to preserve the information of different protein concentrations. Eventually, the protein samples were concentrated in a vacuum concentrator for further processing.

# 4.6.3 Protein digestion and sample preparation for proteome analysis via mass spectrometry

We used a modified version of the "solvent precipitation, single-pot, solid-phase-enhanced sample preparation (SP4) protocol of (Johnston et al. 2022). The concentrations of the protein samples were adjusted to 1  $\mu$ g/ $\mu$ L by adding individual volumes of SDT buffer (4% SDS, 0.1 M dithiothreitol, 0.1 M Tris pH 7.6, (Mikulášek et al. 2021). The TPP extracts were incubated at 60°C for 30 min to solubilize, denature and reduce the proteins. Samples were then sonicated for 10 min and centrifuged at 20,000 ×g for 10 min. Thirty microliters of the supernatant were transferred to new tubes, mixed with 7.5  $\mu$ L iodoacetamide (IAM, 0.1 M) and incubated for 30 min in the dark in order to alkylate the reduced disulfide bridges. Then 2  $\mu$ L DTT (0.1 M) was added to neutralize excess amounts of IAM.

Preparation of the glass beads/ACN suspension, protein precipitation and washing steps were performed as described in (Johnston et al. 2022). We used approx. 400  $\mu$ g of glass beads per sample (approx. 30  $\mu$ g protein). The purified proteins were digested with 0.5  $\mu$ g trypsin (mass spectrometry grade, Promega) for 16 h on a heated shaker at 37°C at 1000 rpm. The peptide-containing supernatants were collected in low peptide binding tubes. The glass beads were rinsed in 60  $\mu$ L ammonium bicarbonate (50 mM) to recover remaining peptides. Eluates were combined and acidified with 1  $\mu$ L formic acid (FA). The peptides were desalted on 50 mg Sep-Pak tC18 columns (WAT054960, Waters) and quantified using the Pierce Quantitative Colorimetric Peptide Assay Kit (Thermo Fisher Scientific). The samples were finally diluted to a final concentration of 400 ng  $\mu$ l<sup>-1</sup> in 0.1% FA.

# 4.6.4 Quantitative proteomics by shotgun mass spectrometry (LC-MS/MS)

400 ng of peptides were injected via a nanoElute2 UHPLC (Bruker Daltonic) and separated on an analytical reversed-phase C18 column (Aurora Ultimate 25 cm x 75 μm, 1.6 μm, 120 Å; lonOpticks). Using a multistage linear gradient (eluent A: MS-grade water containing 0.1% formic acid, eluent B: acetonitrile containing 0.1% formic acid, gradient: 0 min, 2% B; 54 min, 25% B; 60 min, 37% B; 62 min, 95% B; 70 min, 95% B), peptides were eluted and ionized by electrospray ionization using a CaptiveSpray 2 source with a flow rate of 300 nL/min. The timsTOF-HT mass spectrometer followed a data-dependent acquisition parallel accumulation–serial fragmentation (DDA-PASEF) method, covering an ion mobility window of 0.7–1.5 V s/cm² with 4 PASEF ramps, targeting an intensity of 14,500 (threshold 1,200) with a cycle time of ~0.53 s. Ion mobility spectrometry–MS/MS spectra were analyzed with MaxQuant (Cox and Mann, 2008) using default search parameters and the TAIR10 database for protein identification. Additionally, the calculation of label-free quantification (LFQ) values and intensity-based absolute quantification (iBAQ) values for the identified proteins were enabled.

#### 4.6.5 Thermal proteome profiling data analysis

For thermal proteome profiling data analysis, we developed a custom R script (MeCuP, available on demand) which enables automated processing and visualization based on input from MaxQuant. Input data is structured according to the ARC directory format and includes MaxQuant output files (proteingroups.txt with iBAQ values), sample annotation (.csv format), and optional protein annotations. The script normalizes protein abundance data based on BSA-spiked internal standards and applies a starting point (SP) mean normalization at the lowest temperature (e.g. 25°C or user-defined). Normalization can be performed against control, treatment-specific or both respectively SP values. Samples can be filtered based on BSA abundance and the number of valid data points at SP, ensuring only reliable melting curves are included in the analysis. Key user-defined parameters include thresholds for BSA detection, SP data filtering, and minimum valid datapoints. Proteins failing these criteria are

excluded and listed in the output. Filter effects can be explored separately. Melting points (Tm50) are calculated from LOESS-smoothed curves as the temperature corresponding to 50% soluble fraction. Visual outputs include protein melting curves, with optional emphasis on non-overlapping curves between control and treatment. Final outputs include customizable .xlsx files with legends, plots, exclusion logs, and a result table with calculated Tm50 values per protein and condition.

# 4.6.6 Cloning of Arabidopsis cysteine binding candidates

Full-length cDNA for candidate enzymes (STR1: AT1G79230; ETHE1: AT1G53580 Ala-AT: AT1G17290; Asp-AT: AT2G30970; GABA-AT: AT3G22200) were cloned using RT-PCR from total RNA isolated from mature Arabidopsis leaves. Total RNA was extracted using Monarch total RNA Miniprep kit (New England Biolabs) following the manufacturer's protocol. The total RNA was also additionally treated with DNase1 (New England Biolabs) as instructed by the manufacturer. The isolated RNA was quantified using nanophotometer (NanoPhotometer® N60, Implen) and was stored in -80°C immediately. GoScript Reverse Transcriptase (Promega) was used to synthesise cDNA from 5 µg of RNA following manufacture's protocol with the exception of using anchored oligo(dT)20 VN primers instead of oligo(dT)15 primers. Additionally, RNasin (Promega) was also added in the reaction mix. Synthesised cDNA was used for subsequent gene specific PCR's using Phire Hot Start II DNA Polymerase (Thermo Fisher Scientific) with gene specific primers (Suppl. Table S1). The mitochondrial targeting sequences for all enzymes were removed at their cleavage sites and exchanged with Met codon. The primers contained restriction enzyme sites along with compatible overhangs for homology based directional cloning into pET28a(+) (Novogen) vector. The amplified sequences were then ligated into pET28a(+) (Novogen) plasmids using NEBuilder HF DNA assembly kit (New England Biolabs) following the manufacturers' instructions. The ligated plasmids were transformed into NEB 5-alpha competent Escherichia coli cells (New England Biolabs) and grown in Luria-Bertani (Miller) (LB) (Sigma-Aldrich) media supplemented with 50 μg ml-1 kanamycin. Positive clones were screened and sequence verified through sanger sequencing (Microsynth Seqlab).

### 4.6.7 Protein overexpression and purification

The verified plasmids were transformed into expression capable BL21(DE3) competent *E. coli* (New England Biolabs) cells. For some candidates (GABA-AT and ETHE1) the competent BL21(DE3) *E. coli* harboured an additional plasmid- pG-KJE8 (Takara) containing coding sequences for molecular chaperons for assisted folding. Overexpression of the recombinant *E. coli* (OD<sub>600 nm</sub>  $\approx$  0.4) proteins was induced using 1 mM isopropyl  $\beta$ -D-1-thiogalactopyranoside (IPTG) (Thermo Fisher Scientific). For cells harbouring chaperons, addition of 10 ng ml<sup>-1</sup> Tetracycline and 0.5 mg ml<sup>-1</sup> of L-Arabinose preceded IPTG to allow for sufficient production

of chaperons required for assisted folding. Additionally, cultures of candidate aminotransferases (ALA-AT, Asp-AT and GABA-AT) were supplemented with 0.1 mM of pyridoxal 5'-phosphate (PLP) to enhance folding and stability of protein. The cultures were allowed to grow at 18°C overnight for 16h with gentle agitation in baffled flasks.

The cells were harvested by chilling the cultures on ice for 15 min followed by centrifugation at  $16,000 \times g$  for 20 min at 4°C. The pellets were suspended in ice cold lysis buffer (50 mM sodium phosphate, 500 mM NaCl, 10 mM Imidazole, 250 mM Sucrose, 5% Glycerol, pH 8.0 containing 2 mg ml<sup>-1</sup> of Lysozyme, 10 units of DNase1 and RNase1) and incubated at RT for 1 hour. Lysis buffer is also supplemented with EDTA-free protease inhibitor (Roche). GABA-AT was processed differently by using 50 mM Tris(hydroxymethyl)methyl-3-aminopropanesulfonic acid (TAPS) instead of sodium phosphate at pH 9, the rest of buffer components remained the same. The cells were sonicated for 2 minutes with a pulse cycle of 20 sec ON and 30 sec OFF at 70% amplitude. After sonication the supernatant was harvested by centrifugation at 16,000 x g at 4°C for 15 min. The supernatant was passed through 0.45  $\mu$ m filter to remove any cell debris.

Purification of the recombinant enzymes were carried out using affinity chromatography on 5 ml nickel-nitrilotriacetic acid-agarose (NiNTA) columns (Cytiva) coupled to an ÄKTA go system (Cytiva). 50 ml of clarified supernatant was injected into a pre-equilibrated column at a flowrate of 1 ml min<sup>-1</sup> followed by washing with binding buffer for 5 CV (50 mM sodium phosphate/ 50 mM TAPS, 500 mM NaCl, 250 mM sucrose, 5% glycerol, pH 8.0/ 9.0). The bound proteins were eluted using a gradient of imidazole (0-500 mM) for 10 CV at a flowrate of 1 ml min<sup>-1</sup> while collecting 2 ml fractions. The purified protein fractions were pooled and concentrated to 500 µl using Amicon 10K Ultra Centrifugal Filters (Merck). Concentrated samples were subjected to size exclusion chromatography (SEC) using Superdex 200 increase 10/300 (Cytiva) column coupled to an ÄKTA go system (Cytiva). The proteins were separated based on their molecular weights using 2 CV of SEC running buffer (50 mM sodium phosphate, 300 mM NaCl, 10% glycerol, pH 8.0 for ETHE1, STR1, Ala-AT and Asp-AT; 50 mM TAPS, 300 mM NaCl, 10% glycerol, pH 9.0 for GABA-AT) at a flowrate of 0.1 ml min<sup>-1</sup>. 500 µl fractions were collected and fractions containing distinct peaks were screened through 10% (Ala-AT, Asp-AT, GABA-AT) and 15% (STR1 and ETHE1) polyacrylamide gels and visualised using fast Coomassie stain (Serva). The same were also verified using western blot using anti-His mouse monoclonal antibody (Cell Signalling Technologies) and anti-mouse IgG HRP-linked antibody (Cell Signalling Technologies). The purified enzymes fractions corresponding to the right electrophoretic mobility were stored at -20°C in 50% glycerol (v/v). These fractions were quantified using Bradford assay (Thermo Fisher Scientific) and used for enzymatic tests.

### 4.6.8 Enzyme activity tests

Activity assays for Ala-AT and Asp-AT contained 50 mM 4-(2-hydroxyethyl)-1piperazineethanesulfonic acid (HEPES) pH 8.0, 50 µM pyridoxal-5-phosphate (PLP) and 0.25 - 0.3 µg ml<sup>-1</sup> protein for the standard reaction and 200 - 250 µg ml<sup>-1</sup> protein for reactions with cysteine as amino donor. If not indicated otherwise, 9 mM alanine and 12 mM aspartate were used as amino donors for Ala-AT and Asp-AT reactions, respectively, while 6 mM 2oxoglutarate was used as amino acceptor.  $K_m$  and  $V_{max}$  of the respective substrates were determined using 0.25 – 12 mM alanine and 0.125 – 1.5 mM cysteine for Ala-AT; 0.5 – 21 mM aspartate and 3 – 80 mM cysteine for Asp-AT and 0.1 – 6 mM 2-oxoglutarate for both Ala-AT Asp-AT. Standard activity assays for GABA-AT contained and 50 mM tris(hydroxymethyl)methyl-3-aminopropanesulfonic acid (TAPS) pH 9.0, 50 µM PLP and 3.7 -5.9 µg ml<sup>-1</sup> protein. Inhibitory effects of cysteine were determined using 0, 1, 2 and 5 mM cysteine. Forward reactions contained 1 – 8 mM GABA and 6 mM pyruvate. Reverse reactions contained 1 – 7.5 mM alanine and 0.5 mM succinic semialdehyde. Reactions that generated pyruvate or oxaloacetate were coupled to NADH-dependent lactate dehydrogenase (LDH, 0.3 U or 5 µg ml<sup>-1</sup>, pig heart, Roth) or malate dehydrogenase (MDH, 2.4 U or 10 µg ml<sup>-1</sup>, pig heart, Roche), respectively. Continuous assays contained 0.3 mM NADH and the reactions were initiated by the addition of an appropriate amino donor or amino acceptor. The rate of each reaction was monitored as the change in NADH concentration at 340 nm using the spectrophotometer Multiskan Skyhigh (Thermo Fisher Scientific) equipped with temperature control. In assays that were not coupled to LDH or MDH, the formation of amino acids was monitored using reverse-phase high performance liquid chromatography (HPLC). The discontinuous assays were stopped by transferring aliquots into 0.1 M HCl. Samples were neutralized by the addition of 0.5 M potassium borate buffer pH 11. Amino acids were quantified using the Agilent 1260 Infinity II HPLC System (Agilent) and pre-column derivatization with ophthaldialdehyde (OPA) and fluorenylmethoxycarbonyl (FMOC) based on the application note "Automated amino acid analysis using an Agilent Poroshell HPH-C18 Column" by Agilent. Peaks were evaluated and quantified using OpenLabCDS software (Agilent). Reaction rates were determined based on at least 3 time points. All assays were conducted in 30 °C and in triplicates. Kinetic parameters and inhibitory constants were calculated using the non-linear regression least squares fit analysis "Michealis-Menten" and "Competitive inhibition", respectively, in GraphPad Prism (Version 10.4.2 for Windows, GraphPad Software).

### 4.6.9 Pathways Reconstruction

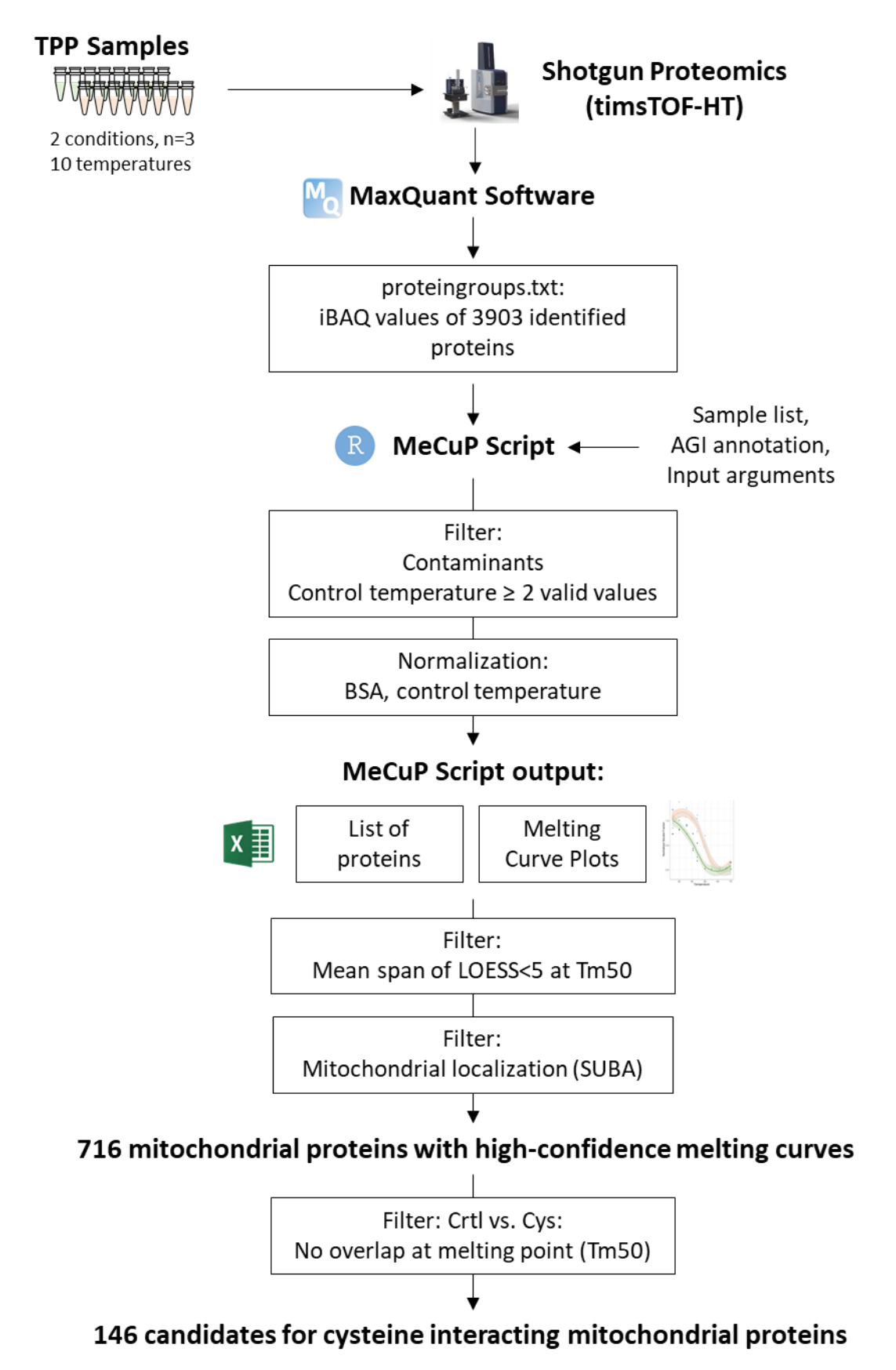
All reactions contained 50 mM HEPES pH 8.0, 1 mM glutathione and 1.1 μg ml<sup>-1</sup> ETHE1. Assays for ETHE1 reactions were started by adding 10 μl of a saturated sulfur solution (in acetone). Assays for combined STR1 and ETHE1 reactions contained additional 7.1 μg ml<sup>-1</sup>

STR1 and were started by adding 1 mM 3-mercaptopyruvate. Assays for full pathway reconstitution contained additional 7.1 µg ml<sup>-1</sup> STR1, 50 µM PLP, 1 mM 2-oxoglutarate, 63 µg ml<sup>-1</sup> Asp-AT or 99 µg ml<sup>-1</sup> Ala-AT and were started by adding 1 mM cysteine. Oxygen content was continuously measured using a clark type oxygen electrode (model DW1, Hansatech Instruments Ltd). All assays were performed in triplicates at 30 °C and reaction rates were determined from the linear phase of oxygen depletion over 20 s. After 50 nmol of oxygen was consumed, samples for thiol quantification were transferred into derivatization buffer (1.5 mM bromobimane; 32% (v/v) acetonitrile; 10.3 mM EDTA and 10.3 mM HEPES pH 8) and incubated for 10 min on ice before the addition of methanesulfonic acid (final conc. 15.9 mM). Samples were diluted and measured using an Agilent 1260 Infinity II HPLC (Agilent) by fluorescence detection (ex. 380 nm; em. 480 nm). Peaks were evaluated and quantified using OpenLabCDS software (Agilent). Assays for oxygen content traces (Fig. 6 B, C, D, E) were started by the addition of 1.1 µg ml<sup>-1</sup> ETHE1 and were repeated at least 3 times with similar results.

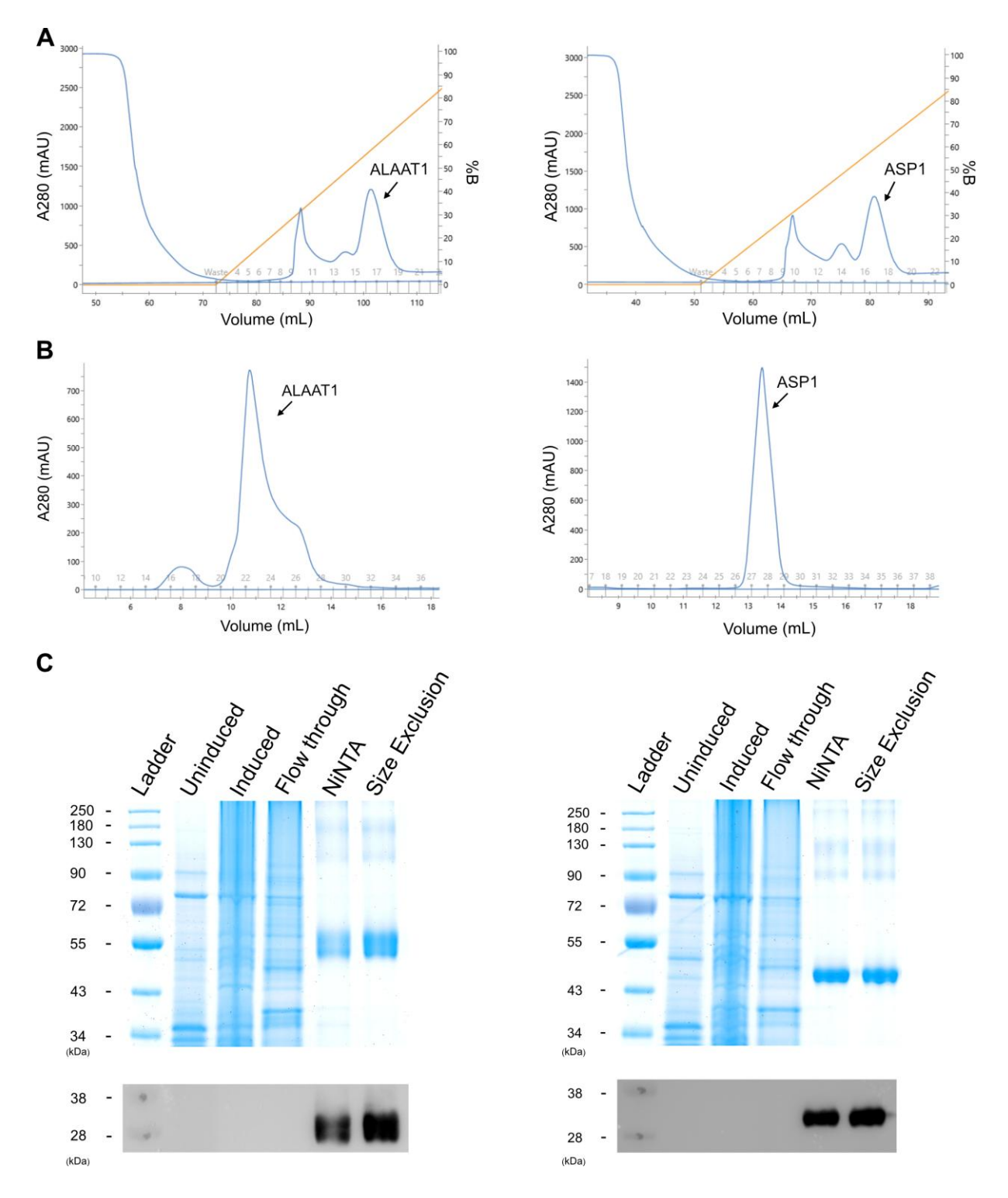
# 4.6.10 Data availability

The mass spectrometry proteomics data have been deposited to the ProteomeXchange Consortium (http://proteomecentral.proteomexchange.org) via the PRIDE partner repository (Perez-Riverol et al. 2022) with the dataset identifier PXD064096.

# 4.7 Supplementary Figures

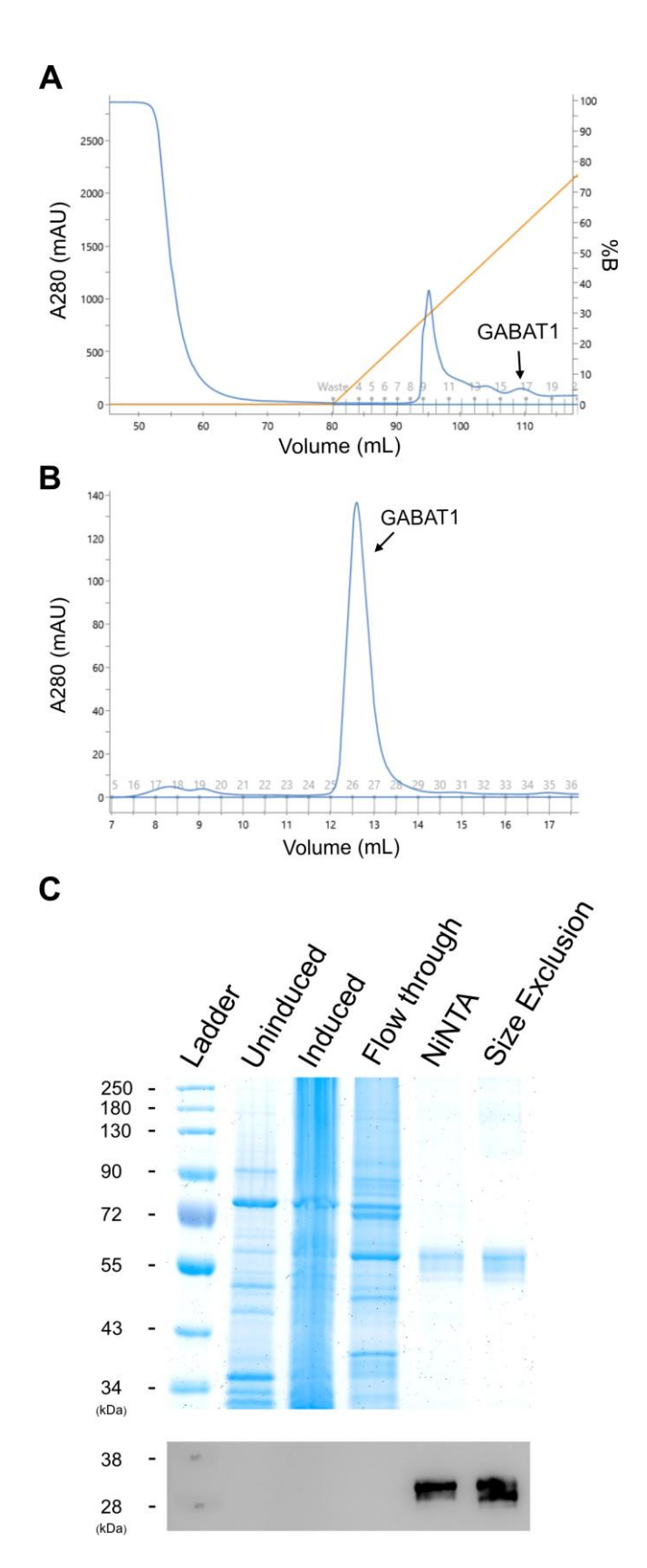


Supplementary Figure 4.1: Thermal Proteome Profiling (TPP) data processing workflow.



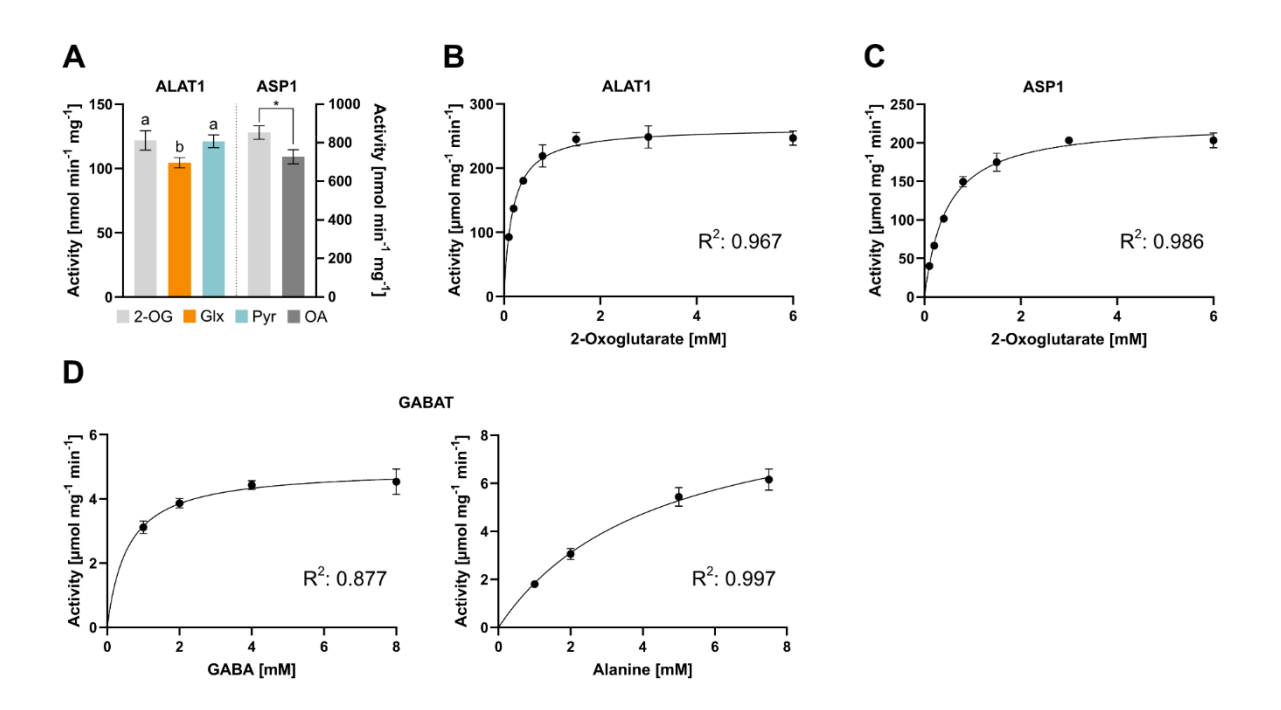
Supplementary Figure 4.2: Purification of recombinant AlaAT and AspAT

**A**. UV chromatograms showing purification peaks for different eluting proteins during gradient elution from Ni-NTA column. ALAAT and ASP. **B**. UV chromatograms showing singular peaks of size excluded fractions for ALAAT and ASP. **C**. SDS-PAGE gel (Lanes 1-6) showcasing, Marker (in kDa), Uninduced, Induced, Flowthrough along with Ni-NTA purified and Size exclusion fractions. ALAAT and ASP correspond to their MW of 54.7 kDa and 45.8 kDa. A Corresponding western blot confirms the purification and presence of our recombinant protein purified from *E. coli* cultures.



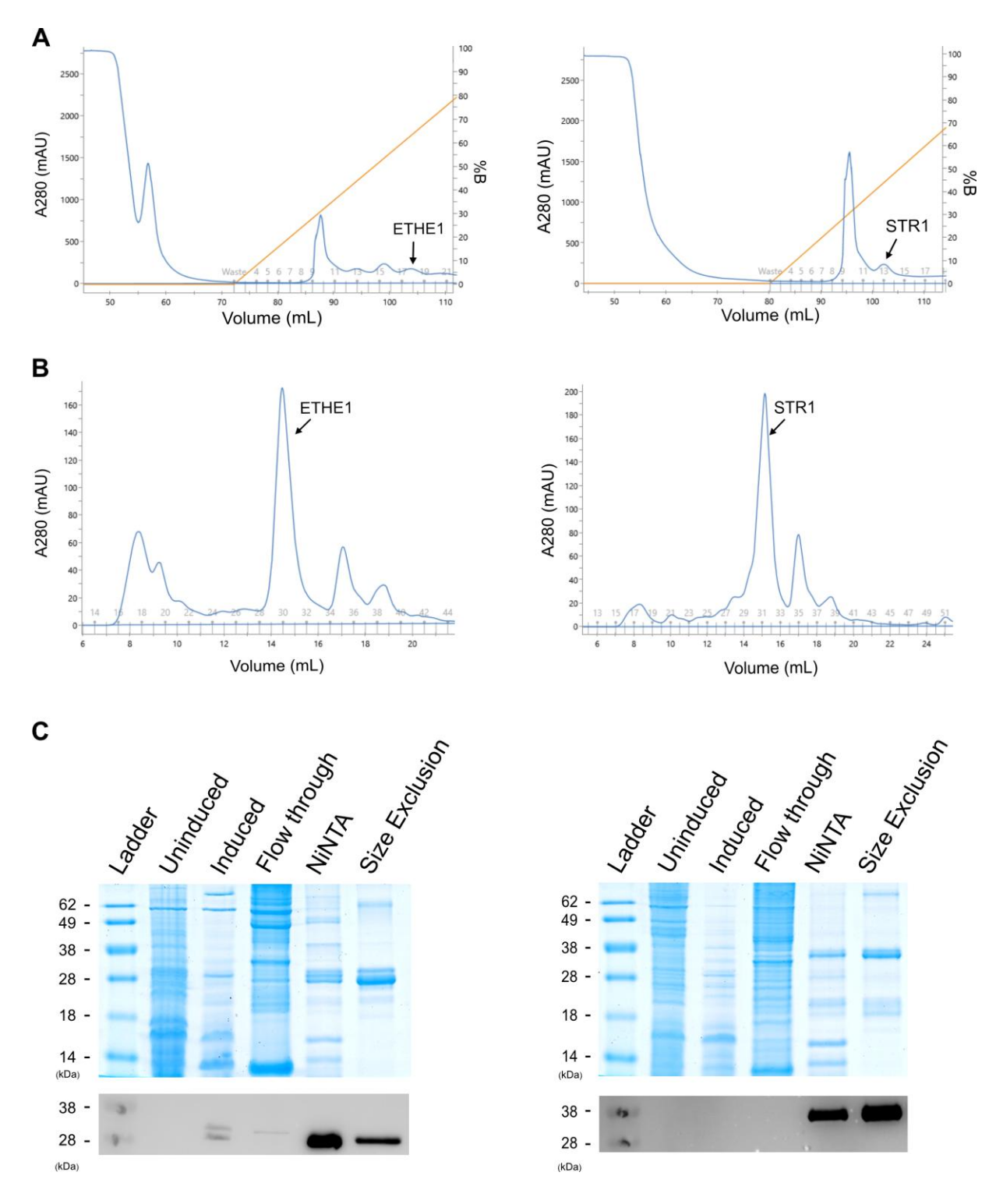
Supplementary Figure 4.3: Purification of recombinant GABA-AT

**A**. UV chromatograms showing purification peaks for different eluting proteins during gradient elution from Ni-NTA column. GABAT. **B**. UV chromatogram showing singular peaks of size excluded fractions for GABAT. **C** SDS-PAGE gel (Lanes 1-6) showcasing, Marker (in kDa), Uninduced, Induced, Flowthrough along with Ni-NTA purified and size exclusion fractions. GABAT correspond to MW of 53.3 kDa. A Corresponding western blot confirms the purification and presence of our recombinant protein purified from e coli cultures.



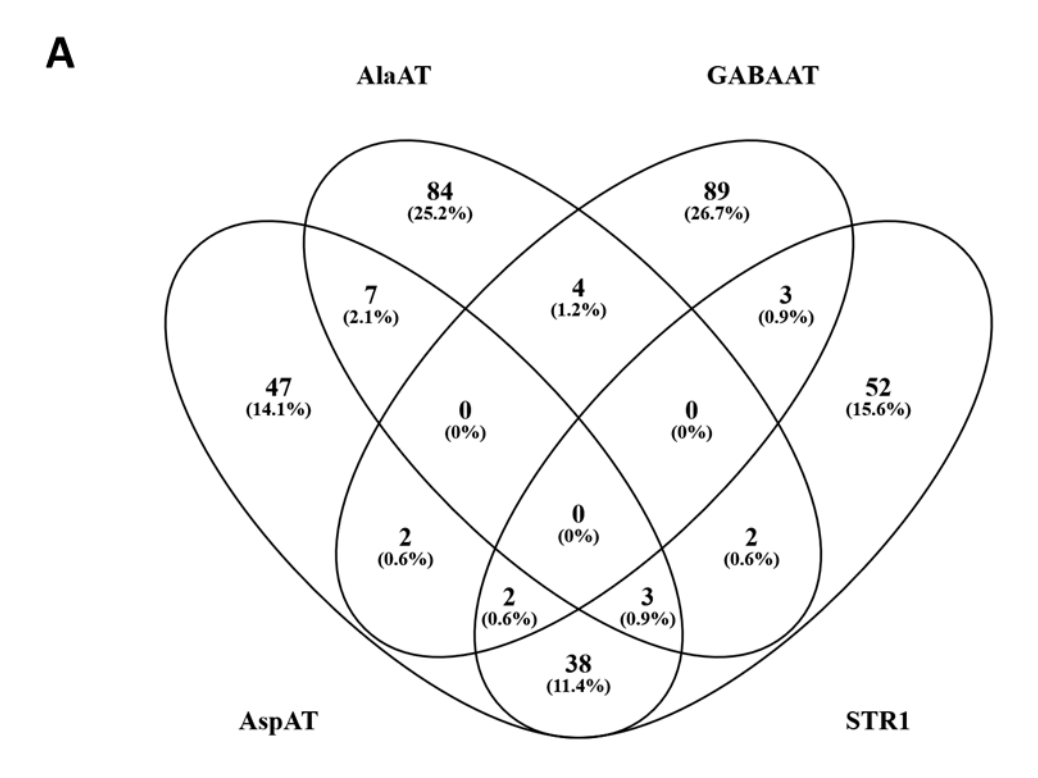
Supplementary Figure 4.4: Biochemical characterization of mitochondrial cysteine aminotransferase candidates

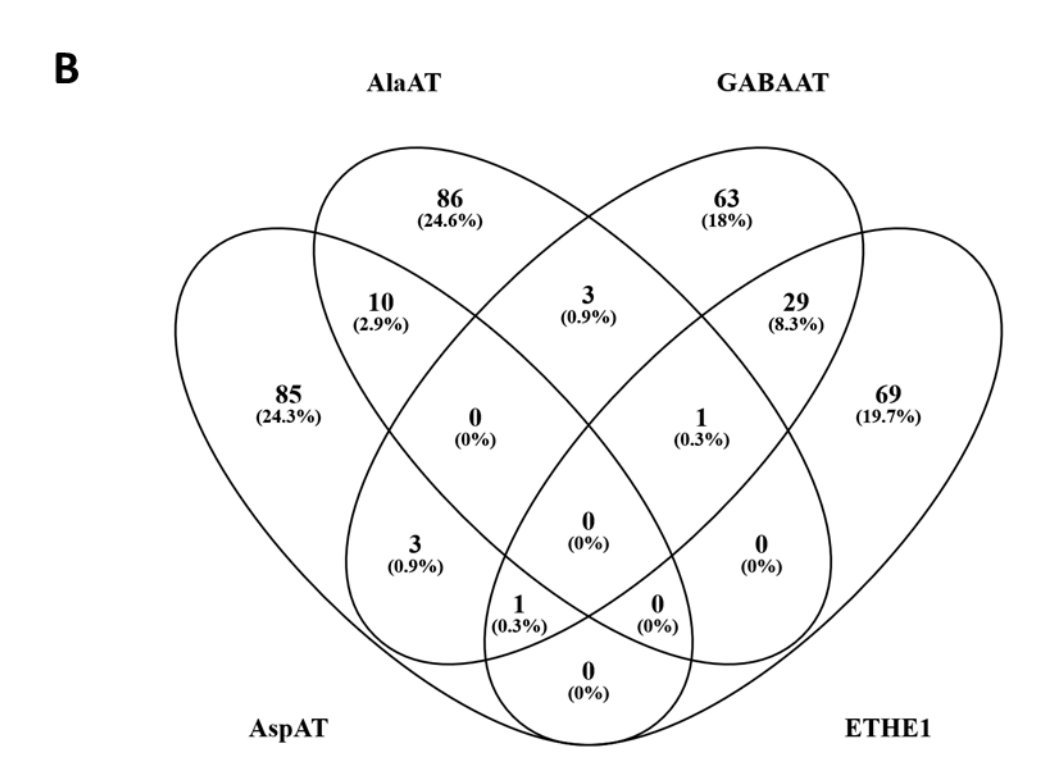
**A**. Aminotransferase activities of Ala-AT with Ala as amino donor and AspAT with Asp as amino donor in combination with different ketoacid substrates. **B**. Michaelis Menten kinetics for alanine aminotransferase 1 (AT1G17290) with L-Ala as fixed and 2-oxoglutarate as variable substrate. **C**. Michaelis Menten kinetics for aspartate aminotransferase 1 (AT2G30970) with L-Asp as fixed and 2-oxoglutarate as variable substrate. **D**. Michaelis Menten kinetics for GABA aminotransferase 1 (AT3G22200) with GABA and Ala as variable substrate.



Supplementary Figure 4.5: Purification of recombinant ETHE1 and STR1

**A**. UV chromatograms showing purification peaks for different eluting proteins during gradient elution from Ni-NTA column. ETHE1 and STR1. **B**. UV chromatogram showing singular peaks of size excluded fractions for ETHE1 and STR1. **C**. SDS-PAGE gel (Lanes 1-6) showcasing, Marker (in kDa), Uninduced, Induced, Flowthrough along with Ni-NTA purified and Size exclusion fractions. ETHE1 and STR1 correspond to their MW of 28.9 kDa and 36.6 kDa. A Corresponding western blot confirms the purification and presence of our recombinant protein purified from *E. coli* cultures.





Supplementary Figure 4.6: Overlap between coexpression profiles of the enzymes involved in mitochondrial cysteine catabolism

To get a first impression about the metabolic integration of the three aminotransferases in mitochondrial sulfur metabolism as well as the physiological context of these networks we compared co-expression profiles available on ATTED (<a href="https://atted.jp/">https://atted.jp/</a>). The top 100 coexpressed genes for the individual enzymes are listed in Suppl. Dataset S2.

### 4.8 References

Araújo, Wagner L. et al. (2010): Identification of the 2-hydroxyglutarate and isovaleryl-CoA dehydrogenases as alternative electron donors linking lysine catabolism to the electron transport chain of Arabidopsis mitochondria. In: *Plant Cell* 22 (5), S. 1549–1563. DOI: 10.1105/tpc.110.075630.

Begara-Morales, J. C. et al. (2016): Protein S-Nitrosylation and S-Glutathionylation as Regulators of Redox Homeostasis During Abiotic Stress Response. In: Dharmendra K. Gupta, José M. Palma und Francisco J. Corpas (Hg.): Redox State as a Central Regulator of Plant-Cell Stress Responses. Cham: Springer International Publishing, S. 365–386.

Birke, Hannah; Heeg, Corinna; Wirtz, Markus; Hell, Rüdiger (2013): Successful Fertilization Requires the Presence of at Least One Major O-Acetylserine(thiol)lyase for Cysteine Synthesis in Pollen of Arabidopsis. In: *Plant Physiol* 163 (2), S. 959–972. DOI: 10.1104/pp.113.221200.

Böttcher, Christoph; Westphal, Lore; Schmotz, Constanze; Prade, Elke; Scheel, Dierk; Glawischnig, Erich (2009): The Multifunctional Enzyme CYP71B15 (PHYTOALEXIN DEFICIENT3) Converts Cysteine-Indole-3-Acetonitrile to Camalexin in the Indole-3-Acetonitrile Metabolic Network of Arabidopsis thaliana. In: *Plant Cell* 21 (6), S. 1830–1845. DOI: 10.1105/tpc.109.066670.

Buchanan, Bob B.; Balmer, Yves (2005): REDOX REGULATION: A Broadening Horizon. In: *Annual review of plant biology* 56 (Volume 56, 2005), S. 187–220. DOI: 10.1146/annurev.arplant.56.032604.144246.

Clark, Shawn M.; Di Leo, Rosa; Dhanoa, Preetinder K.; van Cauwenberghe, Owen R.; Mullen, Robert T.; Shelp, Barry J. (2009): Biochemical characterization, mitochondrial localization, expression, and potential functions for an Arabidopsis gamma-aminobutyrate transaminase that utilizes both pyruvate and glyoxylate. In: *J Exp Bot* 60 (6), S. 1743–1757. DOI: 10.1093/jxb/erp044.

Cobbett, Christopher; Goldsbrough, Peter (2002): Phytochelatins and metallothioneins: roles in heavy metal detoxification and homeostasis. In: *Annual review of plant biology* 53, S. 159–182. DOI: 10.1146/annurev.arplant.53.100301.135154.

Cooper, Chris E.; Brown, Guy C. (2008): The inhibition of mitochondrial cytochrome oxidase by the gases carbon monoxide, nitric oxide, hydrogen cyanide and hydrogen sulfide: chemical mechanism and physiological significance. In: *Journal of Bioenergetics and Biomembranes* 40 (5), S. 533–539. DOI: 10.1007/s10863-008-9166-6.

Couturier, Jérémy; Touraine, Brigitte; Briat, Jean-Francois; Gaymard, Frédéric; Rouhier, Nicolas (2013): The iron-sulfur cluster assembly machineries in plants: current knowledge and

open questions. In: *Frontiers in Plant Science* 4. Online verfügbar unter https://www.frontiersin.org/journals/plant-science/articles/10.3389/fpls.2013.00259.

Dietrich, Katrin et al. (2011): Heterodimers of the Arabidopsis transcription factors bZIP1 and bZIP53 reprogram amino acid metabolism during low energy stress. In: *Plant Cell* 23 (1), S. 381–395. DOI: 10.1105/tpc.110.075390.

Droux, Michel (2003): Plant serine acetyltransferase: new insights for regulation of sulphur metabolism in plant cells. In: *Plant Physiology and Biochemistry* 41 (6), S. 619–627. DOI: 10.1016/S0981-9428(03)00083-4.

Droux, Michel (2004): Sulfur Assimilation and the Role of Sulfur in Plant Metabolism: A Survey. In: *Photosynthesis Research* 79 (3), S. 331–348. DOI: 10.1023/B:PRES.0000017196.95499.11.

Foyer, Christine Helen; Noctor, Graham (2011): Ascorbate and Glutathione: The Heart of the Redox Hub. In: *Plant Physiol* 155 (1), S. 2–18. DOI: 10.1104/pp.110.167569.

Giovanelli, John; Mudd, S. Harvey; Datko, Anne H. (1985): Quantitative Analysis of Pathways of Methionine Metabolism and Their Regulation in Lemna. In: *Plant Physiol* 78 (3), S. 555–560. DOI: 10.1104/pp.78.3.555.

Halkier, Barbara Ann; Gershenzon, Jonathan (2006): Biology and biochemistry of glucosinolates. In: *Annual review of plant biology* 57, S. 303–333. DOI: 10.1146/annurev.arplant.57.032905.105228.

Hatzfeld, Yves; Maruyama, Akiko; Schmidt, Ahlert; Noji, Masaaki; Ishizawa, Kimiharu; Saito, Kazuki (2000): β-Cyanoalanine Synthase Is a Mitochondrial Cysteine Synthase-Like Protein in Spinach and Arabidopsis1. In: *Plant Physiol* 123 (3), S. 1163–1172. DOI: 10.1104/pp.123.3.1163.

Heeg, Corinna et al. (2008): Analysis of the Arabidopsis O-Acetylserine(thiol)lyase Gene Family Demonstrates Compartment-Specific Differences in the Regulation of Cysteine Synthesis. In: *Plant Cell* 20 (1), S. 168–185. DOI: 10.1105/tpc.107.056747.

Heinemann, Björn; Hildebrandt, Tatjana M. (2021): The role of amino acid metabolism in signaling and metabolic adaptation to stress-induced energy deficiency in plants. In: *J. Exp. Bot.* 72 (13), S. 4634–4645. DOI: 10.1093/jxb/erab182.

Heinemann, Björn; Künzler, Patrick; Eubel, Holger; Braun, Hans-Peter; Hildebrandt, Tatjana M. (2021): Estimating the number of protein molecules in a plant cell: protein and amino acid homeostasis during drought. In: *Plant Physiol* 185 (2), S. 385–404. DOI: 10.1093/plphys/kiaa050.

Hell, Rüdiger; Wirtz, Markus (2011): Molecular Biology, Biochemistry and Cellular Physiology of Cysteine Metabolism in *Arabidopsis thaliana*. In: *The Arabidopsis Book* 2011 (9). DOI: 10.1199/tab.0154.

Hildebrandt, Tatjana M.; Nunes Nesi, Adriano; Araújo, Wagner L.; Braun, Hans-Peter (2015): Amino Acid Catabolism in Plants. In: *Molecular Plant* 8 (11), S. 1563–1579. DOI: 10.1016/j.molp.2015.09.005.

Hirota, Takaaki; Izumi, Masanori; Wada, Shinya; Makino, Amane; Ishida, Hiroyuki (2018): Vacuolar Protein Degradation via Autophagy Provides Substrates to Amino Acid Catabolic Pathways as an Adaptive Response to Sugar Starvation in Arabidopsis thaliana. In: *Plant & cell physiology* 59 (7), S. 1363–1376. DOI: 10.1093/pcp/pcy005.

Höfler, Saskia et al. (2016): Dealing with the sulfur part of cysteine: four enzymatic steps degrade I-cysteine to pyruvate and thiosulfate in Arabidopsis mitochondria. In: *Physiologia Plantarum* 157 (3), S. 352–366. DOI: 10.1111/ppl.12454.

Ishizaki, Kimitsune; Larson, Tony R.; Schauer, Nicolas; Fernie, Alisdair R.; Graham, Ian A.; Leaver, Christopher J. (2005): The critical role of Arabidopsis electron-transfer flavoprotein:ubiquinone oxidoreductase during dark-induced starvation. In: *Plant Cell* 17 (9), S. 2587–2600. DOI: 10.1105/tpc.105.035162.

Ishizaki, Kimitsune; Schauer, Nicolas; Larson, Tony R.; Graham, Ian A.; Fernie, Alisdair R.; Leaver, Christopher J. (2006): The mitochondrial electron transfer flavoprotein complex is essential for survival of Arabidopsis in extended darkness. In: *The Plant journal: for cell and molecular biology* 47 (5), S. 751–760. DOI: 10.1111/j.1365-313X.2006.02826.x.

Johnston, Harvey E. et al. (2022): Solvent Precipitation SP3 (SP4) Enhances Recovery for Proteomics Sample Preparation without Magnetic Beads. In: *Analytical chemistry* 94 (29), S. 10320–10328. DOI: 10.1021/acs.analchem.1c04200.

Kinnersley, Alan M.; Turano, Frank J. (2000): Gamma Aminobutyric Acid (GABA) and Plant Responses to Stress. In: *Critical Reviews in Plant Sciences* 19 (6), S. 479–509. DOI: 10.1080/07352680091139277.

Kirsch, J. F. et al. (1984): Mechanism of action of aspartate aminotransferase proposed on the basis of its spatial structure. In: *Journal of molecular biology* 174 (3), S. 497–525. DOI: 10.1016/0022-2836(84)90333-4.

Krüger, Stephan et al. (2009): Analysis of cytosolic and plastidic serine acetyltransferase mutants and subcellular metabolite distributions suggests interplay of the cellular compartments for cysteine biosynthesis in Arabidopsis. In: *Plant, cell & environment* 32 (4), S. 349–367. DOI: 10.1111/j.1365-3040.2009.01928.x.

Krüßel, Lena et al. (2014): The mitochondrial sulfur dioxygenase ETHYLMALONIC ENCEPHALOPATHY PROTEIN1 is required for amino acid catabolism during carbohydrate starvation and embryo development in Arabidopsis. In: *Plant Physiol* 165 (1), S. 92–104. DOI: 10.1104/pp.114.239764.

Liepman, Aaron H.; Olsen, Laura J. (2003): Alanine aminotransferase homologs catalyze the glutamate:glyoxylate aminotransferase reaction in peroxisomes of Arabidopsis. In: *Plant Physiol* 131 (1), S. 215–227. DOI: 10.1104/pp.011460.

Lyu, Hai-Ning et al. (2023): Systematic thermal analysis of the Arabidopsis proteome: Thermal tolerance, organization, and evolution. In: *Cell systems* 14 (10), 883-894.e4. DOI: 10.1016/j.cels.2023.08.003.

Mikulášek, Kamil; Konečná, Hana; Potěšil, David; Holánková, Renata; Havliš, Jan; Zdráhal, Zbyněk (2021): SP3 Protocol for Proteomic Plant Sample Preparation Prior LC-MS/MS. In: *Frontiers in Plant Science* 12, S. 635550. DOI: 10.3389/fpls.2021.635550.

Miyamoto, Ryo; Otsuguro, Ken-Ichi; Yamaguchi, Soichiro; Ito, Shigeo (2014): Contribution of cysteine aminotransferase and mercaptopyruvate sulfurtransferase to hydrogen sulfide production in peripheral neurons. In: *Journal of neurochemistry* 130 (1), S. 29–40. DOI: 10.1111/jnc.12698.

Moormann, Jannis et al. (2025): Cysteine Signalling in Plant Pathogen Response. In: *Plant Cell Environ*. DOI: 10.1111/pce.70017.

Moseler, Anna; Wagner, Stephan; Meyer, Andreas J. (2024): Protein persulfidation in plants: mechanisms and functions beyond a simple stress response. In: *Biological Chemistry* 405 (9-10), S. 547–566. DOI: 10.1515/hsz-2024-0038.

Noctor, Graham; Cohen, Mathias; Trémulot, Lug; Châtel-Innocenti, Gilles; van Breusegem, Frank; Mhamdi, Amna (2024): Glutathione: a key modulator of plant defence and metabolism through multiple mechanisms. In: *J Exp Bot* 75 (15), S. 4549–4572. DOI: 10.1093/jxb/erae194.

Pedre, Brandán et al. (2023): 3-Mercaptopyruvate sulfur transferase is a protein persulfidase. In: *Nature chemical biology* 19 (4), S. 507–517. DOI: 10.1038/s41589-022-01244-8.

Pedrotti, Lorenzo et al. (2018): Snf1-RELATED KINASE1-Controlled C/S1-bZIP Signaling Activates Alternative Mitochondrial Metabolic Pathways to Ensure Plant Survival in Extended Darkness. In: *Plant Cell* 30 (2), S. 495–509. DOI: 10.1105/tpc.17.00414.

Peiser, Galen D.; Wang, Tsu-Tsuen; Hoffman, Neil E.; Yang, Shang Fa; Liu, Hung-wen; Walsh, Christopher T. (1984): Formation of cyanide from carbon 1 of 1-aminocyclopropane-1-carboxylic acid during its conversion to ethylene. In: *Proceedings of the National Academy of Sciences* 81 (10), S. 3059–3063. DOI: 10.1073/pnas.81.10.3059.

Peng, Cheng; Uygun, Sahra; Shiu, Shin-Han; Last, Robert L. (2015): The Impact of the Branched-Chain Ketoacid Dehydrogenase Complex on Amino Acid Homeostasis in Arabidopsis. In: *Plant Physiol* 169 (3), S. 1807–1820. DOI: 10.1104/pp.15.00461.

Perez-Riverol, Yasset et al. (2022): The PRIDE database resources in 2022: a hub for mass spectrometry-based proteomics evidences. In: *Nucleic Acids Res* 50 (D1), D543-D552. DOI: 10.1093/nar/gkab1038.

Reinhard, Friedrich B. M. et al. (2015): Thermal proteome profiling monitors ligand interactions with cellular membrane proteins. In: *Nature Methods* 12 (12), S. 1129–1131. DOI: 10.1038/nmeth.3652.

Romero, Luis C.; Aroca, M. Ángeles; Laureano-Marín, Ana M.; Moreno, Inmaculada; García, Irene; Gotor, Cecilia (2014): Cysteine and Cysteine-Related Signaling Pathways in Arabidopsis thaliana. In: *Molecular Plant* 7 (2), S. 264–276. DOI: 10.1093/mp/sst168.

Ruffet, Marie-Line; Lebrun, Michel; Droux, Michel; Douce, Roland (1995): Subcellular Distribution of Serine Acetyltransferase from Pisum sativum and Characterization of an Arabidopsis thaliana Putative Cytosolic Isoform. In: *European Journal of Biochemistry* 227 (1-2), S. 500–509. DOI: 10.1111/j.1432-1033.1995.tb20416.x.

Savitski, Mikhail M. et al. (2014): Tracking cancer drugs in living cells by thermal profiling of the proteome. In: *Science (New York, N.Y.)* 346 (6205), S. 1255784. DOI: 10.1126/science.1255784.

Su, Tongbing et al. (2011): Glutathione-Indole-3-Acetonitrile Is Required for Camalexin Biosynthesis in Arabidopsis thaliana. In: *Plant Cell* 23 (1), S. 364–380. DOI: 10.1105/tpc.110.079145.

Takahashi, Hideki (2010): Chapter 4 - Regulation of Sulfate Transport and Assimilation in Plants. In: Kwang W. Jeon (Hg.): International Review of Cell and Molecular Biology, Bd. 281: Academic Press, S. 129–159. Online verfügbar unter https://www.sciencedirect.com/science/article/pii/S1937644810810044.

Takahashi, Hideki; Kopriva, Stanislav; Giordano, Mario; Saito, Kazuki; Hell, Rüdiger (2011): Sulfur Assimilation in Photosynthetic Organisms: Molecular Functions and Regulations of Transporters and Assimilatory Enzymes. In: *Annual review of plant biology* 62 (Volume 62, 2011), S. 157–184. DOI: 10.1146/annurev-arplant-042110-103921.

van Hoewyk, Doug; Pilon, Marinus; Pilon-Smits, Elizabeth A.H. (2008): The functions of NifS-like proteins in plant sulfur and selenium metabolism. In: *Plant Science* 174 (2), S. 117–123. DOI: 10.1016/j.plantsci.2007.10.004.

Waltz, Florent; Corre, Nicolas; Hashem, Yaser; Giegé, Philippe (2020): Specificities of the plant mitochondrial translation apparatus. In: *Mitochondrion* 53, S. 30–37. DOI: 10.1016/j.mito.2020.04.008.

Watanabe, Mutsumi; Kusano, Miyako; Oikawa, Akira; Fukushima, Atsushi; Noji, Masaaki; Saito, Kazuki (2008): Physiological Roles of the β-Substituted Alanine Synthase Gene Family in Arabidopsis. In: *Plant Physiol* 146 (1), S. 310–320. DOI: 10.1104/pp.107.106831.

Werhahn, W.; Niemeyer, A.; Jänsch, L.; Kruft, V.; Schmitz, U. K.; Braun, H. (2001): Purification and characterization of the preprotein translocase of the outer mitochondrial membrane from Arabidopsis. Identification of multiple forms of TOM20. In: *Plant Physiol* 125 (2), S. 943–954. DOI: 10.1104/pp.125.2.943.

Wirtz, Markus; Hell, Rüdiger (2006): Functional analysis of the cysteine synthase protein complex from plants: Structural, biochemical and regulatory properties. In: *Journal of plant physiology* 163 (3), S. 273–286. DOI: 10.1016/j.jplph.2005.11.013.

# 5 Closing Remarks

In chapter 2, we summarized the recent progress in the involvement of amino acids in plant microbe interactions. Briefly, we displayed the diversity in which amino acids and their derived specialized metabolites shape the way plants interact with their microbial environment. Thereby, we provided a comprehensive overview of the field and pointed out areas that demand further research. One of them was the role of cysteine metabolism in plant immunity, which we aimed to address in chapter 3. There, we showed that the plant perceives cysteine as a metabolic signal for biotic threat. Cysteine both promotes immune responses artificially and accumulates during infection with Pseudomonas syringae (Pst) naturally. The modulation of phytohormones (abscisic acid & salicylic acid), immune signals (N-hydroxypipecolic acid), defense compounds (Camalexin) as well as of unknown substrates catalyzed by UDPglycosyltransferases (UGTs) and glutathione-S-transferases (GSTs) potentially mediates the cysteine-induced defense response (Fig. 5.1). On the same note, down regulation of the translational controller of immune activation Hem1 also presents a powerful hub for cysteinemediated defense signaling. Notably, shotgun proteome analysis offers great insight into the broader picture of plant metabolism. However, mechanisms of signaling cascades often go beyond changes in protein abundances. Therefore, Chapter 3 presents limited conclusive evidence regarding the mechanistic details of the cysteine-induced defense response. Nevertheless, both GSTs & UGTs as well as Hem1 provide promising targets for further research due to their respective regulatory functions in plant immunity. Further, we revealed compartment-specific differences in the contribution to the cysteine-induced defense response. Remarkably, despite its comparatively small contribution to total cellular cysteine levels, OASTL-C — which is involved in mitochondrial cysteine synthesis — plays a critical role in combatting Pst infection in Arabidopsis. This finding not only presents an additional clue to unravel cysteine-induced immune signaling but also highlights the importance of plant mitochondria in stress adaptation. To build on this idea, we utilized mass spectrometry-based thermal proteome profiling (TPP) on mitochondrial proteome fractions and identified yet unknown aminotransferases that catalyze the transamination of cysteine (chapter 4). Ala-AT and Asp-AT are able to facilitate the first reaction of the mitochondrial cysteine degradation pathway and work in concert with STR1 and ETHE1 in vitro (Fig. 5.1). As enzyme candidates for this step had remained unknown for ten years, our discovery completes the only pathway in plants that fully oxidizes cysteine and advances our understanding of mitochondrial metabolism. Though, physiological significance of Ala-AT & Asp-AT as part of the pathway is yet to be confirmed in vivo. Nonetheless, this research might also aid to unravel potential mitochondrial protein persulfidation via STR1, since the transamination of cysteine is the first committed step in the production of persulfides. Given the importance of mitochondrial cysteine synthesis during Pst infection, future research might also consider protein persulfidation as a means of cysteine signaling in plant immunity. Additionally, GABA-AT is inhibited by cysteine, which we speculated helps to regulate levels of the stress responsive non-proteinogenic amino acid GABA. To build on this point, the proteome of cysteine-treated seedlings showed enriched hypoxia-associated proteins and GABA is known to accumulate under hypoxic conditions. Furthermore, it is worth mentioning that cysteine seems to aid both abscisic acid (abiotic) and salicylic acid (biotic) dependent stress signaling. As stomatal closure helps during both drought and pathogen invasion, cysteine might bridge a gap between the otherwise antagonistically working phytohormones to elicit tissue-specific responses to the same end. However, speculations about synergistic effects of GABA and cysteine during conditions such as hypoxia and cysteines functions in hormonal crosstalk demand more research. Finally, we established and validated TPP as a powerful tool to find plant proteins interacting with a molecule of interest or even to dissect the heat-stability of distinct pathways such as the TCA cycle. Additionally, this technique bears the potential to find proteins that work as cysteine sensors. Hence, future research can capitalize on our data of mitochondrial fractions (chapter 4) or utilize TPP with whole cell fractions to get an even broader picture of candidate proteins binding or interacting with cysteine. Taken together, we confirmed cysteine as an infochemical in plant immunity, dissected proteome responses and, thereby, provided promising targets for further research regarding cysteine-mediated defense responses. Further, we shed light on the importance of mitochondrial cysteine metabolism during pathogen invasion and elucidated an unknown step of the mitochondrial cysteine degradation pathway by establishing TPP. In the end, this dissertation highlights the importance of amino acids generally, but cysteine in particular, during biotic stress responses, provides a framework for follow-up research on cysteine in plant immunity and presents a potent unbiased identification method for protein metabolite interaction in plant research.

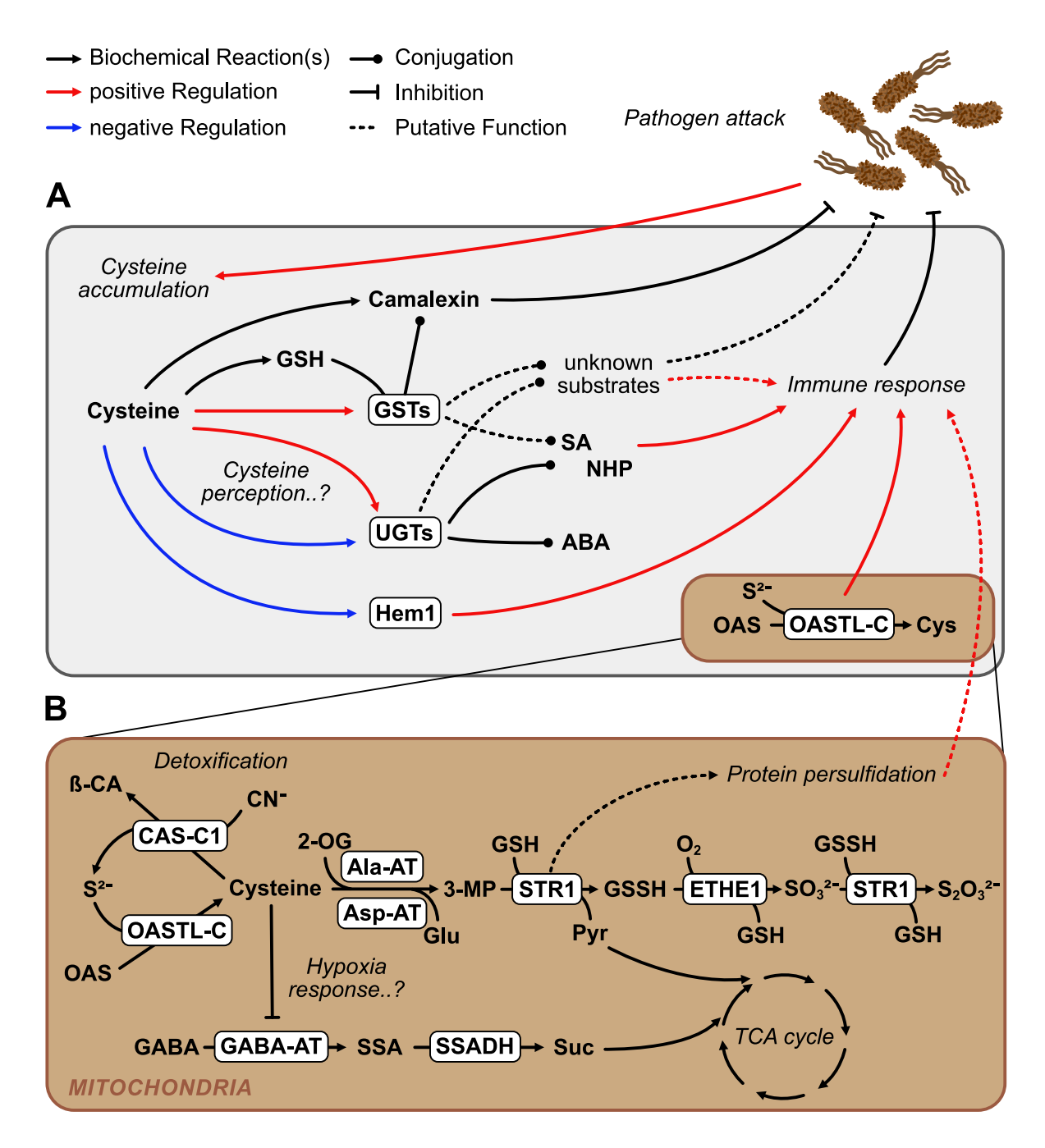


Figure 5.1 Working model of cysteine in signaling and plant pathogen response

Cysteine accumulates in response to pathogen invasion and is interpreted as biotic threat by the plant. It acts as an infochemical and elicits an immune response by different potential mechanisms. (A) Here, we postulated that the modulation of phytohormones (SA & ABA), immune signals (NHP) and defense compounds (camalexin) as well as yet unknown substrates by glutathione-S-transferases and UDP-glycosyltransferases may trigger the cysteineinduced immune response. Additionally, the global immune controller Hem1 is downregulated by elevated cysteine levels and mitochondrial cysteine synthesis by OASTL-C is necessary for a proper defense response. (B) Mitochondrial cysteine metabolism is involved in detoxification of cyanide and sulfide and facilitates the complete oxidation of cysteine. We identified Ala-AT and Asp-AT to catalyze the transamination of cysteine allowing for the generation of (potential protein-) persulfides by STR1. Further, we showed inhibition of GABA-AT by cysteine, which potentially becomes relevant during hypoxic conditions. Enzymes are indicated in white boxes. Abbreviations of enzymes: Ala-AT, alanine aminotransferase; Asp-AT, aspartate aminotransferase; CAS-C1,  $\beta$ -cyanoalanine synthase; ETHE1, persulfide dioxygenase, GABA-AT,  $\gamma$ -aminobutyrate aminotransferase; GSTs, glutathione-S-transferases; Hem1, translational regulator protein; OASTL-C, O-acetylserine(thiol)lyase C; SSAGH, succinic acid semialdehyde dehydrogenase; STR1, 3-mercaptopyruvate sulfurtransferase; UGTs, uridine diphosphate glycosyltranferases. Abbreviations of metabolites: ABA, abscisic acid; β-CA, β-cyanoalanine; Cys, cysteine; GABA, γ-aminobutyrate; Glu, glutamate; GSH, glutathione; GSSH, glutathione persulfide; NHP, N-hydroxypipecolic acid; OAS, O-acetylserine; Pyr, pyruvate; SA, salicylic acid; SSA, succinic acid semialdehyde, Suc, succinate; 2-OG, 2oxoglutarate; 3-MP, 3-mercaptopyruvate.

# **Declaration of Contribution**

**Moormann, Jannis**; Heinemann, Björn; Hildebrandt, Tatjana M. (2022): News about amino acid metabolism in plant microbe interactions. Trends in Biochemical Sciences 47 (10). S. 839 – 850. DOI: 10.1016/j.tibs.2022.07.001

I designed and illustrated all figures. Together with the other authors I defined the scope of the review, compiled relevant primary literature and wrote the manuscript.

**Moormann, Jannis**; Heinemann, Björn; Angermann, Cecile; Koprivova, Anna; Armbruster, Ute; Kopriva, Stanislav; Hildebrandt, Tatjana M. (2025): Cysteine signaling in plant pathogen response. *Plant Cell Environ*. DOI: 10.1111/pce.70017

I performed all thiol quantifications, infection assays, GST activity tests and  $H_2O_2$  staining experiments. Additionally, I acquired, processed and evaluated the shotgun proteomics data of Pst and mock-infected samples. I performed statistical analysis and designed and illustrated all figures except the Suppl. Fig. 3.3B & Suppl Fig. 3.4. I wrote the manuscript with support from TMH and feedback from the other co-authors.

Heinemann, Björn; **Moormann, Jannis**; Bady, Shivsam; Angermann, Cecile; Schrader, Andrea; Hildebrandt, Tatjana M. (2025): Thermal proteome profiling identifies mitochondrial aminotransferases involved in cysteine catabolism via persulfides in plants. BioRxiv. DOI: 10.1101/2025.05.23.655777

I participated in cloning and heterologous expression of candidate genes. I performed all enzyme activity tests including aminotransferase activity tests and pathway reconstruction and determined kinetic parameters including inhibitory constants for GABA-AT. I designed and illustrated Fig. 5 & Fig. 6 and contributed to manuscript writing.